

Experimental and Numerical Investigations on Stress Laminated Timber Bridges

*Master's Thesis in the Master's Programme Structural Engineering and Building
Performance Design*

EMIL ANDERSSON

JOHAN BERGENDAHL

Department of Civil and Environmental Engineering

Division of Structural Engineering

Steel and Timber Structures

CHALMERS UNIVERSITY OF TECHNOLOGY

Göteborg, Sweden 2009

Master's Thesis 2009:93

MASTER'S THESIS 2009:93

Experimental and Numerical Investigations of Stress Laminated Timber Bridges

Master's Thesis in the *Master's Programme Structural Engineering and Building
Performance Design*

EMIL ANDERSSON

JOHAN BERGENDAHL

Department of Civil and Environmental Engineering
Division of Structural Engineering
Steel and Timber Structures
CHALMERS UNIVERSITY OF TECHNOLOGY
Göteborg, Sweden 2009

Experimental and Numerical Investigations of Stress Laminated Timber Bridges

Master's Thesis in the *Master's Programme Structural Engineering and Building Performance Design*

EMIL ANDERSSON

JOHAN BERGENDAHL

© EMIL ANDERSSON, JOHAN BERGENDAHL, 2009

Examensarbete 2009:93

Department of Civil and Environmental Engineering

Division of Structural Engineering

Steel and Timber Structures

Chalmers University of Technology

SE-412 96 Göteborg

Sweden

Telephone: + 46 (0)31-772 1000

Cover:

Figure shows the principal behaviour of a Stress Laminated Timber Deck under point-load at edge.

Chalmers Reproservice / Department of Civil and Environmental Engineering
Göteborg, Sweden 2009

Experimental and Numerical Investigations of Stress Laminated Timber Bridges

Master's Thesis in the *Master's Programme Structural Engineering and Building Performance Design*

EMIL ANDERSSON

JOHAN BERGENDAHL

Department of Civil and Environmental Engineering

Division of Structural Engineering

Steel and Timber Structures

Chalmers University of Technology

ABSTRACT

Today, a greater part of the timber bridges built in Sweden are utilized as bridges for pedestrians and bicycles. As a step towards a more sustainable society and building industry, the use of concrete and steel needs to be reduced. A low-footprint alternative is sustainable harvested wood. Research on the behaviour of stress laminated timber decks (SLTD) for road traffic has been very extensive in, for example USA and Australia, but limited in Sweden.

The aim of this project was to study some of the design guides that are proposed and used when designing timber bridges as a SLTD. Special attention has been put on studying the methods with, regards to deflection, for load application at the edge. It has also been to study the uplift behaviour in the supports of an orthotropic plate loaded at mid-span. Another part of the project has been to examine if elastic foundation theory can be used to approximate deflection in orthotropic plates like SLTD. Finally, it was also investigated if a failure mechanism could be predicted for edge loads in a SLTD.

The aims were fulfilled using data from two tests. Firstly, a full scale test performed at SP Träteknik was used. Secondly, downscaled tests were carried out on plates of LVL in the laboratory of the Division of Structural Engineering at Chalmers University of Technology, Göteborg.

From the investigated hand calculation methods, it was found that Eurocode is the only method that gives results on the safe side for load applied at the edge. Relations between the uplift per applied load versus the length-width ratio was noticed.

The elastic foundation theory rendered higher maximal deflections than the measured values and thus leading to a result more on the safe side. However, for practical implementation of the theory, more test data needs to be analysed. A possible failure mechanism was also derived using elastic foundation theory.

Key words: stress laminated timber deck bridge, SLTD, orthotropic plate, beam on elastic foundation theory

Experimentell och Numerisk Utredning av Tvärspända Limträbroar

Examensarbete inom Magisterprogrammet 'Structural Engineering and Building Performance Design'

EMIL ANDERSSON

JOHAN BERGENDAHL

Institutionen för bygg- och miljöteknik

Avdelningen för Konstruktionsteknik

Stål- och Träbyggnad

Chalmers tekniska högskola

SAMMANFATTNING

Den största delen av träbroar som byggs i Sverige idag används som gång- och cykelbroar. Som ett steg mot ett mer hållbart samhälle och en mer hållbar byggnadsindustri finns det ett behov av att minska användningen av betong och stål. Ett alternativ till att bygga med stål och/eller betong är att bygga med trä, vilket är ett ur miljöhänsyn bra material. Forskning om broar som byggs som tvärspända träplattor och används för vägtrafik har varit mycket omfattande i länder som USA och Australien, men har varit begränsad i Sverige.

Syftet med detta projekt var att studera några av de mest använda metoderna vid dimensionering av träbroar. Särskild uppmärksamhet har riktats till vilka nedböjningar metoderna ger vid kantlast. Studier av upplyfts beteende vid stöd har även genomförts för ortotropa plattor. En annan del av projektet har varit att undersöka om teorin om balk på elastiskt underlag kan användas för att approximera nedböjningar i en träplatta. Slutligen så har en undersökning gjorts för att se om en brottsmod går att förutspå för träplattor som utsätts för kantlast.

Målen uppfylldes med hjälp av resultaten från två tester. Det ena från ett test utfört av SP Träteknik och det andra från ett test som genomfördes av författarna på Chalmers Tekniska Högskola.

Undersökningen av handberäkningsmetoderna visade att Eurocode är den enda metoden som ger resultat på den säkra sidan för kantlast. Relationen mellan upplyft per pålagd last mot längd- bredd förhållandena kunde noteras.

Teorin om balk på elastiskt underlag gav högre maximala nedböjningar än de uppmätta värdena vilket ger ett resultat på den säkra sidan. För praktisk användning av teorin anser författarna att mer analys av testdata bör genomföras. En möjlig brottsmekanism kunde beräknas med hjälp av teorin om balk på elastiskt underlag.

Nyckelord: tvärspänd träplatta, ortotropisk platta, teorin om balk på elastiskt underlag

Contents

ABSTRACT	I
SAMMANFATTNING	II
CONTENTS	III
PREFACE	VII
NOTATIONS	IX
1 INTRODUCTION	1
1.1 Background	1
1.1.1 Historical background	1
1.1.2 Manufacturing process	2
1.1.3 Mechanical behaviour	3
1.2 Aim of the thesis	5
1.3 Method and objectives	5
1.4 Limitations	5
1.5 Outline	6
2 SP TEST	7
2.1 Background	7
2.2 Test	7
2.3 Results from test	8
3 HAND CALCULATION METHODS	9
3.1 Ritters design guide	9
3.2 Eurocode 5	14
3.3 Crews design guide	16
3.4 West Virginia University method	17
3.5 Summary of hand calculation methods	18
4 BEAM ON ELASTIC FOUNDATION	19
4.1 Theory	19
4.1.1 Guiding differential equation	19
4.1.2 Finite element formulation	20
4.1.3 Evaluation of the elastic foundation stiffness matrix	21
4.2 Calculation methodology	23
4.3 Verification of model	24
4.3.1 Convergence	24
4.3.2 Beam behaviour	24

5	DOWNSCALED TESTS	25
5.1	Background	25
5.2	Test procedure	25
5.3	Expected test results	28
5.3.1	Support behaviour	28
5.3.2	Effective width	28
5.4	Test results	29
6	EVALUATION	31
6.1	Hand calculation methods	31
6.2	Elastic foundation stiffness	32
6.3	Failure load	35
7	DISCUSSION	39
7.1	Downscaled tests	39
7.2	Hand calculation methods	39
7.3	FE model	40
7.4	Failure load	40
7.5	Suggestions for further research	40
8	REFERENCES	41
8.1	Literature	41
8.2	Verbal	41
	APPENDIX A1 – USED DEFLECTIONS FROM SP TEST	42
	APPENDIX A2 – PARAMETERS FROM THE SP TEST	43
	APPENDIX B1 – RITTER	45
	APPENDIX B2 – EUROCODE 5	48
	APPENDIX B3 – CREWS	50
	APPENDIX B4 – WEST VIRGINIA UNIVERSITY METHOD	52
	APPENDIX C1 – CONVERGENCE FOR NUMBER OF ELEMENTS	54
	APPENDIX C2 – BEHAVIOUR OF BEAM ON ELASTIC FOUNDATION	55
	APPENDIX D1 – CONVERGENCE FOR CREEP	59

APPENDIX D2 – COMPUTATIONS FOR MODULUS OF ELASTICITY	60
APPENDIX D3 – PROCEDURE FOR TESTING OF LVL	63
APPENDIX D4 – EXPECTED PLATE DEFLECTIONS	65
APPENDIX D5 – RESULTS FROM PLATE BEHAVIOUR TEST	69
APPENDIX E1 – RESULTS FROM PARAMETER STUDY	89

Preface

In this study, experimental and numerical investigations of stress laminated timber bridges were performed. This was done by analysing downscaled tests on LVL-plates, brand “Kerto-Q” and a full scale test performed by SP Trätek. The results were compared to different hand calculation methods and the theory of a beam on elastic foundation. The theory was also used to investigate if a failure mechanism could be predicted in a SLTD. The thesis was carried out from March 2009 to November the same year. The work is a part of the research project “Competitive timber bridges”, and it was carried out at the Division of Structural Engineering, Steel and Timber Structures, Chalmers University of Technology. The research project is financed as a part of VINNOVA’s trade research programme with the two timber bridge manufactures, Moelven Töreboda AB and Martinsons Träbroar AB as the main financiers. The tested LVL plates in this study came from Moelven Töreboda AB and their contribution was highly appreciated.

The project was carried out with PhD-student Kristoffer Karlsson as supervisor and adjunct Professor Roberto Crocetti as examiner. All downscaled tests were carried out in the laboratory of the Division of Structural Engineering at Chalmers University of Technology. Our supervisor Kristoffer Karlsson and our examiner Roberto Crocetti were of great help with planning our test and we would like to thank them for all their help during the whole process with this thesis.

An appreciated thanks to Lars “Lasse” Wahlström for all the help in the laboratory even though he was not part of our tests.

Thanks to Robert Bengtsson and Mikael Widén who could serve as opponent group with a short notice.

We would also like to thank PhD-student Fredrik Öisjöen for his comments, concerning language, when reading our report.

Finally we would like to thank the persons close to us for their support, and especially to have endured us during our work.

Göteborg, November 2009

Emil Andersson

Johan Bergendahl

”Knowledge and timber shouldn't be much used till they are seasoned”

Oliver Wendell Holmes (1809 – 1894)

"If the facts don't fit the theory, change the facts."

Albert Einstein (1879-1955)

Notations

In the notation table, all variables occurring in the report are listed alphabetically.

Roman upper case letters

B	Width of specimen
C_b	Reduction factor for butt joints
D_w	Effective width
E_i	Young's modulus in i-direction
$F_{v,Ed}$	Design shear force
G	In plane shear modulus
I_i	Second moment of inertia in i-direction
L	Effective bridge span
M_i	Bending moment in i-direction
N	Prestressing force
P	Load
R^2	Coefficient of determination
S	Section modulus, Elastic foundation stiffness
SS	Sum of squares
V_i	Shear force in i-direction

Roman lower case letters

a	Deck plate system factor
b	Width of bridge
b_{ef}	Effective width according to Eurocode
b_{lam}	Width of laminate
b_w	Wheel-width
c	Distance between pre-stressing rods
f_{md}	Dimensioning bending resistance
f_{mk}	Characteristic bending resistance
f_{vd}	Dimensioning shear resistance
f_{vk}	Characteristic shear resistance
h	Height of specimen
k	Fictive spring stiffness
k_{ls}	Load distribution factor
k_{sys}	System strength factor
n	Number of loaded laminates, Number of butt-joints
q	Distributed load
t	Thickness of specimen
w	Effective width for "elastic foundation beam"

Greek letters

α	Parameter for torsional stiffness, Unknown values in shape matrix
β	Parameter for choice of transversal shear, Load distribution angle
δ	Deflection
η	Scale factor
θ	Stiffness ratio, Rotation angle
μ	Friction coefficient
σ_i	Stress

σ_f	Minimum level of prestress
$\sigma_{f-initial}$	Initial prestress
σ_{p-min}	Long term stress caused by prestressing force
τ	Shear
χ_{je}	Combined shear and moment utilization ratio

Signs and mathematical symbols

°	Degree
%	Percent
∫	Integral
[]	Matrix/vector parentheses, Unit parenthesis
cos, cosh	Cosine, Hyperbolic cosine
sin, sinh	Sine, Hyperbolic sine
d^i	i^{th} order derivate
∑	Summation
$w(x)$	Deflection as a function of x

Matrix notation letters

a	Deflection vector
c	Arbitrary vector
f	Force vector
B	Shape gradient vector
K	Stiffness matrix
N	Shape function vector

Abbreviations

AASHTO	American Association of State Highway and Transportation Officials
CALFEM	Computer Aided Learning of the Finite Element Method
CEN	Comité Européen de Normalisation
FE	Finite Element
G	Giga-
k	kilo-
l	Length
LVL	Laminated Veneer Lumber
m	Meter
m	milli-
M	Mega-
MOE	Modulus of Elasticity
MTO	Ontario Ministry of Transportation
N	Newton
OHBD	Ontario Highway Bridge Design Code
SLS	Serviceability Limit State
SLTD	Stress-Laminated Timber Deck
SP	Sveriges Tekniska Forskningsinstitut (Swedish Institute for Technical Research)
ULS	Ultimate Limit State

1 Introduction

1.1 Background

The environmental consciousness among the population is constantly increasing, along with the need for a more sustainable building industry. For countries that can produce their own timber, bridges that utilise much of this material has definitely a smaller environmental footprint compared to concrete and steel. A commonly used timber bridge type is the Stress Laminated Timber Deck (SLTD). The SLTD is constructed of wooden laminates that are placed next to each other and stressed together by steel rods, leading to a plate-wise behaviour instead of a beam-like behaviour.

1.1.1 Historical background

The idea of reinforced timber deck bridges was first developed in Ontario, Canada during the 1970's. Many of the existing nail-laminated timber bridges in the area were heavily loaded due to intensified traffic load, leading to partition of the nailed laminates. The loss of force between the laminates caused fractures and separation in the asphalt layer, making the bridge more vulnerable to external loading. To temporarily solve the problem, engineers at Ontario Ministry of Transportation (MTO) used a pre-stressing technique that already had been tested in other applications of civil engineering. Steel rods together with anchor plates were mounted on both sides of the bridge deck and compressed together with pre-stressing rods, *Figure 1.1.*

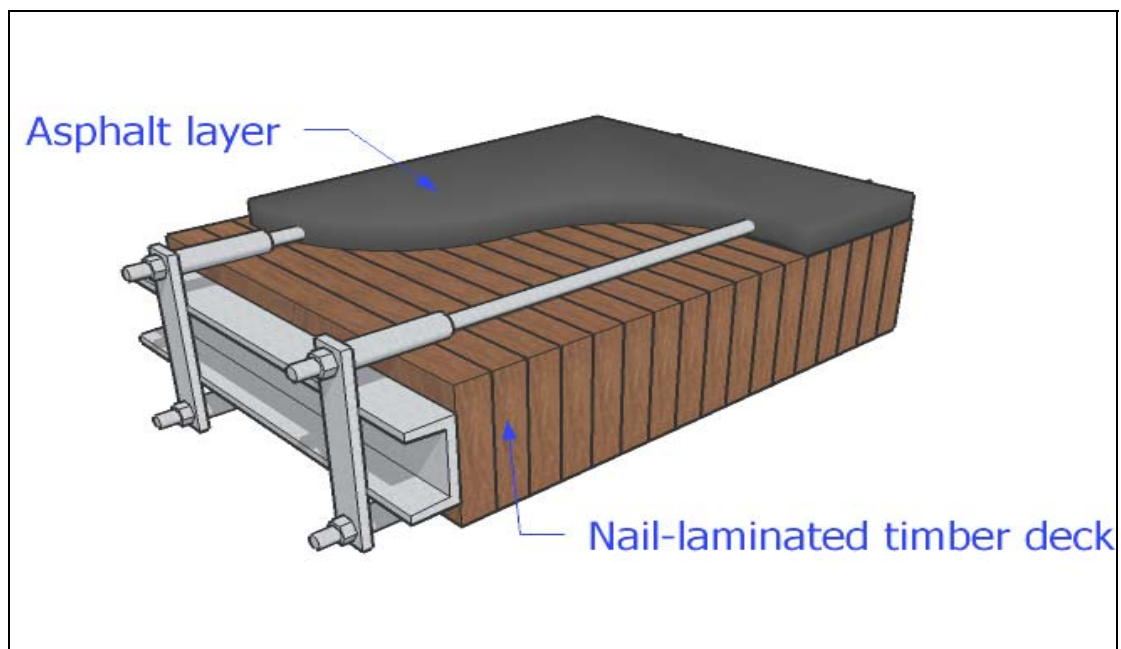


Figure 1.1 Parts for pre-stressing mounted on nail-laminated bridge, thus increasing the capacity of the structure.

Tests performed after the mounting showed that the pre-stressing equipment not only recovered the original capacity of the bridge, but also increased it. To develop the method, MTO initiated cooperation with the Queen's University in Ontario.

The studies conducted at the University included tests of small stress laminated decks in laboratory and the results from these studies showed that the pre-stressed plate had orthotropic behaviour, i.e. different stiffness properties in the directions perpendicular and parallel to the grain. The studies also showed that the stiffness perpendicular to the grain, called the transverse stiffness, could be expressed as a constant fraction of the stiffness parallel to the grain, called longitudinal stiffness. In 1979, the first design procedure for stress laminated timber (SLT) decks was proposed and implemented in the Ontario Highway Bridge Design Code (OHBDC), Ritter (1990).

1.1.2 Manufacturing process

The design of stress laminated timber bridges built today differs from the original design used in Canada. Bridges in Sweden are often made with glulam beams which are pressed together with high-strength steel, thereby creating a lamination effect between the glulam, see *Figure 1.2*.

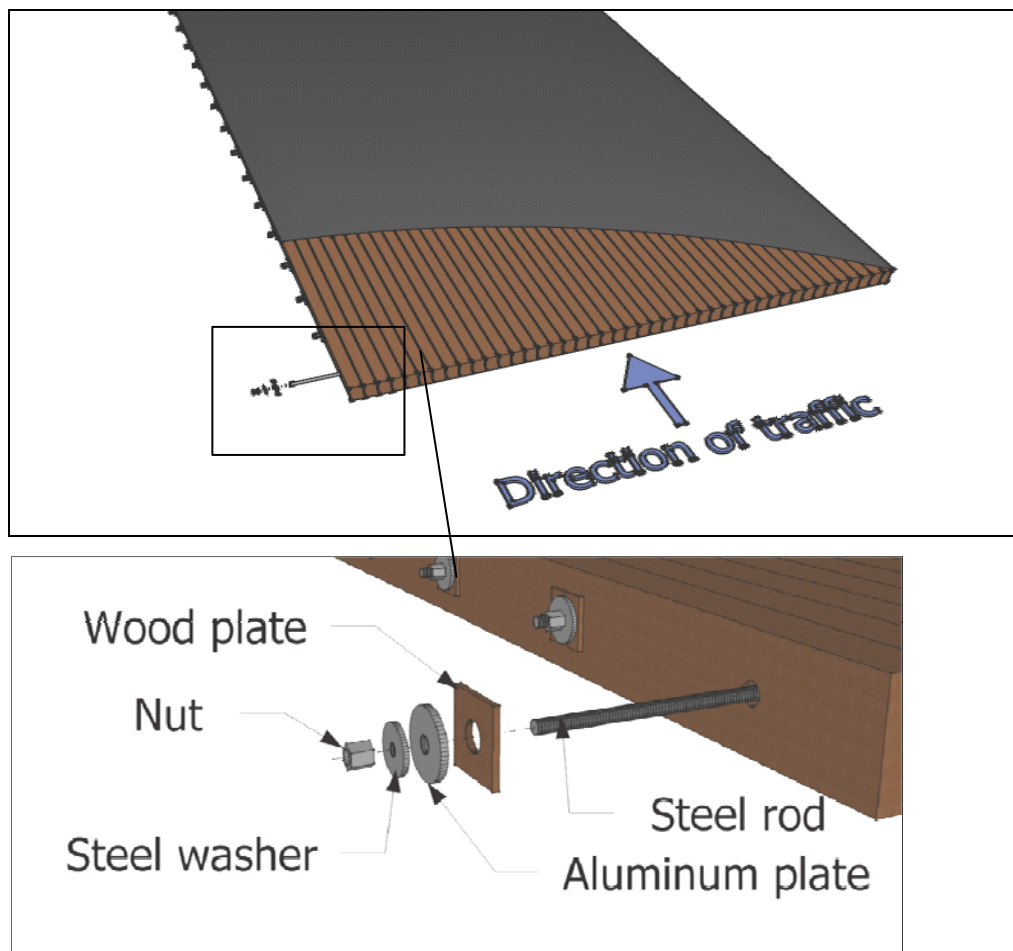


Figure 1.2 Details on a stress laminated timber bridge.

Usually the bridges are assembled in a factory; this is common for smaller bridges. Due to restriction of transportation width, larger bridges have to be assembled on the site of construction. The on-site assembly can be done in two ways, either by assembling the structure directly on its final resting ground, or assemble it next to the construction site, whereby the structure is lifted into its final position. The latter is a convenient method if there is a demand for little disturbance of the existing traffic.

No glue is used between the laminates and one of the reasons for this is due to the high cost. In addition some of the bridges are assembled on site, and the Swedish regulations prohibit load carrying structures to be glued outside of a factory environment, Crocetti (2009).

On modern stress laminated timber bridges, pre-stressing rods are integrated in the bridge body either in one or two layers. The pre-stressing force is transferred from the steel-rods to the timber with a nut and different plates. Upon assembly, the rods are stepwise stressed at different time intervals, thus allowing the creep effect in the wood to occur in a controlled way. After assembly on-site the bridge usually has a re-stressing plan that prescribes re-stressing of the rods in a 10-20 years cycle.

The pre-stressing force introduces a concentrated compressive stress perpendicular to the grain. This stress may cause a ductile failure which reduces the pre-stressing force, and as a consequence of this the overall performance of the deck is reduced. One way of treating this problem is to reinforce the deck at the anchor region by using full-threaded screws as reinforcement. With reinforcement of compression perpendicular to the grain the anchor capacity can be increased as much as 80%. Another advantage of reinforcement with screws is that the loss of pre-stressing force over time is reduced, Formolo and Granström (2007).

1.1.3 Mechanical behaviour

The most important attribute of the stress laminated timber deck is its pre-stressing system. It enables the laminates to act as a solid timber deck with orthotropic behaviour, allowing greater distribution of loads, and leading to smaller deflections, see *Figure 1.3*. The orthotropic behaviour is realised through the compression-friction connection between the laminates, created by the pre-stressed force in the steel rods.

By failure in SLS, the deck changes its properties but can still carry load. There are two major ways that the deck can fail in serviceability limit state, SLS. Firstly the shear force created by a vehicle may overcome the friction effect created by the pre-stressing system, leading to a slip between the laminates, see *Figure 1.4 A*. Secondly the vehicle may create a bending moment in the plate, thereby inducing a delaminating effect, *Figure 1.4 B*. The forces created in these failure modes have to be overcome by the pre-stressing system.

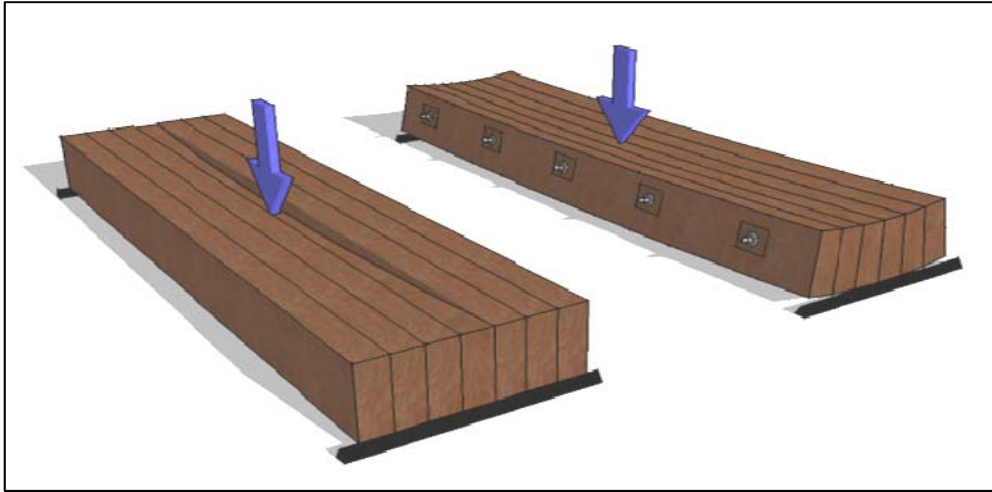


Figure 1.3 Load behaviour in simply supported beams, with no prestress (left) and with prestressing (right.).

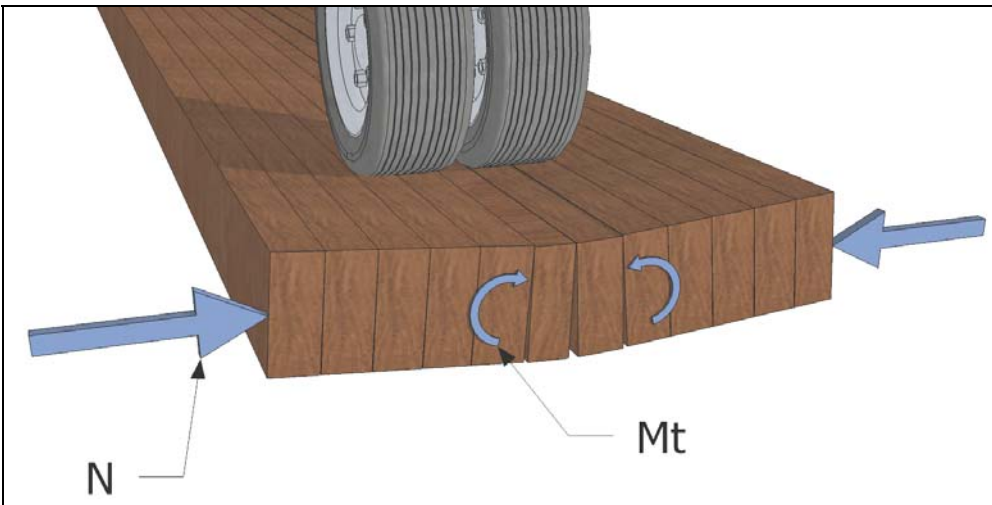
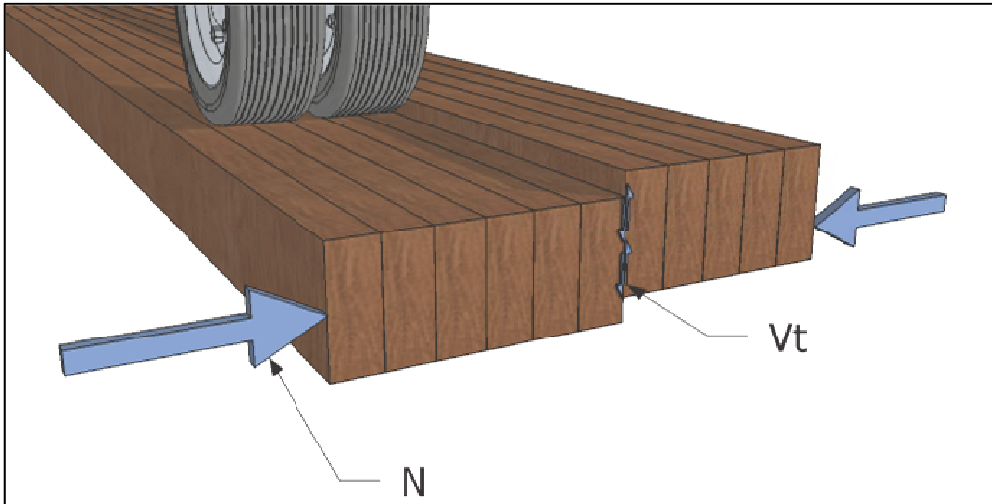


Figure 1.4 A) Top – Shear failure
B) Bottom – Moment failure

The governing equation for the failure modes is (with notations as in *Figure 1.4*):

$$N = \max \left(\frac{1.5 \cdot V_t}{t \cdot \mu}, \frac{6 \cdot M_t}{t^2} \right) \quad [\text{Nmm}^{-2}] \quad (1.1)$$

where:

N	Pre-stressing force in SLS
V_t	Transversal shear force
t	Thickness of the plate
μ	Friction coefficient between the laminates
M_t	Transversal bending moment

1.2 Aim of the thesis

The aim of this thesis is to investigate different hand calculation methods that are used for design of SLTD and to compare which one has the best deflection approximation for edge-load. Moreover, a study of the uplift-behaviour at supports when a SLTD is loaded in mid-span is shown. Continuing, it was also decided to check the hypothesis that deflection in a SLTD can be approximated using the theory of beam on elastic foundation. And finally, the last aim is to investigate a possible failure mechanism for a SLTD.

1.3 Method and objectives

Deflections from the different hand calculation methods were compared with results from a full scale test, hereby denoted as the SP test, and downscaled tests performed at Chalmers. The test data was also used to analyse the uplift behaviour for orthotropic plates.

The theory of beam on elastic foundation was investigated numerically together with the experiment test results to find out how good the deflection approximations were. These were all studied in MATLAB, especially using the toolbox CALFEM.

For the failure mechanism, values obtained from the elastic foundation theory were used together with the failure equation presented in Chapter 1, Section 1.1.3.

1.4 Limitations

Due to the range of each hand calculation method, the authors had to limit the extent to what was found of interest for the thesis. The studied hand calculation methods were chosen with respect to the amount of available literature.

The FE model was only validated using edge-loads on simply supported one-span plates, mainly due to the amount of input data that was available for this load-case.

1.5 Outline

To get a better overview of the thesis, a short description of the chapters is presented here. The outline follows the order of how the thesis work has been carried out.

1. **Introduction:** The feature of the thesis is present. Background information together with aims and facts about the implementations of the aims is presented.
2. **SP Test:** Information and relevant data from a full scale test performed by SP Trätekt is presented.
3. **Hand Calculation Methods:** The different hand calculation methods that are studied in this thesis are presented.
4. **Beam on Elastic Foundation:** A presentation of the FE-implementation to the elastic foundation theory is presented and analysed. It also contains a calculation methodology together with a convergence study.
5. **Downscaled Tests:** Experiments performed on LVL plates was carried out at Chalmers. These plates represented a downscaled SLTD and test procedures together with results from the test are presented.
6. **Evaluation:** The different hand-calculation methods, the elastic foundation theory and the failure load that have been studied in this thesis are evaluated. The evaluation is based on data from the SP test and the downscaled tests.
7. **Discussion:** Discussion and conclusions are presented together with recommendations for further research.
8. **References:** A summary of the literature used in the thesis are listed in alphabetic order.
9. **Appendices:** The major results from the tests and calculations are presented.

2 SP Test

2.1 Background

In August 2008, SP Trätekt performed a full scale test of an SLTD bridge on behalf of Martinsons Träbroar AB. The test was performed to check the deck strength when loaded with a concentrated force placed on the longitudinal edge, see *Picture 2.1*, SP Trätekt (2008). The intent of the test was also to test the strength when loaded in the centre of the deck, but since the deck failed at the edge-test, this was not possible.



Picture 2.1 Test of full scale bridge. Force plate mounted at edge in mid-span, top-centre of picture (Courtesy of Martinsons Träbroar).

2.2 Test

The tested bridge had the dimensions 10600 x 5350 x 495 mm (l x w x h) and the deck was simply supported with a free span of 10 m. To measure the deflection of the deck, eleven measurement devices were placed on the deck, three at each support and five in the middle of the span. The deck was loaded cyclically with five loadings for each increase of applied load between 100 kN up to 500 kN. When the applied load got close to 600 kN a failure in the deck appeared, SP Trätekt (2008). For the measured deflections with applied load around 100 kN, 20 data points were given in five different measure-points. The data from the measure-point that gave the largest deflections are presented as the darker points in *Figure 2.1*.

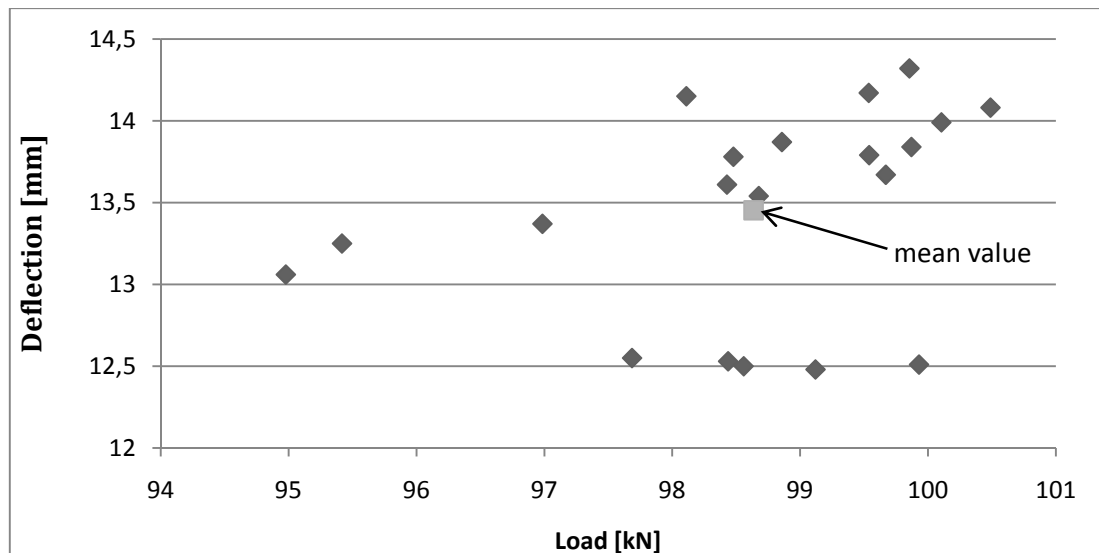


Figure 2.1 Measured deflections from different load series. The darker points are the measured deflections for different load series and the lighter point is the one used in the analysis.

The value that was chosen to be analysed is the value of the brighter point, which is a mean value from both the applied load and measured deflection. Data was also given for higher loads and the analysis procedure was done for applied loads around 200 and 300 kN. These results are presented in *Appendix A1* together with the data from the other measure-points that were chosen to be analysed.

2.3 Results from test

The analysis of the test data showed that the point load caused an upwards deflection on the unloaded side, leading to a twist-like behaviour. This positive deflection was also measurable at the supports, leading to a smaller load-carrying area, thus leading to higher concentrated stresses, SP Tråtek (2008). However, this was neglected. Dimensions and parameters of the deck are presented in *Appendix A2*.

3 Hand Calculation Methods

When designing a SLTD there are different hand calculation methods that can be used. Which method that is used partly depends on where in the world the bridge should be built, due to the fact that different countries have different regulations which the methods take into account. A common calculation method, which has been the most commonly used in Sweden, is Ritter's design guide. This method was developed by Michael A. Ritter in 1990. In addition to Ritter's design guide, EC5 also proposes a design method for SLTD. Another method that is commonly used, mostly in Australia, was developed by Keith Crews in 2002, while the West Virginia University method was developed in USA in 1993, Dahl (2002). All the methods that are studied in this thesis are simplified analyses where the deck is designed as a fictive beam, see *Figure 3.1*. The difference in the above mentioned methods is how to find the effective width, D_w , of the fictive beam. However, Eurocode uses the notation b_{ef} for the effective width. Hereby follows a summary of the different models, where special attention has been put on the differences in the effective width.

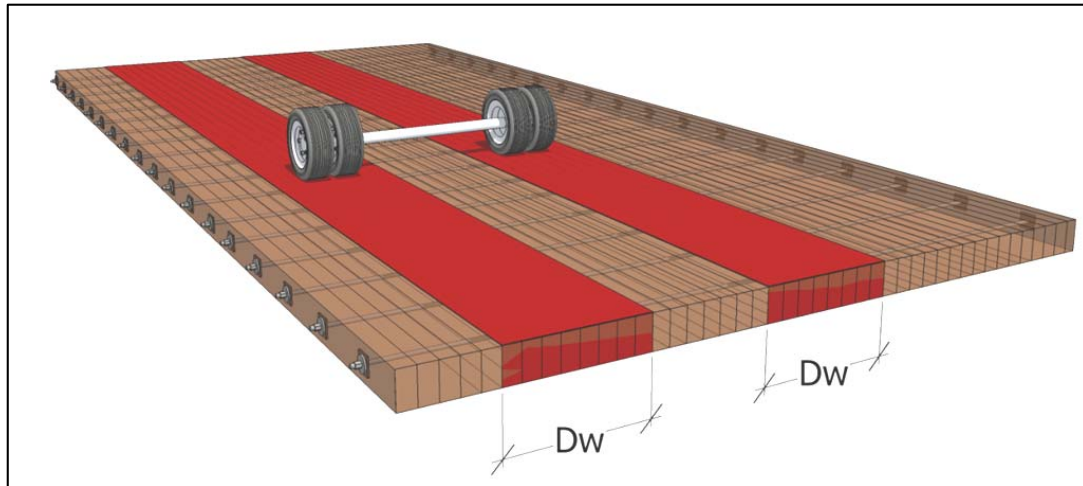


Figure 3.1 Effective width visualized.

3.1 Ritters design guide

In the 1990 Michael A. Ritter presented his design guide for SLTD. When designing according to Ritters guide there are some general design criterion that you have to fulfil, Ritter (1990).

- The deck should be constructed from sawn lumber laminations and have the typical design of a SLTD
- The deck width is constant
- The deck thickness is constant and not less than 178 mm (8 inches)
- The deck is rectangular in plane, or skewed by less than 20°
- All supports should be continuous across the deck width

- The presence of butt joints should be limited to a maximum of one joint for any four adjacent laminations within a distance of 1220 mm (4 feet) in the longitudinal direction

Design loads are based on AASHTO¹ loading requirements. For timber bridges it is allowed to increase the design stresses by 33% for overloads. In addition to this you calculate with load distribution factor k_{ls} that increase the bending stiffness with 30% or 50% depending on lumber grade. These values come from the lumbers possibility to redistribute from weak lamellas to stronger. The calculation model has been verified for quality graded timber from Douglas Fir-Larch, Hem-Fir, Red Pine and Eastern White Pine, Ritter (1990).

AASHTO does not specify any demand regarding live load deflection. Instead it is up to the engineer to put up reasonable demands for every single bridge, based on specific design circumstances. However, Ritter highly recommends that the designer follows the guide lines, regarding maximum deflection, given for other timber bridges, Ritter (1990).

Designing a SLTD according to Ritter is basically done in two parts. The first part is designing the deck for bending, shear and deflection as if it was a beam. The second part in the design procedure is designing the pre-stressing system. Both design procedures use graphs that are based on variable relationships developed by analytic modelling, verified by tests performed by M. Ritter, Ritter (1990).

The design procedure that follows is a shortening from Ritter's design procedure:

1. Define the deck geometry and design loads. The geometry concerns bridge span, width and number of traffic lanes. The effective bridge span L is defined as the distance between centre to centre of two supports. Both the span length, L , and the width, b , is given in millimetre.
2. Choose of timber class. This gives the designer the maximum allowable value for the bending moment f_{mk} and E-modulus is thereby known.
3. Preliminary design of butt joints. The presence of butt joints creates discontinuity in the deck. To compensate for this the reduction factor C_B is used. C_B is involved in different deck properties such as the effective deck section modulus, S , and the effective deck moment of inertia, I .
4. Compute values for the transverse bending modulus of elasticity, E_{90} , and the in-plane shear modulus, G . In Ritter's design guide the following two expressions are given to compute E_{90} and G :

$$E_{90} = 0,013 * E_0 \quad [\text{Nmm}^{-2}] \quad (3.1)$$

$$G = 0,03 * E_0 \quad [\text{Nmm}^{-2}] \quad (3.2)$$

¹ American Association of State Highway and Transportation Officials

It should be taken into account that the expressions are only valid for the Douglas Fir-Larch, Hem Fir, Red Pine and Eastern White Pine.

5. The maximum moment M_0 from live load caused by one wheel line of the design vehicle is found from beam analysis. If the deck is continuous over several supports the deck is calculated as continuous beams.
6. Determine wheel load distribution width, D_w , from diagram produced by Ritter, see *Figure 3.2*. SLTD are designed as beams and D_w is then the effective width of that fictive beam. D_w is dependent on the two parameters α and θ which are computed as:

$$\alpha = \frac{2 \cdot G}{\sqrt{E_0 \cdot C_B \cdot E_{90}}} \quad [-] \quad (3.3)$$

$$\theta = \frac{b}{2 \cdot L} * \left[\frac{E_0 \cdot C_B}{E_{90}} \right]^{0,25} \quad [-] \quad (3.4)$$

- where:
- α Parameter for the torsional stiffness of the deck
 - θ Ratio between the deck stiffness in longitudinal and transversal direction
 - C_B Coefficient regarding butt joints
 - E_0, E_{90} E-modulus in longitudinal and transversal direction respectively
 - G In-plane shear modulus of elasticity
 - b, L Dimensions of width and span of the deck

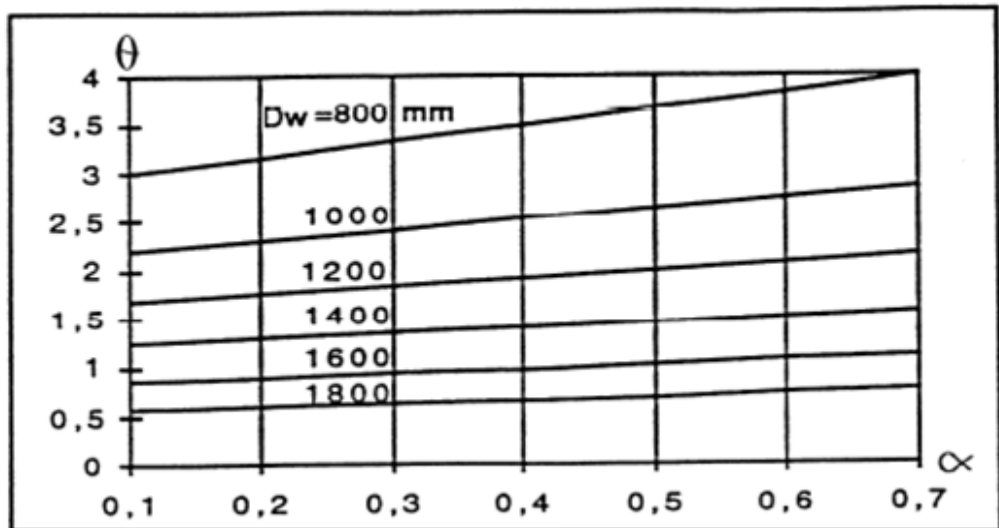


Figure 3.2 Graph used to determine D_w for a single lane bridge, Ritter (1990) and modified by Dahl (2002).

7. Estimate deck thickness and compute deck-section properties. Ritter gives some recommended values for the thickness, t , depending on span length and number of traffic lanes. The thickness is estimated so that the designer is able to compute the effective deck section modulus, S , and the effective deck moment of inertia, I :

$$S = \frac{C_B * D_w * t^2}{6} \quad [\text{mm}^3] \quad (3.5)$$

$$I = \frac{C_B * D_w * t^3}{12} \quad [\text{mm}^4] \quad (3.6)$$

where: t Deck thickness

8. Compute the design bending moment, M_γ , acting on the deck by adding the bending moment due to dead weight, M_g , to the bending moment due to live load, M_0 .
9. Compute maximum bending stresses in the deck by dividing the design moment by S , the effective deck sectional modulus, Ritter (1990).

$$\sigma_\gamma = \frac{M_\gamma}{S} \leq f_{md} * k_{ls} \quad [\text{Nmm}^{-2}] \quad (3.7)$$

where: k_{ls} Load distribution factor

10. Live load deflection is computed according to elastic analysis of a beam. Since the orthotropic behaviour of the deck results in a wider distribution width for deflection than for bending, the effective deck moment of inertia, I , could be increased by 33% for the design in Serviceability Limit State (SLS). AASHTO does not give any guidelines for maximum deflection but Ritter recommend that for a SLTD with asphalt layer should be limited to $L/360$.
11. To avoid sagging caused by dead load deflection the deck should be cambered at least 2 times, and preferably 3 times, the amount of dead load deflection.
12. The level of prestress for SLTD must be determined for two conditions, in service and at installation. The amount of prestress in service state represents the minimum compressive prestress level for adequate performance. At installation the level of prestress is the amount that needs to be introduced to the deck at time of prestressing, to be able meet the demand in service state.

The amount of prestress depends on the size of transverse bending moment and transverse shear from applied load. Values for both transverse bending moment, M_{90} , and transverse shear, V_{90} , are found in *Figure 3.3*. For M_{90} values α and θ are used and for the transverse shear, β is used.

$$\beta = \pi * \left(\frac{b}{L}\right) * \sqrt{\frac{E_0 * C_B}{2 * G_0}} \quad [-] \quad (3.8)$$

Both diagrams are developed for a wheel load of 71 kN. When other loads are used, the designer should multiply this load with the load ratio. Minimum

level of prestress, σ_f , is found as the maximum of *Equation 3.9 and Equation 3.10*, but not less than 0.276 Nmm^{-2} , Ritter (1990):

$$\sigma_f \geq \frac{6 \cdot M_{90}}{t^2} \quad [\text{Nmm}^{-2}] \quad (3.9)$$

$$\sigma_f \geq \frac{3}{2} * \frac{V_{90}}{t * \mu} \quad [\text{Nmm}^{-2}] \quad (3.10)$$

where:

- σ_f Minimum prestressing-force
- t Deck thickness
- M_{90} Magnitude of transverse bending moment per unit length
- V_{90} Magnitude of transverse shear force per unit length
- μ Friction coefficient (0,35 for surfaced, 0,45 for rough-sawn or surfaced on one side)

Because of the loss of prestressing-force over time, the initial prestressing, $\sigma_{f-initial}$, should be 150% larger than the computed prestressing-force.

$$\sigma_{f-initial} = 2,5 * \sigma_f \quad [\text{Nmm}^{-2}] \quad (3.11)$$

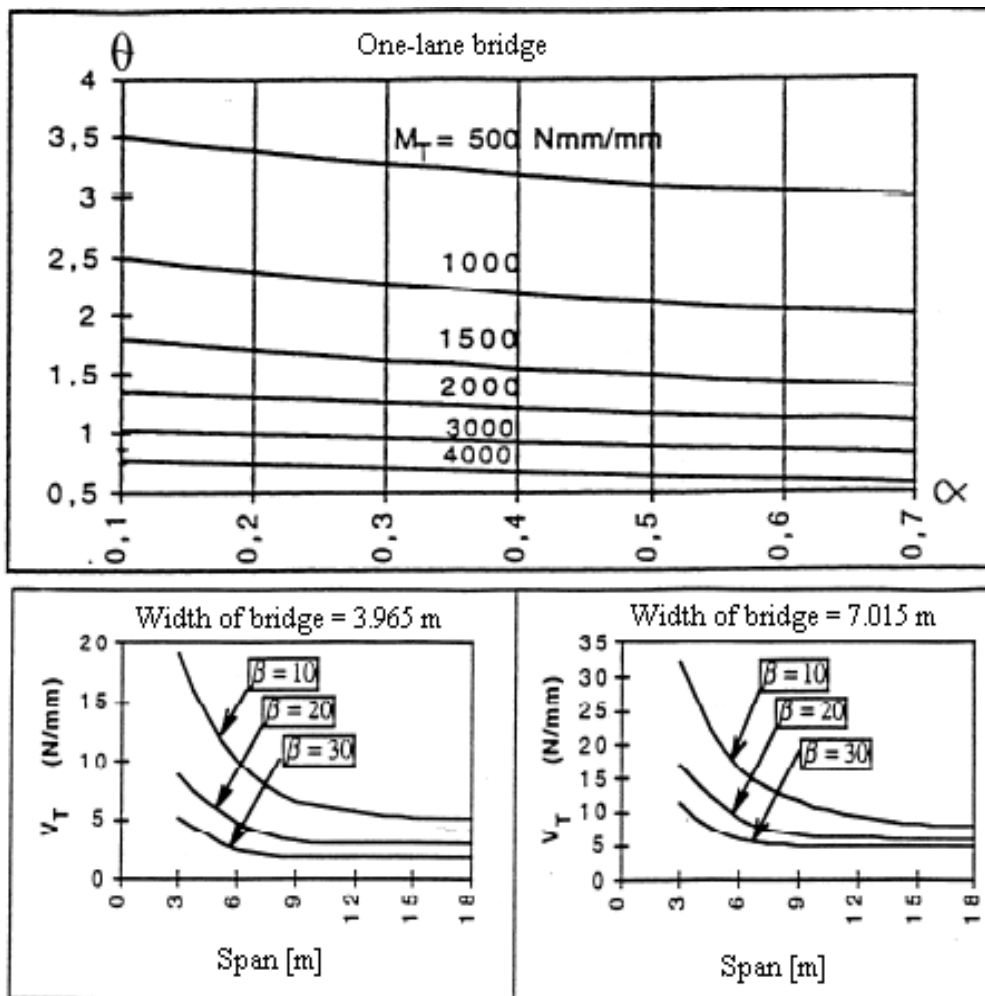


Figure 3.3 Graphs used to determine $M_T (M_{90})$ and $V_T (V_{90})$, Ritter (1990) and modified by Dahl (2002).

3.2 Eurocode 5

The general recommendations in Eurocode² when designing SLTD is to use one of the following three analysis methods:

- Orthotropic plate theory
- Grid-modelling of the deck
- A simplified method suggested in Eurocode

In the analysis, it was chosen to use the simplified method, since the analysis procedure have some similarities to Ritter's design guide. The greatest similarity between the two methods is that both use a fictional width, given in Eurocode as b_{ef} (compare to Ritters width D_w). The use of the fictional width allows the load to distribute to the middle plane of the deck, thus making the stresses smaller and thereby allowing smaller dimensions on the bridge. To obtain b_{ef} , the following equations are used:

$$b_{w,middle} = b_w + h/2 * \sin(\beta) \quad [m] \quad (3.12)$$

$$b_{ef} = b_{w,middle} + a \quad [m] \quad (3.13)$$

The notations used are visualized in *Figure 3.4*. The load distribution angle, β , is a material constant whose values differ according to *Table 3.1*. The constant a is dependent on what deck plate system that is used, see *Table 3.2*, Eurocode (2004).

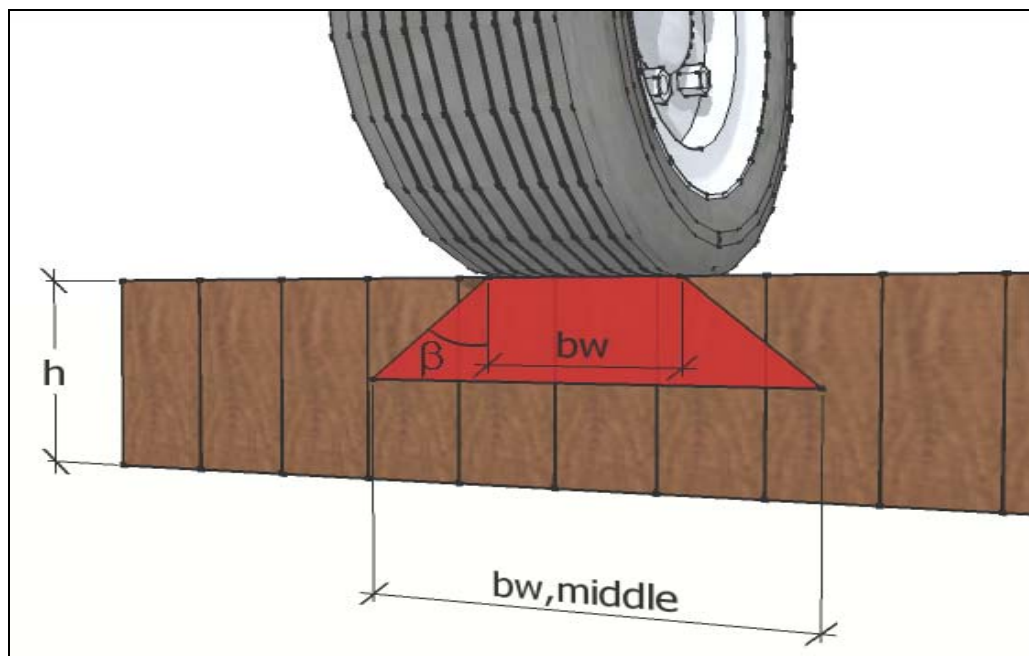


Figure 3.4 Load distribution under a contact surface with the width b_w .

² Eurocode 1995-2: 2004, hereby referred to as "Eurocode (2004)" or "Eurocode"

Table 3.1 Dispersion angle, β , for various materials.

Materials used on bridge	Dispersion angle β
Pavement	45°
Laminated timber deck bridges	
- In direction of the grain	45°
- Perpendicular to the grain	15°

Table 3.2 Width, a , for various deck plate systems.

Deck plate system	a [m]
Nail laminated deck plate	0.1
Stress-laminated or glue laminated	0.2
Cross-laminated timber	0.5

The effective width, b_{ef} is then used as a width of an equivalent beam, allowing the design of the glulam used in the SLTD.

To verify the design, checks on bending moment and shear forces in the fictive beam needs to be preformed according to following:

$$f_{m,d,deck} = k_{sys} * f_{m,d,lam} \quad [\text{Nmm}^{-2}] \quad (3.14)$$

$$f_{v,d,deck} = k_{sys} * f_{v,d,lam} \quad [\text{Nmm}^{-2}] \quad (3.15)$$

where: $f_{m,d,lam}$ Bending strength of the lamination material
 $f_{v,d,lam}$ Shear strength of the lamination material
 k_{sys} System strength factor as can be read from *Figure 3.5*

To calculate number of loaded laminations, the following equations are suggested, Eurocode (2004):

$$n = \frac{b_{ef}}{b_{lam}} \quad [-] \quad (3.16)$$

where: b_{lam} Width of the lamination material

The deck strengths are then checked against the design moments and shear.

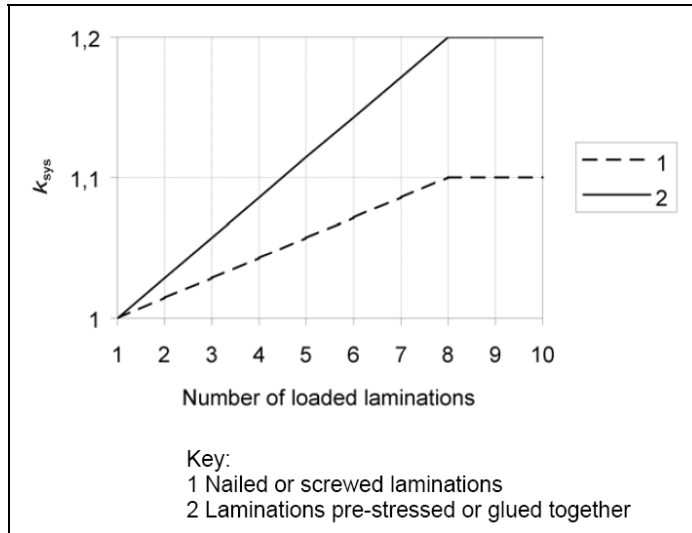


Figure 3.5 The system strength factor k_{sys} and its dependence of loaded laminations, Eurocode 1995-1-1:2004, clause 6.6.

To avoid laminar slip, Eurocode also recommends that the following requirement is fulfilled:

$$F_{v,Ed} \leq \mu_d * \sigma_{p,min} * h \quad [\text{Nmm}^{-1}] \quad (3.17)$$

where:

$F_{v,Ed}$	Design shear force per unit length
μ_d	Design friction coefficient
$\sigma_{p,min}$	Long-term stress caused by the prestressing force
h	Height of deck

Eurocode recommends that the long term residual stress $\sigma_{p,min}$ should be greater than 0.35 Nmm^{-2} , provided that the initial pre-stress is at least 1.0 Nmm^{-2} , Eurocode (2004).

3.3 Crews design guide

Designing a SLTD deck according to Crews model is to design the deck with equivalent beam analysis. The beam can be either simply supported or continuous over several spans, depending on support conditions. To be able to design the deck as a beam the designer needs to find the effective width of the fictive beam. This effective width, D_w , varies depending on whether the designer would like to compute deflections (SLS) or longitudinal flexural capacity (ULS) for the deck. The equivalent beam is the part of the orthotropic deck that is supposed to carry the load, Crews (2002).

In comparison with Ritter, Crews model is a bit more straightforward. This is since the only material parameter involved in the computation of the effective width is E_ρ .

The transverse modulus of elasticity E_{90} and the in-plane shear modulus G are already included in the model.

Distribution width, D_w , for a single lane bridge and a two lane bridge respectively is calculated as:

$$D_w = \left[\left(\frac{E_0}{10\,000} \right)^{0,5} + \frac{L}{25} + 0,45 \right] * C_B \quad [\text{m}] \quad (3.18)$$

$$D_w = \left[\left(\frac{E_0}{18\,000} \right)^{0,40} + \frac{L}{30} + 0,45 \right] * C_B \quad [\text{m}] \quad (3.19)$$

where: E_0 Longitudinal modulus of elasticity

L Effective design span

C_B Butt joint modification factor

$$C_B = \frac{\left(\frac{n-1}{n} \right)}{0,75} \geq 1,0 \quad \text{For hardwood} \quad [-] \quad (3.20)$$

$$C_B = \frac{\left(\frac{n-1}{n} \right)^{0,5}}{0,85} \geq 1,0 \quad \text{For Australian pine} \quad [-] \quad (3.21)$$

where: n Number of butt joints transverse the deck in the range of 1200 mm in longitudinal direction.

These expressions are based on a prestress of 1.0 Nmm^{-2} which is the assumed serviceability prestress in Australia. The recommended initial pre-stressing forces in Australia are 1.2 to 1.5 Nmm^{-2} for hardwood and 1.0 to 1.3 Nmm^{-2} for softwood, Crews (2002).

From this part, the design of bending moment and shear force is done in the same manner as according to the method proposed by Ritter and is therefore not presented, Crews (2002).

3.4 West Virginia University method

Like Ritter and Crews the University of West Virginia has developed a design procedure for stress-laminated timber decks. The design procedure in many ways corresponds to Ritter's design guide which is described in Chapter 3.1. The most obvious differences are described below, Dahl (2002):

$$D_w = [b_w + 2 * t] * C_B \quad [\text{mm}] \quad (3.22)$$

where: b_w Total wheel width

t Thickness of the cross-section

C_B Butt joint factor as described by Crews in Chapter 3.3

The method assumes a 45° distribution over the whole cross-section in transverse direction. For deflection caused by a concentrated force the designer can assume an increase in load distribution by 15%. So when designing against deflection it is possible to use $1,15 * D_w$ as distribution width, Dahl (2002).

For a single line bridge the maximum moment and shear force, per unit length, in transverse direction is calculated as:

$$M_{90} = \frac{1,54 * M_0}{1000 * C_B^{1/4}} * \frac{b_w}{2 * L} \quad [\text{Nmm/mm}] \quad (3.23)$$

$$V_{90} = \frac{P_w}{1000} * \left(10,4 - \frac{b_w}{2 * L} \right) \quad [\text{Nmm}^{-1}] \quad (3.24)$$

where: M_0 Moment in longitudinal direction caused by a single wheel set
 L Span width
 P_w Maximum load from one wheel

Like Crews the calculations from this point follows Ritter and are therefore not presented, Dahl (2002).

3.5 Summary of hand calculation methods

As described in the introduction to Chapter 3 one of the biggest differences between the methods is how to achieve the effective width. This effective width affects the calculated deflections to a great extent. For the SP test described in Chapter 2, calculations for the deflections were computed for every method described in this thesis and these calculations are presented in *Appendix B1-B4* respectively.

4 Beam on Elastic Foundation

An approach when designing a SLTD could be to approximate the deflection of the cross-section in a section of the plate according to the theory of beam on elastic foundation, Marklund K.A. (1997). Having a simple method of approximating the deflection behaviour could make the design process faster and easier. This would also mean that it would be possible to determine internal forces without using a plate-theory. The cross-section would in this case be assumed as a beam which should have the length l_{beam} and an effective width, w , see *Figure 4.1*.

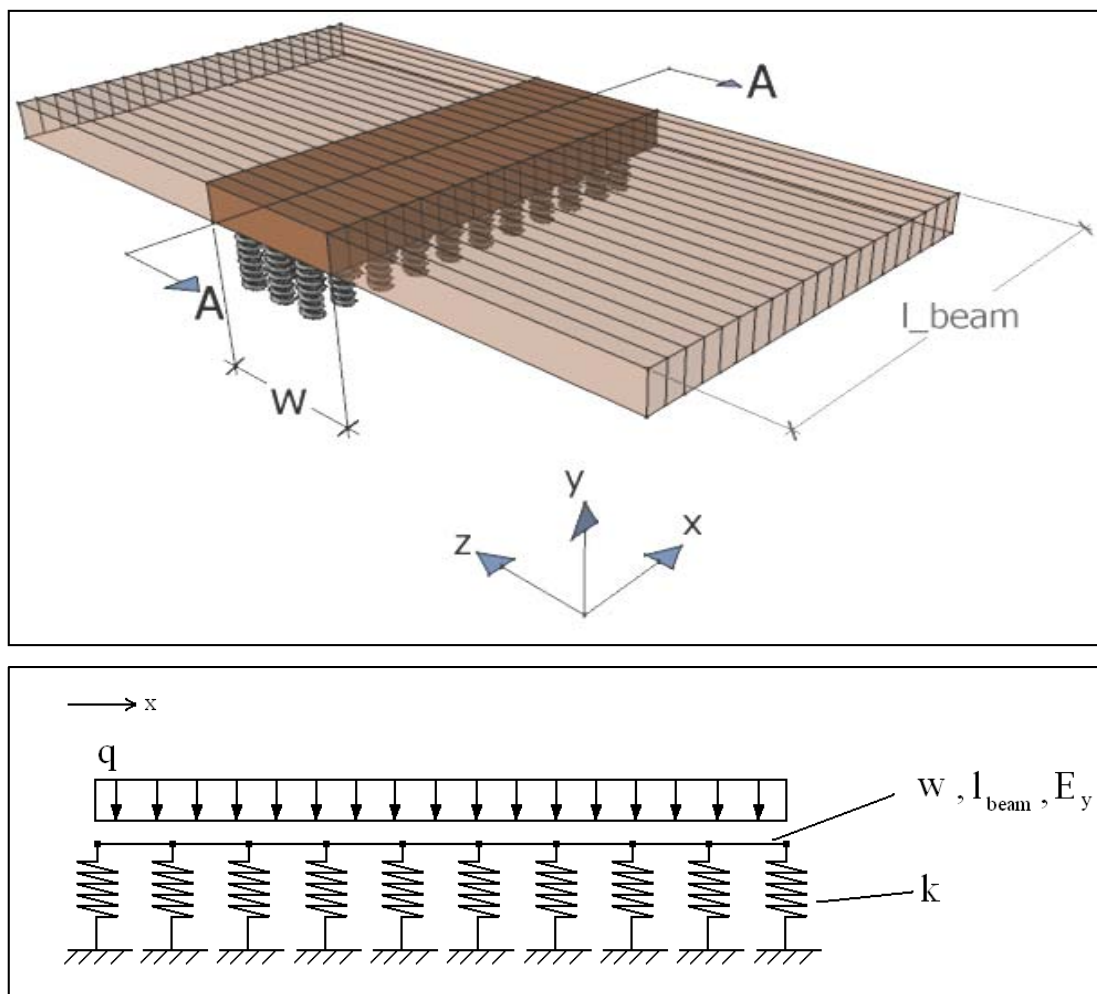


Figure 4.1 Top) Section of SLT deck that acts as the imagined beam on elastic foundation

Bottom) Schematic figure of section A-A from top figure

4.1 Theory

4.1.1 Guiding differential equation

The elastic foundation theory is often used in civil engineering applications such as plates and beams on soil where the structure of the soil can be modelled as a foundation of elastic springs. For the case of a beam on elastic foundation, the following differential equation for deflection, y , is used, Bing Y.Ting et al (1983):

$$EI * \frac{d^4 y}{dx^4} + k * y = q \quad (4.1)$$

where: k Modulus of sub grade reaction
 EI The beams flexural rigidity
 q The transversal load acting on the beam.

4.1.2 Finite element formulation

To be able to compare the theory of elastic foundation to the measured deflections from the SP-test, a FE-model was established. The derivation of the FE-expression was made without any consideration of axial forces and assuming that the beam rests on Winkler foundation, i.e. a foundation that has a linear relationship between the force on the foundation and the deflection. As a first step, *Equation 4.1* was multiplied with a weight function, $v(x)$, and integrated over the domain as suggested in Ottosen & Petersson (1993), leading to the following expression:

$$\int_a^b v \frac{d^2 M}{dx^2} dx - \int_a^b k y dx + \int_a^b v q dx = 0 \quad (4.2)$$

Integration by parts of the first expression in *Equation 4.2* and using that $dM/dx = V$, we obtain:

$$\int_a^b \frac{dv}{dx} \frac{dM}{dx} M dx = [vV]_a^b - \int_a^b k y dx + \int_a^b v q dx \quad (4.3)$$

By integrating the left hand side, the following expression is defined:

$$\int_a^b \frac{d^2 v}{dx^2} M dx + \int_a^b k y dx = \left[\frac{dv}{dx} M \right]_a^b - [vV]_a^b + \int_a^b v q dx \quad (4.4)$$

Where M and V are the natural boundary conditions. The expression obtained is the weak form of the equilibrium equation, and to obtain the strong form the following approximation for the deflection is introduced:

$$y = \mathbf{N} \mathbf{a} \quad (4.5)$$

where:

$$\mathbf{N} = [N_1 \ N_2 \ \dots \ N_n] \quad \mathbf{a} = \begin{bmatrix} u_1 \\ u_2 \\ \vdots \\ u_n \end{bmatrix} \quad (4.6)$$

From *Equation 4.5* it can be shown that:

$$\frac{d^2 y}{dx^2} = \mathbf{B} \mathbf{a}, \text{ where } \mathbf{B} = \frac{d^2 \mathbf{N}}{dx^2} \quad (4.7)$$

The next step is to adopt the Galerkin expression for the weight function:

$$v = \mathbf{N} \mathbf{c} \quad (4.8)$$

This means:

$$\frac{dv}{dx} = \mathbf{c}^T \frac{d\mathbf{N}^T}{dx}; \quad \frac{d^2 v}{dx^2} = \mathbf{c}^T \mathbf{B}^T \quad (4.9)$$

Observing that the weight function is arbitrary and thereby concluding that c also is arbitrary, *Equation 4.4* is rewritten as:

$$\mathbf{c}^T \left(\int_a^b \mathbf{B}^T M dx + \int_a^b \mathbf{N}^T k \mathbf{N} a - \left[\frac{d\mathbf{N}^T}{dx} M \right]_a^b + [\mathbf{N}^T V]_a^b - \int_a^b \mathbf{N}^T q dx \right) = 0 \quad (4.10)$$

The arbitrary property of c makes it possible to back this function out of the equation, and with the constant flexural rigidity we introduce:

$$M = -EI * \mathbf{B} \mathbf{a} \quad (4.11)$$

leading to the final FE formulation defined as:

$$\left(\int_a^b \mathbf{B}^T * EI * \mathbf{B} dx + \int_a^b \mathbf{N}^T k \mathbf{N} dx \right) \mathbf{a} = [\mathbf{N}^T V]_a^b - \left[\frac{d\mathbf{N}^T}{dx} M \right]_a^b + \int_a^b \mathbf{N}^T q dx \quad (4.12)$$

or:

$$(\mathbf{K} + \mathbf{K}_{spring}) \mathbf{a} = \mathbf{f} \quad (4.13)$$

where:

$$\mathbf{K} = \int_a^b \mathbf{B}^T * EI * \mathbf{B} dx \quad (4.14)$$

$$\mathbf{K}_{spring} = \int_a^b \mathbf{N}^T k \mathbf{N} dx \quad (4.15)$$

$$\mathbf{f} = [\mathbf{N}^T V]_a^b - \left[\frac{d\mathbf{N}^T}{dx} M \right]_a^b + \int_a^b \mathbf{N}^T q dx \quad (4.16)$$

4.1.3 Evaluation of the elastic foundation stiffness matrix

In order to solve the FE equation, an approximation of the deflection is required. For infinitely small beam elements, inner deflection will be given by an arbitrary rigid-body motion superposed by an arbitrary constant curvature. This means that the approximation of the deflection must be able to represent both an arbitrary rigid-body motion as well as an arbitrary constant curvature, often referred to as the completeness requirements.

The approximation also has to fulfil the compatibility requirements, i.e. the approximation w must vary continuously and with continuous slopes over the element boundaries.

The following equation is used to approximate the deflection:

$$y = \alpha_1 + \alpha_2 x + \alpha_3 x^2 + \alpha_4 x^3 \quad (4.17)$$

To determine the α -values, the selected beam element must possess four unknown, which are chosen as u_1 , u_2 , u_3 and u_4 , where u_1 and u_3 are the deflection of the nodes in y-direction and u_2 and u_4 are the counter-clockwise slopes in the nodes, as in *Figure 4.2*.

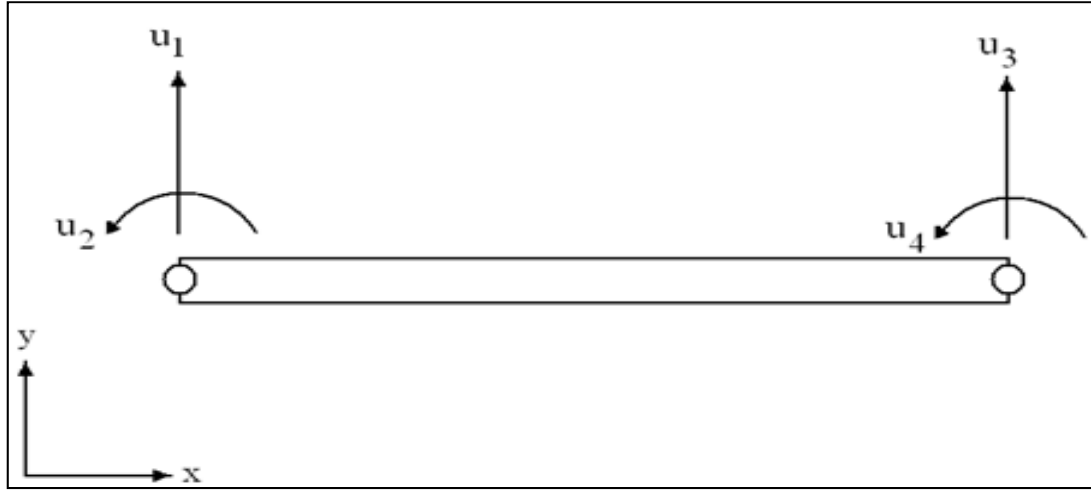


Figure 4.2 Simple beam element and the selected degrees of freedom.

Applying the C-matrix method suggested by Ottosen and Petersson (1993) the element shape functions will be expressed as:

$$\mathbf{N} = [N_1^e \ N_2^e \ N_3^e \ N_4^e] \quad (4.18)$$

where:

$$N_1^e = 1 - 3\frac{x^2}{L^2} + 2\frac{x^3}{L^3} \quad (4.19)$$

$$N_2^e = x \left(1 - 2\frac{x}{L} + \frac{x^2}{L^2}\right) \quad (4.20)$$

$$N_3^e = \frac{x^2}{L^2} \left(3 - 2\frac{x}{L}\right) \quad (4.21)$$

$$N_4^e = \frac{x^2}{L} \left(\frac{x}{L} - 1\right) \quad (4.22)$$

In the first step of developing the foundation stiffness matrix, \mathbf{K}_{spring} , it is assumed that the stiffness properties of the fictive springs do not vary along the beams axis. Thereby it is possible to move the spring stiffness constant, k [Nmm^{-2}], outside of the integral expression. From the element shape functions, the stiffness contribution to the beam from the elastic foundation can together with Equation 4.18 be expressed as:

$$\mathbf{K}_{spring} = \int_a^b \mathbf{N}^T k \mathbf{N} dx = k \int_a^b \mathbf{N}^T \mathbf{N} dx = k \int_a^b \begin{bmatrix} N_1^e N_1^e & N_1^e N_2^e & N_1^e N_3^e & N_1^e N_4^e \\ N_2^e N_1^e & N_2^e N_2^e & N_2^e N_3^e & N_2^e N_4^e \\ N_3^e N_1^e & N_3^e N_2^e & N_3^e N_3^e & N_3^e N_4^e \\ N_4^e N_1^e & N_4^e N_2^e & N_4^e N_3^e & N_4^e N_4^e \end{bmatrix} dx \quad (4.23)$$

After integrating the expression, the elastic foundation stiffness matrix is given by:

$$K_{spring} = \frac{L \cdot k}{420} \begin{bmatrix} 156 & 22L & 54 & -13L \\ 22L & 4L^2 & 13L & -3L^2 \\ 54 & 13L & 156 & -22L \\ -13L & -3L^2 & -22L & 4L^2 \end{bmatrix} \quad (4.24)$$

4.2 Calculation methodology

The FE-calculations, which were performed in MATLAB, were created using the finite element toolbox CALFEM. To find a reliable model that was somewhat consistent with physical relationships, the following steps were performed, in chronological order:

1. The establishment of a MATLAB FE-model, where the deflections of a beam on elastic foundation could be calculated. The CALFEM routine beam2w.m was primarily used.
2. A convergence-study was performed on the model to be able to find a conforming number of elements for the model.
3. The behaviour of the model was then verified by a Swedish handbook for Civil Engineering, BYGG1 (1961).
4. The model was then analysed using only dead-weight where the main purpose was to get a better understanding of how the different parameters controlled the beams deflection behaviour. The self-weight used in the model were chosen from Structural Timber Design to Eurocode 5 (2007).
5. The next step was to introduce a load on the beam, to find out how the beam would react.
6. The MATLAB routine fminsearch.m was then used to vary the effective width w , and the elastic foundation stiffness, k .
7. The routine fminsearch.m was set to try to minimize the changes of the measured deflections and the calculated ones, using the coefficient of determination, R^2 . For the coefficient of determination, f_i were the modelled values and y_i were the observed values. The regression sum of squares was calculated as:

$$SS_{reg} = \sum_i (f_i - \bar{f}_i)^2 \quad (4.25)$$

And the sum of squared errors was calculated as:

$$SS_{err} = \sum_i (y_i - f_i)^2 \quad (4.26)$$

The coefficient of determination was then calculated as:

$$R^2 = \frac{SS_{reg}}{SS_{tot}} = \frac{SS_{reg}}{SS_{err} + SS_{reg}} \quad (4.27)$$

For a good match between calculated deflections and measured ones, the value of R^2 should be close to 1. The routine fminsearch.m was set to minimize the function $1 - R^2$, thus leading to a minimum of deflection difference.

8. After establishing a good FE model with comforting values on the elastic foundation stiffness in SLS, the model was used to try to predict the failure mode. This was done by searching exponents x and y that satisfies:

$$\left(\frac{\tau_E}{\tau_R}\right)^x + \left(\frac{\sigma_E}{\sigma_R}\right)^y \leq 1.0 \quad (4.28)$$

where:	τ_E	Shear stress effect
	τ_R	Shear stress resistance
	x	Exponent, > 0 , for the shear stress utilization
	σ_E	Bending stress effect caused by bending moment
	σ_R	Bending stress resistance
	y	Exponent, > 0 , for the bending stress utilization

This was done by choosing exponents so that the failure in the model appeared in the same area as the failure from the SP test. The internal stresses were obtained from the CALLFEM routine beam2ws.m.

4.3 Verification of model

4.3.1 Convergence

The convergence was tested using the change of mean moment and the change of max shear force with increasing number of elements, see *Appendix C1*. The study was performed on a plate with the dimensions according to the bridge tested by SP and with an elastic foundation stiffness of 6995 kN/m². The load was placed in the middle of the plate and had a magnitude of 100 kN. After the analysis according to *Appendix C1*, it was decided to use approximately 150 elements in the FE analysis.

4.3.2 Beam behaviour

To get familiar with the behaviour of a beam on elastic foundation, a series of calculations were executed with different load combinations and stiffness properties. The moment distribution from the analysis was then controlled against BYGG1 to get a confirmation that the model behaved as expected. Examples of the behaviour of the beam can be found in *Appendix C2*.

5 Downscaled Tests

5.1 Background

The support behaviour results from the SP test were somewhat surprising. When the deck was loaded with a point load at the edge in the middle span, as in *Figure 5.1*, the positive deflection at the supports was larger than expected. This behaviour could result in sway of the structure, something that is not often taken into account when designing supports for SLTD bridges with small widths (Crocetti 2009).

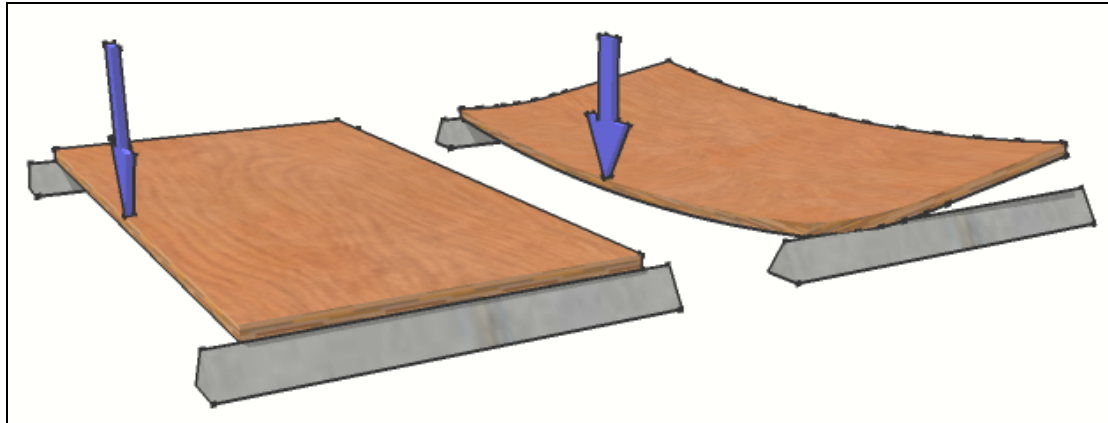


Figure 5.1 Behaviour of the tested specimen, in exaggerated scale.

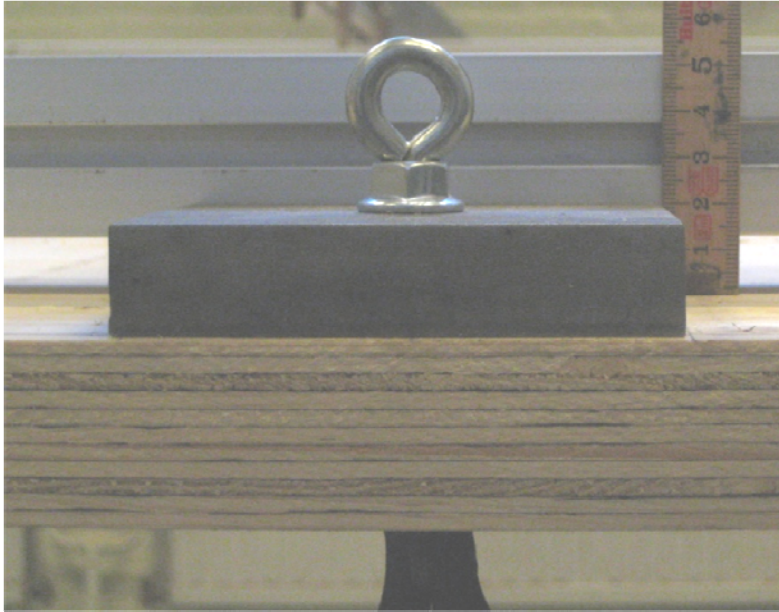
Because of this, it was decided to carry out additional downscaled tests at Chalmers to verify and document the behaviour of an orthotropic plate, and especially examine:

- The support behaviour when loaded with point load
- How well the test data could be approximated by the theory of beam on elastic foundation

The outcome from this test was to better understand the behaviour of a plate and to be able to verify that the effective width actually is a good approximation when designing SLTD.

5.2 Test procedure

The test was performed on plates of LVL, brand “Kerto-Q”, a material that also possesses orthotropic properties. However, the correlation between the stiffness properties is larger than for a SLTD. The test was performed on five different plates with different sizes, this especially to observe the differences in sway behaviour. Before the test started, estimation was done of how large the load-plate would need to be to avoid local compression of the wood. This was done by estimating the highest loads that were to affect the plates and thereafter calculating which area that would be necessary to not exceed the compression resistance in the specimen, which was obtained from Moelven (2009). The plate that was used and the load-anchoring screw can be seen in *Picture 5.1*.



Picture 5.1 Load plate with dimensions $0.1 \times 0.1 \times 0.02 \text{ m}^3$, and anchor screw.

The first test performed was a convergence study for creep to be able to see after how long time the deflections should be measured. This was done by loading one plate and get the initial deflection, then measurements were done every tenth second during the first minute, 20 seconds during the second minute, twice during the third minute and then once every minute for another 16 minutes. The convergence study showed that the deformation after five minutes was 0.26% larger than after 10 seconds, whereby it was decided to measure the deflections five minutes after load application. Measurements were also done when the plate was unloaded to see how large the remaining deformations were. Results from the convergence study are shown in *Figure 5.2*, for the measured deflections see *Appendix D1*. The measurements showed that there were remaining deformations in the plate, which was not expected. However, this remaining deformation is probably due to disturbance of the measurement equipment when unloading, which was a critical moment in this test.

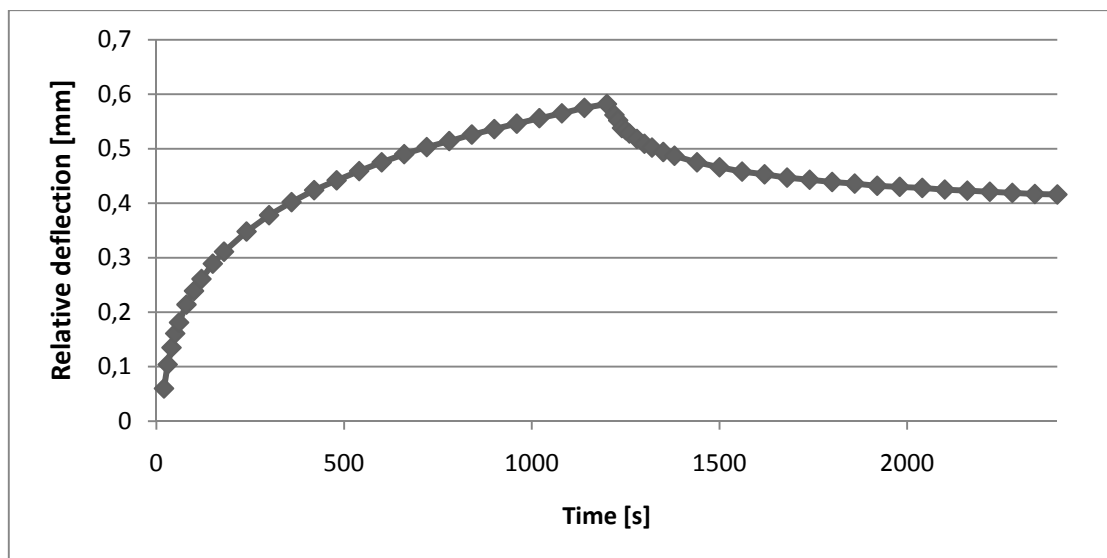


Figure 5.2 Relative viscoelastic creeps.

Another constant of great importance for the test was to compute the modulus of elasticity, MOE, for the tested plates. This was done by adding two line loads, 100 mm from the middle of the plate, and measure the deflection caused by these loads. This was done both for the longitudinal and transversal direction. When the deflections were known, E_x and E_y could be calculated according to BYGG1 (1961) and verified by Timber Engineering STEP1 (1995), these results are presented in Table 5.1, where a comparison of the values suggested by Moelven (2009) is presented. For calculations of MOE, see *Appendix D2*.

Table 5.1 Values of modulus of elasticity

	E_x [GPa]	E_y [GPa]
BYGG1	11.887	2.051
STEP1	11.361	2.612
Moelven	10.500	-

The handbook from Moelven (2009) did not give any suggestions for the transversal modulus of elasticity, E_y . As can be seen, the calculated values were higher than then the manufactures values, while the correlations between the calculated values were acceptable. For any further calculations regarding LVL, the values calculated according to BYGG1 were used. *Figure 5.3* shows the placement of the line loads and *Picture 5.2* shows practical implementation.

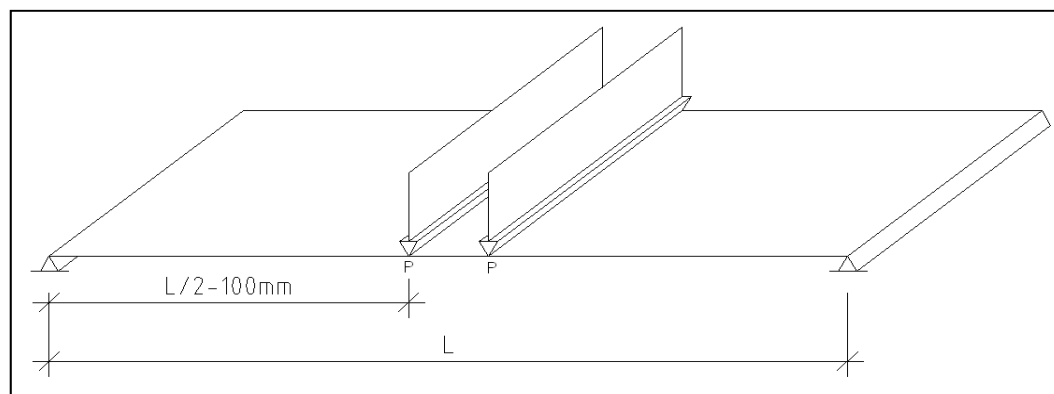
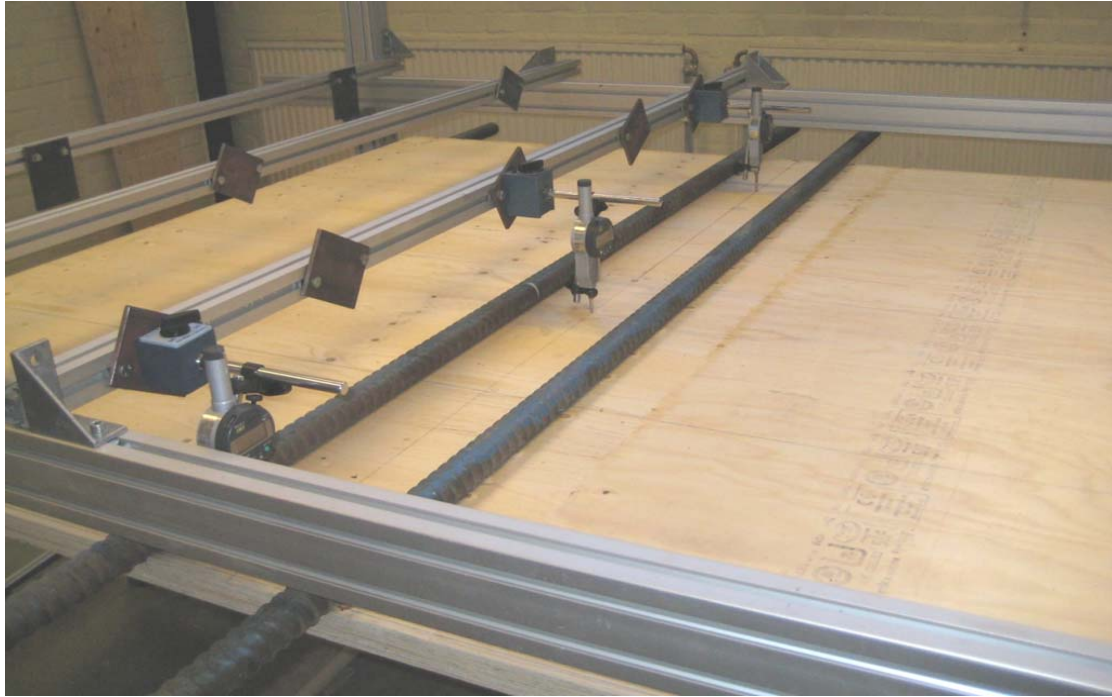


Figure 5.3 Placement of line loads for computing MOE.



Picture 5.2 Line loads for computing MOE.

When the creep time and MOE was computed, the test could be performed. Each plate was tested in a similar way. The test procedure, load placement/ magnitudes and placement of deflection detectors can be found in *Appendix D3*.

5.3 Expected test results

5.3.1 Support behaviour

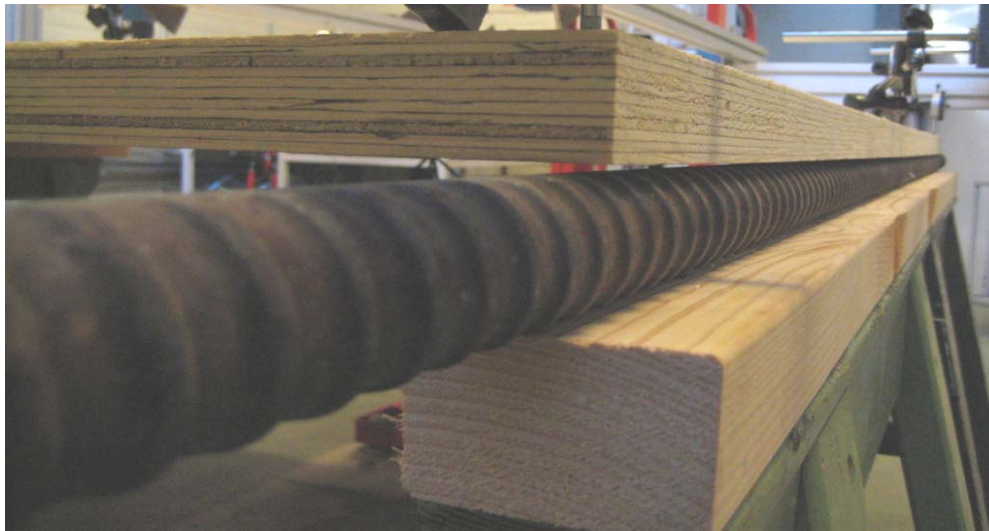
The results from the test were not expected to differ much from the SP test, concerning uplift at the support. However, it was hard to approximate to what extent the plate would get uplift.

5.3.2 Effective width

The hand calculation methods used to design SLTD-bridges is partly based on the relationship between the stiffness properties in longitudinal and transversal direction. This fact together with the large difference in dimensions between the plates that the methods are designed for and the test plates, the behaviour of the test specimen was hard to estimate. To verify if the hand calculation methods were good approximations compared to the test results, it was decided to use the calculated deflections divided by the measured ones as a verification factor and this is further presented in Chapter 6.1. Since the hand calculation methods are adapted to bridges of full size, the calculated distribution width had to be downscaled with a factor η . This factor was based on the relation between a bridge with a length of 15 m and the length of the test plates which were only 2 m. For the calculated deflections, see *Appendix D4*.

5.4 Test results

The plates that were tested showed the same behaviour as the SLTD tested by SP, concerning the uplift at the supports. It could easily be seen with the naked eye that the plate lifted from the support at the corners, which is shown in *Picture 5.3*. Results from the plate with dimensions $L \times B = 2 \times 1.8 \text{ m}^2$, is shown in *Figure 5.4* and *Figure 5.5* for applied load at the edge and in the middle respectively. For the other results from the plate behaviour test, see *Appendix D5*.



Picture 5.3 Uplift at support when loaded at the edge of the plate.

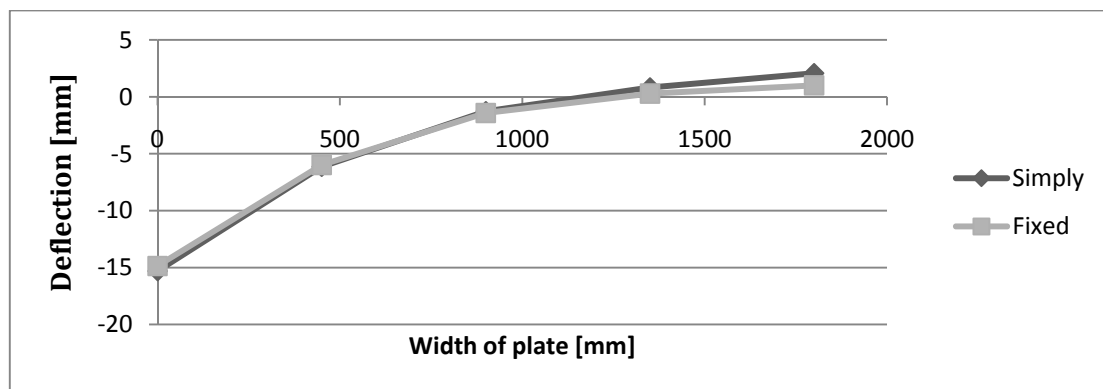


Figure 5.4 Deflections in mid span for simply supported and fixed plate, with dimensions $L \times B = 2 \times 1.8 \text{ m}^2$. Applied load $P=1.303 \text{ kN}$ at the edge of the plate.

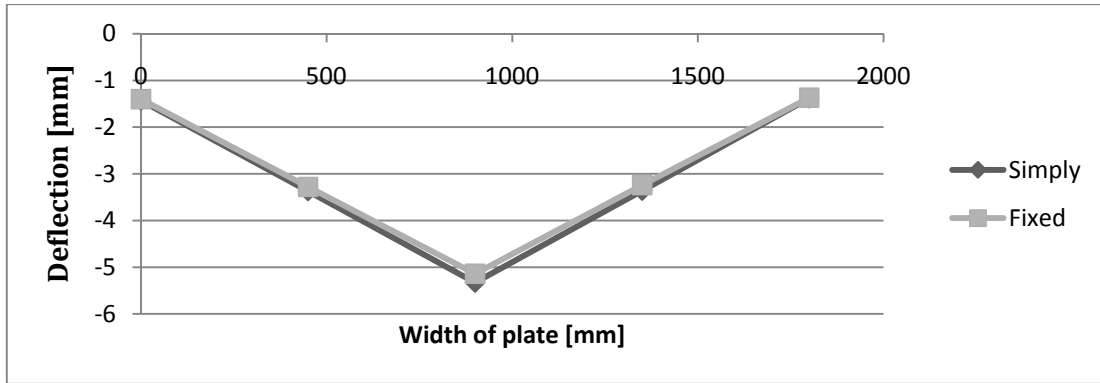


Figure 5.5 Deflections in the mid span for simply supported and fixed plate, with dimensions $L \times B = 2 \times 1.8 \text{ m}^2$. Applied load $P=1.303 \text{ kN}$ in the middle of the plate.

Another thing of interest is the relation between uplift at the corner of the supports/applied load, δ/P , versus the length/width, L/B , relation, which is presented in Figure 5.6 for edge load and Figure 5.7 for load in the middle of the plate. As can be seen, the plates are more prone to get uplift for a length/width relation around one than for the other relations.

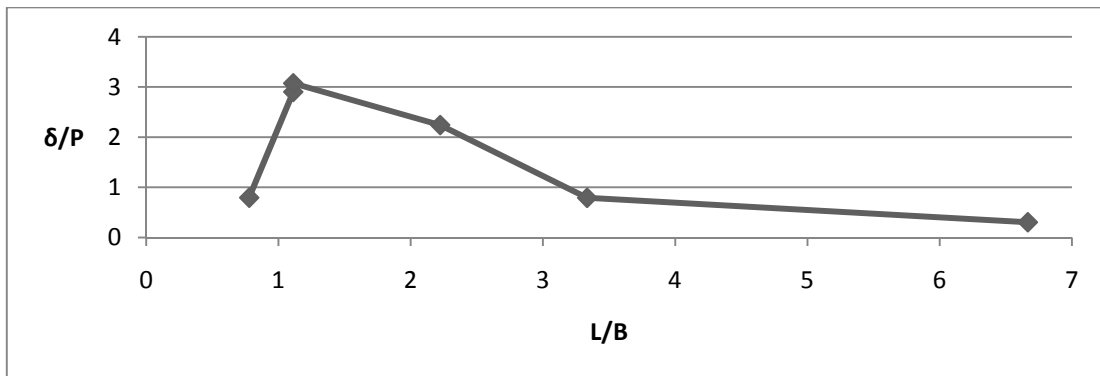


Figure 5.6 Uplift/load versus length/width for applied load at the edge of the plate.

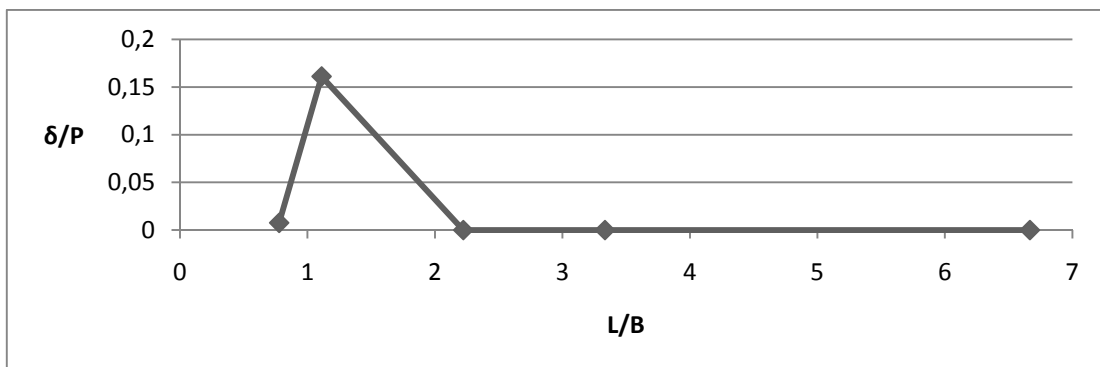


Figure 5.7 Uplift/load versus length/width for applied load in the middle of the plate.

6 Evaluation

6.1 Hand calculation methods

To be able to evaluate the different hand calculation methods described in this thesis it was decided to compare them with the results from both the SP test and the downscaled tests. This was done by comparing calculated deflections with the measured deflections for the different cases. *Figure 6.1* shows the results from the hand calculation methods, described in Chapter 3, compared to the SP test, as well as the effective width. It can be seen in *Figure 6.1* that the effective width is not the only thing that affects the deflection. For example, in the case of designing with Crews design guide, the effective width has a very high value, while the ratio between the calculated deflections and the measured ones are relatively small. One important thing is if the designer could increase the second moment of inertia, I , when designing for deflections, which is suggested in Ritter's design guide and in the method suggested from West Virginia University. Another thing of great importance is how close to the edge the models allow the designer to place the load. In the test performed by SP the load was placed 0.335 m from the edge, which is something that only Eurocode takes into account. Finally the deck tested at SP had a prestress of 0.4 Nmm^{-2} and for example Crews model do not allow prestress to be smaller than 0.5 Nmm^{-2} . This could explain why this model gives a higher deflection compared to the other models.

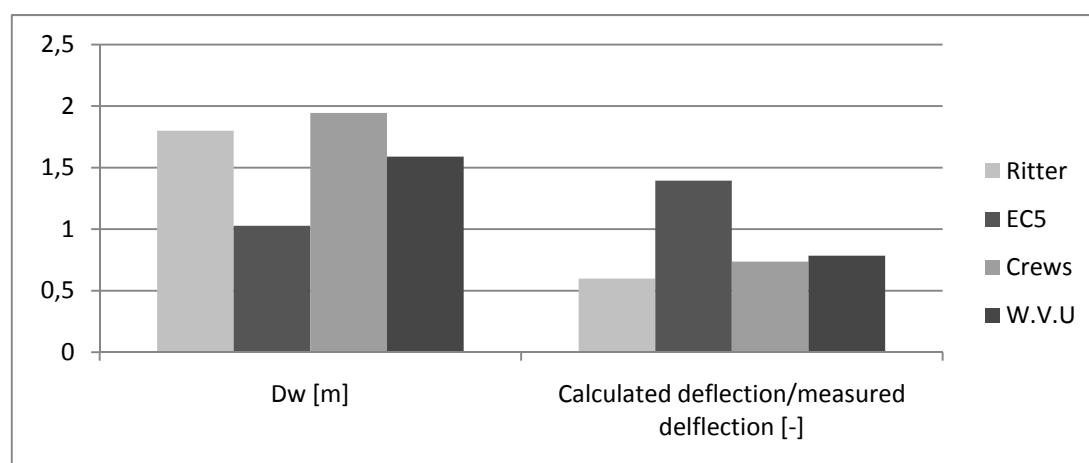


Figure 6.1 Calculated D_w and relation between calculated deflection and measured deflection for the SP test, applied load 100 kN.

A similar comparison as the one done for the full scale test was done for the tested LVL plates. *Figure 6.2* shows the same relations as *Figure 6.1* but for the downscaled test. The studied plate in this case was the plate with $L \times B = 2 \times 0.3 \text{ m}^2$ and the applied load 0.46 kN placed at the edge of the plate. What can be seen when studying *Figure 6.1* and *Figure 6.2* is that the relations concerning calculated deflection/measured deflection is not the same. One of the reasons for this is that the relation between E_x and E_y is not the same for a SLTD and the tested plates. Another reason is that the hand calculation methods are not designed for downscaled tests, which was something that had to be taken into account when calculating the deflection for the downscaled tests. The author's way of treating this by scaling the

effective width was maybe not the best approach when treating downscaled bridges. Another matter of great importance is to what extent the different dimensions of the deck affect the effective width. A more proper way of scaling the plates would be to have different scale factors for different methods, dependent on which parameter affecting D_w the most.

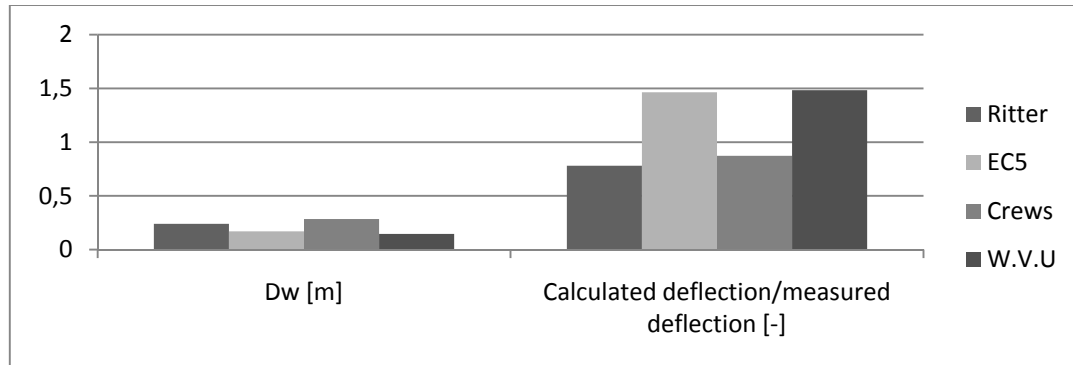


Figure 6.2 Calculated D_w and relation between calculated deflection and measured deflection for a downscaled test, applied load 0.46 kN.

6.2 Elastic foundation stiffness

The data points that were to be investigated were compared to the results obtained from the CALFEM routine mentioned in Chapter 4. The idea was to see if the beam on elastic foundation could get the same deflections as the deflection from the SP- and downscale-tests. This would be done by varying the stiffness properties of the beam. After being confident that the FE-model gave accurate results, the measured results from the LVL downscaled tests and from the SP-test were compared. The width of the beam was fixed according to:

$$w = w_{load\ plate} + h_{test\ specimen} \quad [m] \quad (6.1)$$

A visualization of how the deflection varied with different values of the foundation stiffness can be seen in Figure 6.3.

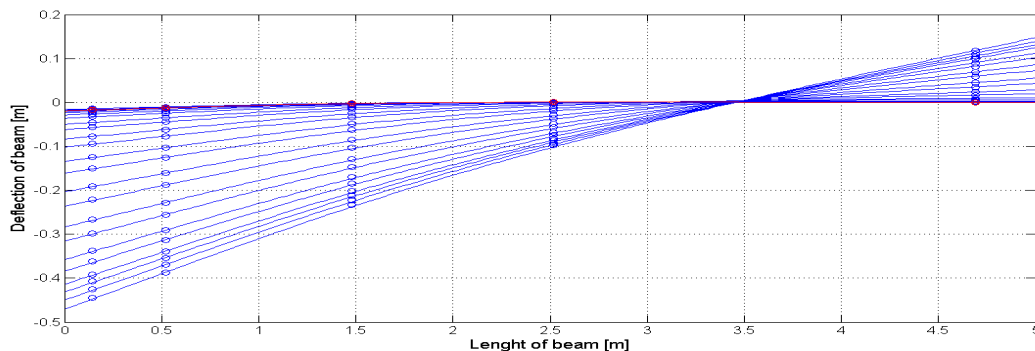


Figure 6.3 Visualisation of the search function in the MATLAB routine `fminsearch.m`. The applied load is 100 kN, at $x=0.355$ m and the width of the beam is 0.695m. The foundation stiffness is increased from 170 kN/m^2 to 7171 kN/m^2 , leading to a maximal deflection of 0.0194 m.

For the case in *Figure 6.3*, the start-value on the elastic foundation stiffness were 170 kN/m², leading to a maximal deflection of 0.47 m, and the end-value were 7171 kN/m² leading to a maximal deflection of 0.0194 m. The red deflection curve is the calculated optimal one with a coefficient of determination value of 84.6%.

As a step of confirming that the foundation stiffness of the different test specimens was correct, a simplified way of calculating the stiffness was applied. For a fictive simply supported beam with a width of D_w that is charged with a point-load, the deflection can be calculated as:

$$\delta = \frac{PL^3}{4E * D_w * h^3} \quad [\text{m}] \quad (6.2)$$

where: P Load on beam
 L Length of the span
 E Beams longitudinal modulus of elasticity
 D_w Width of fictive beam
 h Height of beam

The general expression for the stiffness of one fictive spring is:

$$k_S = \frac{P}{\delta} \quad [\text{Nmm}^{-1}] \quad (6.3)$$

where: P Load on beam
 δ Deflection under the point-load

When combining *Equation 6.2* and *Equation 6.3*, the expression for the spring stiffness can be obtained as:

$$k_S = \frac{4E * D_w * h^3}{L^3} \quad [\text{Nmm}^{-1}] \quad (6.4)$$

To be able to utilise the spring stiffness for an elastic foundation, *Equation 6.4* must be divided over the width of the beam resting on these fictive springs. In this case, the notation w has been used as width of the beam, leading to the expression for the elastic foundation stiffness:

$$S = \frac{k_S}{w} = \frac{4E * D_w * h^3}{L^3 * w} \quad [\text{Nmm}^{-2}] \quad (6.5)$$

To compare the elastic foundation stiffness obtained from the FE analysis and the value obtained from *Equation 6.5*, the value D_w was calculated by integration of the deflection curves from the FE analysis and using the simplified method as indicated in *Equation 6.6*:

$$D_w = \sum_{i=1}^n \int w(x) dx * \delta_{max}^{-1} = \frac{A}{\delta_{max}} \quad [\text{m}] \quad (6.6)$$

where:	n	Number of roots that satisfies $w(x) = 0$
	$w(x)$	Function that describes deflection
	A	Total area between the deflection curve and a zero-vector
	δ_{\max}	Maximal deflection

Example 6.1

Length of plate $L = 10\text{m}$

Width of plate $B = 5\text{m}$

Longitudinal modulus of elasticity $E = 11\text{ GPa}$

Height of plate $h = 0.495\text{ m}$

Effective width of plate $D_w = 1\text{ m}$

Width of fictive beam on elastic foundation $w = 0.5\text{ m}$

Spring stiffness:

$$k = \frac{4E * D_w * h^3}{L^3} = \frac{4 * 11 * 10^9 * 1 * 0.495^3}{10^3} = 5336.6 \frac{\text{kN}}{\text{m}}$$

Elastic foundation stiffness:

$$S = \frac{4E * D_w * h^3}{L^3 * w} = \frac{4 * 11 * 10^9 * 1 * 0.495^3}{10^3 * 0.5} = 10673.3 \frac{\text{kN}}{\text{m}^2}$$

The results from the FE analysis can be found in *Table 6.1*. The last column shows how well the elastic foundation from the hand calculation method agrees with the one from the FE-analysis.

Table 6.1 Results from FE-analysis

L [m]	B [m]	P [kN]	w [m]	S_{FE} [Nmm ⁻²]	R ² [%]	D _w [m]	S/S _{FE} [-]
10	5	98.63	0.695	7.35	83.7	0.848	0.966
10	5	198.34	0.695	7.31	84.3	0.915	1.048
10	5	298.39	0.695	7.19	86	1.023	1.191
2	1.8	1.3	0.133	0.39	86	0.237	0.96
2	0.9	1.3	0.133	0.35	90	0.252	1.16
2	0.6	0.87	0.133	0.36	75.4	0.217	0.97
2	0.3	0.46	0.133	0.28	58.3	0.122	0.69
1.4	1.8	1.3	0.133	0.11	91.7	0.257	1.14

6.3 Failure load

After having established a comforting FE model of the elastic foundation theory, an attempt was made of trying to explain the failure mechanism in the SP test by analysing the shear and moment distribution over the beam on elastic foundation. The term “failure” in this chapter is as described in Chapter 1, Section 1.1.3, i.e. SLS failure, where the deck changes its properties but still have load carrying capacity.

An example of the shear and moment distribution from the SP test can be seen in *Figure 6.4*.

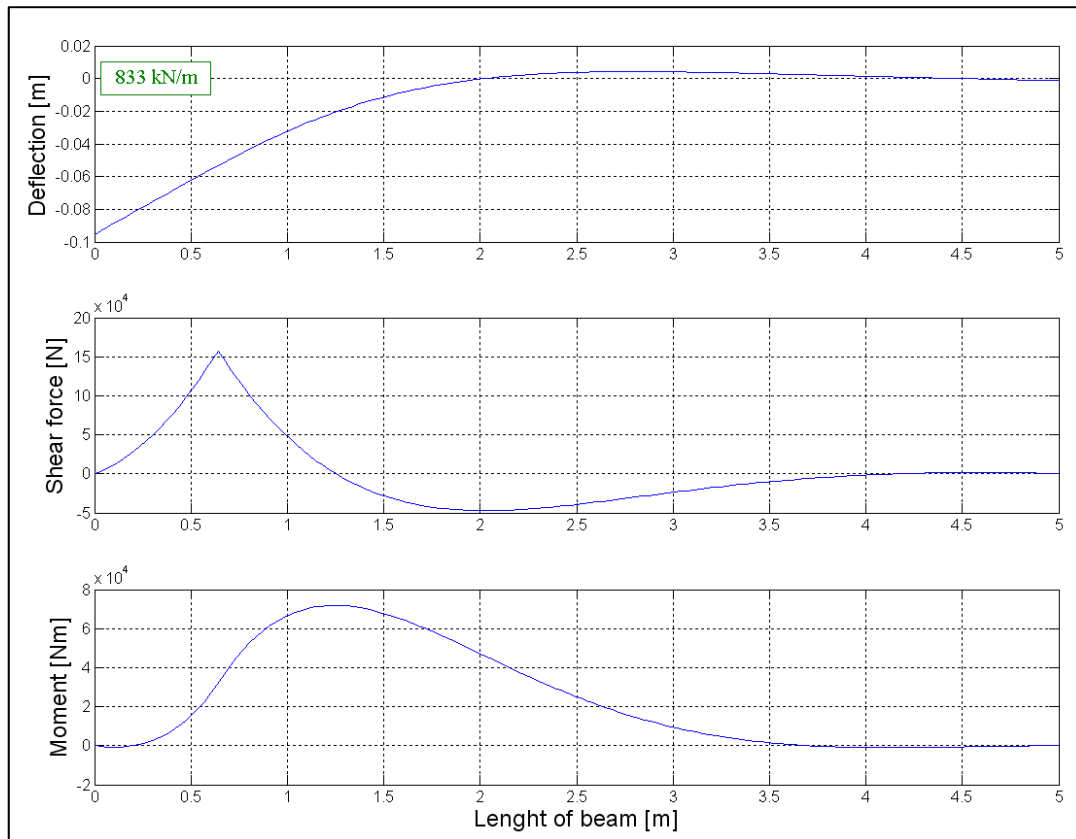


Figure 6.4 Deflection, shear and moment distribution for a beam on elastic foundation. $S = 7.25 \text{ Nmm}^{-2}$, $w = 0.695 \text{ m}$, Load = 833 kN/m distributed on 0.6 m

In the SP test, slip failure was registered around 0.6 m from the loaded edge when the load got close to 600 kN. Since the force distributions in the longitudinal direction were hard to approximate, a parameter study was made to see if there were some correlation between the load distribution length, l_{dist} , and the exponents of the failure equation. Similar to Equation 4.28, the failure could mathematically be described as:

$$\left(\frac{\tau_E}{\tau_R}\right)^x + \left(\frac{\sigma_E}{\sigma_R}\right)^y = \chi_{je} \leq 1.0 \quad (6.7)$$

where:

$$\tau_E = \frac{1.5 \cdot V}{l_{dist} \cdot h}$$

$$\sigma_E = \frac{6 \cdot M}{l_{dist} \cdot h^2}$$

$$\sigma_R = \frac{N}{c \cdot h}$$

$$\tau_E = \sigma_R \cdot \mu$$

V Shear force

l_{dist} Distribution length for stresses in longitudinal direction

h Height of deck

M Moment

N Prestressing force

- c Distance between prestressing rods
- μ Coefficient of friction

When applying *Equation 6.7* to the shear and moment-distribution from the elastic foundation FE-analysis, it was found that failure appeared in the same area as in the SP test for the exponent-relation:

$$y \lesssim 0.5 * x \quad [-] \quad (6.8)$$

With this relation, the principal behaviour of the combined stress utilization can be seen in *Figure 6.5*. This exponent-relation suppresses the contribution from the shear stress utilization, while the bending stress utilization is magnified. Like in the failure from SP, the beam has sufficient resistance for the 500 kN load, but suffers failure, i.e. $\chi_{je} \geq 1$ for the applied load of 600 kN.

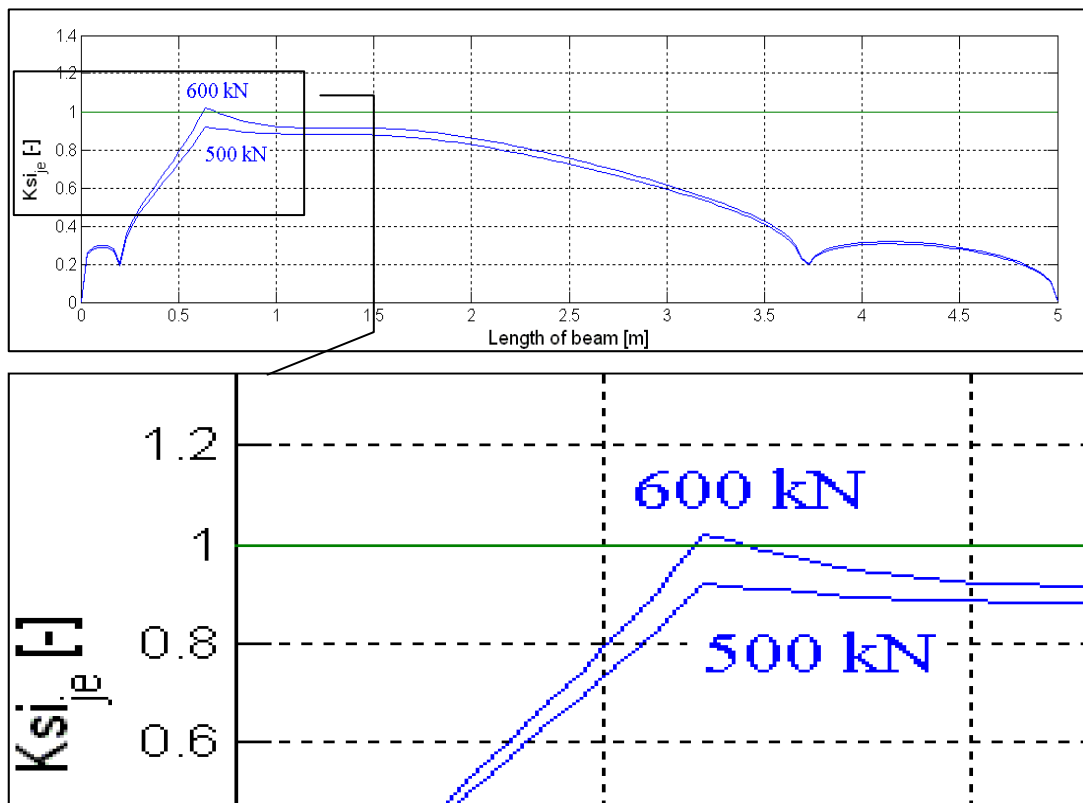


Figure 6.5 Combined stress utilization for a load distribution length of 8 m, $x=2.00$ and $y=0.2$.

A part of the parameter study can be found in *Table 6.2* shows the value of x , y and χ_{je} for different l_{dist} . For values of l_{dist} below 5 m, the relation between σ_E and σ_R in *Equation 6.8* reaches one and there exists no exponents that satisfy the equation. Further results for different relations between x and y are presented in *Appendix E1*.

Table 6.2 Values from parameter study.

l_{dist} [m]	x [-]	y [-]	X_{je} (500 kN)	X_{je} (600 kN)
10	1.60	0.160	0.94	1.02
9	1.75	0.175	0.93	1.02
8	2.00	0.200	0.92	1.02
7	2.35	0.235	0.91	1.03
6	2.90	0.290	0.89	1.05
5	4.43	0.443	0.81	1.06

7 Discussion

7.1 Downscaled tests

The results from the downscaled tests could be somewhat misleading, especially in the creep behaviour test where it seems that a relative large deflection remains after unloading. This behaviour is surprising, since the loads on the plate were not of the magnitude to create remaining deformations in the test specimen. A possible explanation for the remaining deflection from the test could be that there were some disturbances in the measure equipment when loading and unloading. Another possibility for the remaining deflection is if the loaded screw were displaced in the plate, as seen in *Figure 7.1*. This might have led to that the plate was prevented to get to its ordinary state when we thought it was unloaded. A factor that had an important role in the test results was if the loading procedure was totally centric, i.e. if the load actually were acting in the true centre of the plates span.

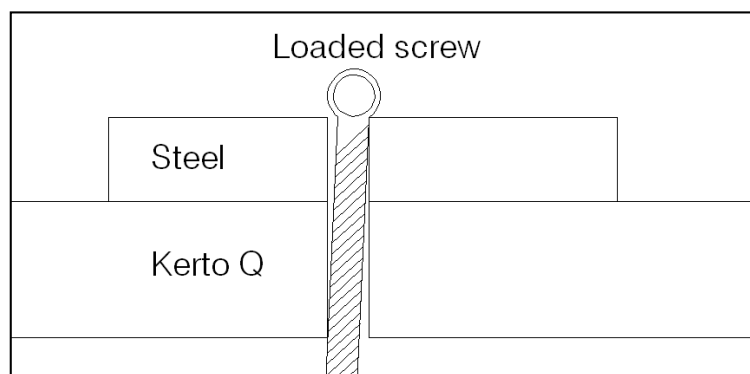


Figure 7.1 Misplaced load-application in load-carrying screw

7.2 Hand calculation methods

The different hand calculation methods described in this thesis are a good way of designing SLTD in SLS. The different methods give suggestions for how to calculate D_w , and changes in these calculations partly depends on different regulations in different countries. One thing that the methods do not take into account is the uplift at the corner of the supports which has been noticed both by the SP test and our downscaled tests. The uplift in our tests showed to be worst for the plate with L/B close to one. However this uplift is not a big problem when designing SLTD since the covering layers will keep the corners in place and this might be one reason for why no methods takes this into account. Another reason for why uplift is not a big issue in SLS is that the uplift is greatest for large point-loads applied at the edge of the plate. This is an extreme load case and is something that only takes place in tests.

When comparing the hand calculation methods to the different tests there was a clear difference in what maximum deflection one could expect. This deflection differs in a great extent and one important thing is how close to the edge the designer is allowed to place the load. What could be seen in both the test from SP and the test performed at Chalmers was that when designing with Eurocode the calculated deflections were on the safe side. This is due to the fact that Eurocode allows the designer to place the load closer to the edge than the other methods discussed in this thesis.

The scale factor, η , affected the calculated deflections for the downscaled test. As mentioned in Chapter 6.1, a better way of treating this would be to have different scale factors for different methods. For example, in the method from West Virginia University the thickness of the plate affect the distribution width and thereby the deflection. With the used scale factor, that only takes the length of the plate into account, the distribution width is lower than it would have been if the scale factor also would have been dependent of the thickness of the plate.

7.3 FE model

The CALFEM routines beam2w.m and beam2ws.m has proven to be a reasonable good method of predicting deflections, shear forces and moments in the SLS for SLTD bridges. However, the deflections are on the safe side, thus leading to higher deflections and internal forces. According to the results from the FE analysis, the best way of predicting the elastic foundation stiffness for a SLTD loaded with edge-load would be to estimate the effective width, D_w according to Eurocode and then calculate the elastic foundation stiffness according to *Equation 6.4*. The authors of this thesis thinks that this correlation is due to the fact that Eurocode takes into account the effect of high loads close to the edge in the span.

For the downscaled test plates the results contained some consistency for the larger plates, but gave unsatisfying results for the smallest plate.

Due to the limitation of this thesis, discussions of how well the approximation would be for a beam with point-load in the centre cannot be made. For a practical use of the elastic foundation theory, more full scale test data would be needed to analyse.

7.4 Failure load

To establish a good model of the failure load, consideration of how the stress distributes in the transversal direction probably needs to be taken into account. The distributed lengths, l_{dist} , from Chapter 6, Section 6.3 would probably be smaller if the stresses are allowed to distribute in both directions.

7.5 Suggestions for further research

- Modify the elastic foundation model against more full-scale tests
- Examine the failure load in ABAQUS
- Use different l_{dist} for the shear and moment utilization

8 References

8.1 Literature

- Bing Y. Ting, Eldon M. (1984): Beams on elastic foundation finite element, *Journal of Structural Engineering*, Vol. 110, No. 10, October, 1984, ASCE, ISSN.
- Blass H.J et al. (1995): *Timber Engineering – STEP 1*. First Edition, Centrum Hout, The Netherlands.
- BYGG1 – *Allmänna Grunder*, AB Byggmästarföreningens förlag, Stockholm 1961, (BYGG1 - *General Basics*).
- Comité Européen de Normalisation, CEN (2004),: EN 1995-1:2004. Eurocode 5 – Design of Timber Structures Part 1 – General – Common rules and rules for buildings, 2004.
- Comité Européen de Normalisation, CEN (2004),: EN 1995-2:2004. Eurocode 5 – Design of Timber Structures Part 2 – Bridges, 2004.
- Crews, K. (2002): *Behaviour and Critical Limit States of Transversely Laminated Timber Cellular Bridge Decks*. Ph.D. Thesis. Faculty of Engineering, University of Technology, Sydney.
- Crews, K. (2006): *Recommended Procedures for Determination of Distribution Widths in the Design of Stress Laminated Timber Plated Decks*, CIB W18/39-12-1.
- Dahl, K. (2002): *Tverspente Dekker i Tre*. Master's Thesis, (Stress Laminated Timber Decks), Institutt for tekniske fag, Norges Landbrukshøgskole, (The Institute for technical research, Norwegian Agricultural School).
- Formolo S, Granström R (2007): *Compression Perpendicular to the Grain and Reinforcement of a Pre-Stressed Timber Deck*. Master's Thesis. Department of Civil and Environmental Engineering, Chalmers University of Technology, Göteborg.
- Marklund K.A (1997): *Nordic Timber Bridge Project – Deflection of Measuring of Stress-Laminated Deck Bridge*, Institutet för Träteknisk Forskning (Institute for timber research).
- Moelven (2009): *Moelvens handbok om Kerto*, tabell 2.6 och 2.7 (*Moelven's handbook about Kerto*, table 2.6 and 2.7).
- Ottosen N, Petersson H. (1992): *Introduction to the finite element method*. Prentice Hall, Great Britain, 1992.
- Porteous J, Kermani A (2007): *Structural Timber Design to Eurocode 5*. Blackwell Publishing, United Kingdom.
- Ritter, M, A (1990): *Timber Bridges – Design, Construction, Inspection and maintenance*.
- SP Träteknik (2008): Report, Denotation P803586.

8.2 Verbal

- Crocetti, R (2009)

Appendix A1 – Used deflections from SP test

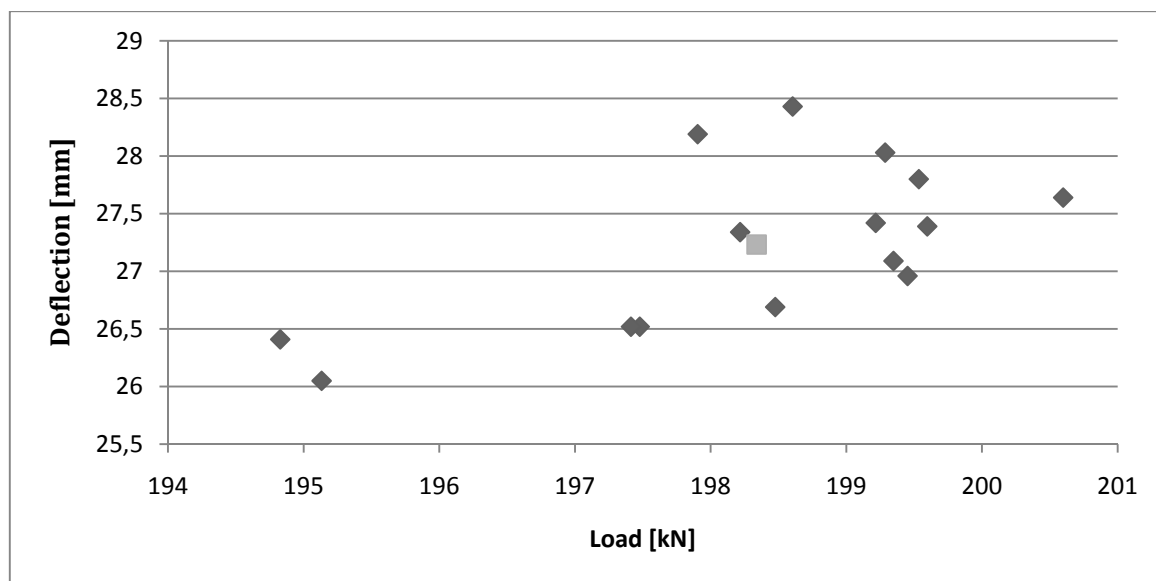


Figure A.1 Measured deflections from different load series around 200 kN.

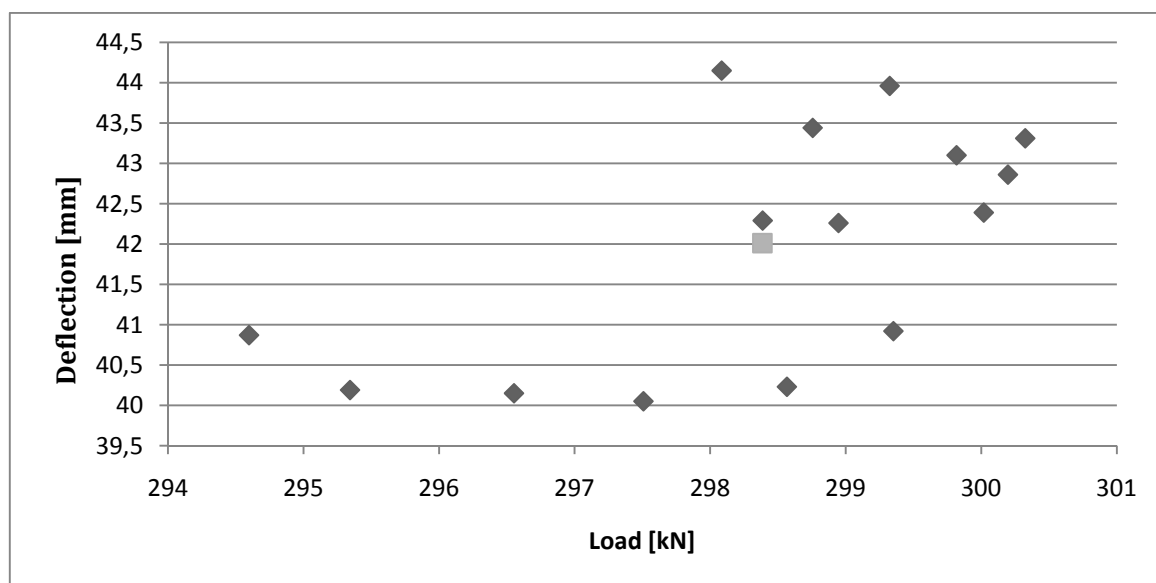


Figure A.2 Measured deflections from different load series around 300 kN.

Table A.1 Measured deflections used for analysis of elastic foundation stiffness.

Load [kN]	Measure point [m] - Deflection [mm]				
	0,143	0,523	1,477	2,518	4,689
98,6362	13,453	11,4645	6,602	3,102	-1,394
198,3392	27,232	23,068	12,96467	5,677333	-3,71067
298,3852	42,01133	35,25733	19,116	7,574	-7,27533

Appendix A2 – Parameters from the SP test

Dimensions and parameters of the bridge

Dimensions

$l_{\text{span}} := 10\text{m}$	Length of bridge
$w_{\text{bridge}} := 5035\text{mm}$	Width of bridge
$w_{\text{glulam}} := 95\text{mm}$	Width of glulam beam
$h_{\text{glulam}} := 495\text{mm}$	Height of glulam beam
$x := (0, 0.01\text{m}.. l_{\text{span}})$	
$y := (0, 0.01\text{m}.. w_{\text{bridge}})$	

Crossectional units

$$I_{x\text{beam}} := \frac{w_{\text{glulam}} \cdot h_{\text{glulam}}^3}{12} = 9.602 \times 10^{-4} \text{ m}^4$$

$$I_{y\text{beam}} := \frac{h_{\text{glulam}} \cdot w_{\text{glulam}}^3}{12} = 3.537 \times 10^{-5} \text{ m}^4$$

$$W_{x\text{beam}} := \frac{w_{\text{glulam}} \cdot h_{\text{glulam}}^2}{6} = 3.88 \times 10^{-3} \cdot \text{m}^3$$

$$W_{y\text{beam}} := \frac{w_{\text{glulam}}^2 \cdot h_{\text{glulam}}}{6} = 7.446 \times 10^{-4} \cdot \text{m}^3$$

Modification factors

Size effect

$$k_h := \min \left[\left(\frac{600\text{mm}}{h_{\text{glulam}}} \right)^{0.1}, 1.1 \right] = 1.019$$

Load duration and service class

$$k_{\text{mod}} := 0.9$$

System effect

$$k_{\text{sys}} := 1.1$$

Deformation coefficient

$$k_{\text{def}} := 2.0$$

Partial coefficient for material properties

$$\gamma_{M_{\text{glulam}}} := 1.3$$

Defining units in Mathcad

$$\text{Nm} := \text{N} \cdot \text{mm}$$

$$\text{kNm} := \text{kN} \cdot \text{m}$$

Strength and stiffness properties, combined glulam

$$\gamma_{\text{spruce}} := 380 \frac{\text{kg}}{\text{m}^3} \cdot g = 3.727 \frac{\text{kN}}{\text{m}^3}$$

Characteristic values

Bending strength

$$f_{\text{mgk}} := 28 \frac{\text{N}}{\text{mm}^2} = 28 \text{MPa}$$

Tension strength

$$f_{\text{t0gk}} := 16.5 \frac{\text{N}}{\text{mm}^2} = 16.5 \text{MPa}$$

$$f_{\text{t90gk}} := 0.4 \frac{\text{N}}{\text{mm}^2} = 0.4 \text{MPa}$$

Compression strength

$$f_{\text{c0gk}} := 24 \frac{\text{N}}{\text{mm}^2} = 24 \text{MPa}$$

$$f_{\text{c90gk}} := 2.7 \frac{\text{N}}{\text{mm}^2} = 2.7 \text{MPa}$$

Shear strength

$$f_{\text{vgk}} := 2.7 \frac{\text{N}}{\text{mm}^2} = 2.7 \text{MPa}$$

Modulus of elasticity

$$E_{0\text{mean}} := 12.0 \frac{\text{kN}}{\text{mm}^2} = 12 \text{GPa}$$

Shear modulus

$$G_{\text{mean}} := 0.72 \frac{\text{kN}}{\text{mm}^2} = 0.72 \text{GPa}$$

Dimensioning values

Bending strength

$$f_{\text{mgdb}} := \frac{k_t \cdot k_{\text{mod}} \cdot k_{\text{sys}} \cdot f_{\text{mgk}}}{\gamma_{\text{Mglulam}}} = 21.737 \text{MPa}$$

$$f_{\text{vgdb}} := \frac{k_{\text{mod}} \cdot k_{\text{sys}} \cdot f_{\text{vgk}}}{\gamma_{\text{Mglulam}}} = 2.056 \text{MPa}$$

Appendix B1 – Ritter

Ritters Design guide

☞ Reference: Z:\Skolan\Exjobb\Till Storegate\MathCad\Dimensioner och parametrar på bron.xmcd(R)

Loads acting on the deck

$$P_{\text{test}} := \begin{pmatrix} 100 \\ 200 \end{pmatrix} \text{kN} \quad \text{Loads for comparison with SP test}$$

According to Ritter Design guide, the following points have been calculated.

1) Input data from Appendix A2

$$\begin{aligned} b_{\text{deck}} &:= w_{\text{bridge}} & b_{\text{deck}} &= 5.035\text{m} & \text{Width of deck} \\ l_{\text{span}} &= 10\text{m} & & & \text{Length of span} \\ h_{\text{glulam}} &= 0.495\text{m} & & & \text{Height of deck} \\ E_{0\text{mean}} &= 1.2 \times 10^4 \cdot \text{MPa} & & & \end{aligned}$$

2) Timber class GL28c

$$\begin{aligned} f_{\text{mgdb}} &= 21.737\text{MPa} \\ E_{0\text{mean}} &= 12 \cdot \text{GPa} \end{aligned}$$

3) C_B - Coefficient for butt joints

$$C_B := 1.0 \quad \text{No butt joints}$$

4) Stiffness properties

$$\begin{aligned} E_0 &:= E_{0\text{mean}} \\ E_{90} &:= 0.013 E_0 = 156\text{MPa} \\ G_0 &:= 0.03 E_0 = 360\text{MPa} & \text{According to Ritter} \end{aligned}$$

5) Maximal pointload moment

$$M_0 := \frac{P_{\text{test}} \cdot l_{\text{span}}}{4} = \begin{pmatrix} 250 \\ 500 \end{pmatrix} \cdot \text{kNm}$$

6) Effective width D_w

$$\alpha := \frac{2 \cdot G_0}{\sqrt{E_0 \cdot C_B \cdot E_{90}}} = 0.526$$

Parameter for the Decks torsional stiffness

$$\theta := \frac{b_{\text{deck}}}{2 \cdot l_{\text{span}}} \cdot \left(\frac{E_0 \cdot C_B}{E_{90}} \right)^{0.25} = 0.746$$

Relation between the deck stiffness in longitudinal and transversal direction

$$D_w := 1800 \text{ mm}$$

From diagram according to Ritter (1990), and modified by Dahl (2002).

7) Deck section modulus and effective deck moment inertia

$$I := C_B \cdot \frac{D_w \cdot h_{\text{glulam}}^3}{12} = 0.018 \text{ m}^4$$

$$S := C_B \cdot \frac{D_w \cdot h_{\text{glulam}}^2}{6} = 0.074 \text{ m}^3$$

8) Design moment

$$q_d := \gamma_{\text{spruce}} \cdot D_w \cdot h_{\text{glulam}}$$

$$M_y := M_0 - q_d \cdot \frac{l_{\text{span}}^2}{4} = \begin{pmatrix} 116.35 \\ 366.35 \end{pmatrix} \cdot \text{kNm}$$

9) Bending strenght check

$$\sigma_y \leq f_{\text{mgdb}} \cdot C_{I_s}$$

$$C_{I_s} := 1.3$$

$$\sigma_y := \frac{M_y}{S} = \begin{pmatrix} 1.583 \\ 4.984 \end{pmatrix} \cdot \text{MPa}$$

$$f_{\text{mgdb}} \cdot C_{I_s} = 28.258 \text{ MPa}$$

10) Deflection w from uniform load and point load

$$w_{\text{tot}} \leq w_{\text{lim}}$$

$$I_w := \frac{D_w \cdot h_{\text{glulam}}^3}{12}$$

$$w_{\text{bend_pointload}} := \frac{P_{\text{test}} \cdot l_{\text{span}}^3}{48 \cdot E_{0\text{mean}} \cdot 1.33 I_w} \quad \text{Increase } I \text{ for deflection calculations}$$

$$w_{\text{bend_uniform}} := \frac{5 \cdot q_d \cdot l_{\text{span}}^4}{384 E_{0\text{mean}} \cdot 1.33 I_w}$$

$$\Psi_{\text{shear_amplification_point}} := \left[1 + 1.2 \left(\frac{E_{0\text{mean}}}{G_0} \right) \cdot \left(\frac{h_{\text{glulam}}}{l_{\text{span}}} \right)^2 \right] = 1.098$$

$$\Psi_{\text{shear_amplification_uniform}} := \left[1 + 0.96 \left(\frac{E_{0\text{mean}}}{G_0} \right) \cdot \left(\frac{h_{\text{glulam}}}{l_{\text{span}}} \right)^2 \right] = 1.078$$

$$w_{\text{totfin}} := w_{\text{bend_pointload}} \cdot \Psi_{\text{shear_amplification_point}} + w_{\text{bend_uniform}} \cdot \Psi_{\text{shear_amplification_uniform}} = \begin{pmatrix} 9.484 \\ 17.362 \end{pmatrix} \cdot \text{mm}$$

$$w_{\text{lim}} := \frac{l_{\text{span}}}{360} = 27.778 \text{ mm}$$

$$w_{\text{bend_pointload}} = \begin{pmatrix} 7.175 \\ 14.35 \end{pmatrix} \cdot \text{mm}$$

Appendix B2 – Eurocode 5

Eurocode

☞ Reference: Z:\Skolan\Exjobb\Till Storegate\MathCad\Dimensioner och parametrar på bron.xmcd(R)

Input data from Appendix A2

$$b_{\text{deck}} := w_{\text{bridge}} \quad b_{\text{deck}} = 5.035\text{m} \quad \text{Width of deck}$$

$$l_{\text{span}} = 10\text{m} \quad \text{Length of span}$$

$$h_{\text{glulam}} = 0.495\text{m} \quad \text{Height of deck}$$

$$E_{0\text{mean}} = 12\text{GPa}$$

Loads acting on the deck

$$P_{\text{test}} := \begin{pmatrix} 100 \\ 200 \end{pmatrix} \text{kN} \quad \text{Loads to compare with SP test}$$

Effective width

$$b_w := 0.6\text{m} \quad \text{Width of wheel}$$

$$\beta := 15\text{deg} \quad \text{Dispersion angle, according to Table 3.1}$$

$$a := 0.3\text{m}$$

$$b_{w_middle} := b_w + h_{\text{glulam}} \sin(\beta) = 0.728\text{m}$$

$$b_{\text{ef}} := b_{w_middle} + a$$

$$b_{\text{ef}} = 1.028\text{m}$$

Deck strenght

$$b_{\text{lam}} := w_{\text{glulam}}$$

$$n := \frac{b_{\text{ef}}}{b_{\text{lam}}} = 10.822$$

$$k_{\text{sys}} = 1.1$$

$$f_{m_d_lam} := f_{\text{mgdb}}$$

$$f_{v_d_lam} := f_{\text{vgdb}}$$

$$f_{m_d_deck} := k_{sys} \cdot f_{m_d_lam} = 23.911 \text{ MPa}$$

$$f_{v_d_deck} := k_{sys} \cdot f_{v_d_lam} = 2.262 \text{ MPa}$$

Action effects

$$q_d := \gamma_{spruce} \cdot b_{ef} \cdot h_{glulam} = 1.896 \frac{\text{kN}}{\text{m}}$$

$$I := b_{ef} \cdot \frac{h_{glulam}^3}{12}$$

$$R_A := \frac{P_{test}}{2} + q_d \cdot \frac{l_{span}}{2}$$

$$M_{max} := R_A \cdot \frac{l_{span}}{2} - q_d \cdot \frac{l_{span}^2}{4} = \left(\frac{250}{500} \right) \cdot \text{kNm} \quad \text{Design moment}$$

$$w_{bend} := \frac{P_{test} \cdot l_{span}^3}{48 \cdot E_{0mean} \cdot I} = \left(\frac{16.707}{33.414} \right) \cdot \text{mm} \quad \text{Deflection due to applied loads}$$

Appendix B3 – Crews

Crews

☞ Reference: Z:\Skolan\Exjobb\Till Storegate\MathCad\Dimensioner och parametrar p å bron.xmcd

Defining units in Mathcad

$$\text{kNm} := \text{kN} \cdot \text{m}$$

Input data from Appendix A2

$$b_{\text{deck}} := w_{\text{bridge}} \quad b_{\text{deck}} = 5.035\text{m} \quad \text{Width of deck}$$

$$l_{\text{span}} = 10\text{m} \quad \text{Length of span}$$

$$h_{\text{glulam}} = 0.495\text{m} \quad \text{Height of deck}$$

$$E_{0\text{mean}} = 12 \cdot \text{GPa}$$

Loads acting on the deck

$$P_{\text{test}} := \begin{pmatrix} 100 \\ 200 \end{pmatrix} \text{kN} \quad \text{Loads to compare with SP test}$$

Distribution width

$$D_{w1} = \left[\left(\frac{E_0}{10000} \right)^{0.50} + \frac{l_{\text{span}}}{25} + 0.45 \right] \cdot C_B \quad \text{for a single lane bridge}$$

$$D_{w2} = \left[\left(\frac{E_0}{18000} \right)^{0.40} + \frac{l_{\text{span}}}{30} + 0.45 \right] \cdot C_B \quad \text{for a two lane bridge}$$

Where:

$$E_0 := E_{0\text{mean}} = 12 \cdot \text{GPa}$$

$$C_{B_hardwood} = \frac{\left(\frac{n-1}{n} \right)}{0.75} \geq 1.0$$

where n is number of buttjoints

$$C_{B_australian.pine} = \frac{\left(\frac{n-1}{n} \right)}{0.85} \geq 1.0$$

Since we have glulam and therefore there is no effect of butt joints, $C_B=1.0$

$$C_B := 1.0$$

$$D_{w1} := \left[\left(\frac{E_0}{10000 \text{ MPa}} \right)^{0.50} + \frac{l_{\text{span}}}{25 \cdot \text{m}} + 0.45 \right] \cdot C_B$$

$$D_{w2} := \left[\left(\frac{E_0}{18000 \text{ MPa}} \right)^{0.40} + \frac{l_{\text{span}}}{30 \cdot \text{m}} + 0.45 \right] \cdot C_B$$

$$D_w := \begin{pmatrix} D_{w1} \\ D_{w2} \end{pmatrix} \cdot \text{m} = \begin{pmatrix} 1.945 \\ 1.634 \end{pmatrix} \text{m}$$

$$D_w := D_{w1} \cdot \text{m}$$

Since we have a single line bridge

$$D_w = 1.945 \text{m}$$

Calculated distribution width according to Crews

Second moment of inertia, I, and deflection, w.

$$I := \frac{C_B \cdot D_w \cdot h_{\text{glulam}}^3}{12} = 0.02 \text{m}^4$$

$$w := \frac{P_{\text{test}} \cdot l_{\text{span}}^3}{48 \cdot E_0 \cdot I}$$

$$w = \begin{pmatrix} 8.829 \\ 17.659 \end{pmatrix} \cdot \text{mm}$$

Appendix B4 – West Virginia University method

West Virginia University method

☞ Reference: Z:\Skolan\Exjobb\Till Storegate\MathCad\Dimensioner och parametrar på bron.xmcd

☞ Reference: Z:\Skolan\Exjobb\Till Storegate\MathCad\Gammalt\Crews.xmcd

Defining units in Mathcad

$$\underline{kNm} := kN \cdot m$$

$$\underline{Nmm} := N \cdot mm$$

$$Nm := N \cdot m$$

Loads acting on the deck

$$P_{\text{test}} = \begin{pmatrix} 100 \\ 200 \end{pmatrix} \cdot kN$$

Loads to compare with SP test

Input data from Appendix A2

$$\underline{b_{\text{deck}}} := w_{\text{bridge}} \quad b_{\text{deck}} = 5.035m$$

Width of deck

$$l_{\text{span}} = 10m$$

Length of span

$$h_{\text{glulam}} = 0.495m$$

Height of deck

$$E_{0\text{mean}} = 12 \cdot GPa$$

Distribution width

$$D_w = (b_f + 2 \cdot t) \cdot C_B$$

$$b_f := 600mm$$

wheel width

$$C_B = 1$$

No effects of butt joints

$$\underline{D_w} := (b_f + 2 \cdot h_{\text{glulam}}) \cdot C_B$$

$$\underline{D_w} = 1.59m$$

calculated distribution width according to W.V.U method

Second moment of inertia, I, and deflection, w.

$$\underline{I} := \frac{D_w \cdot h_{\text{glulam}}^3}{12} = 0.016m^4$$

$$w := \frac{P_{\text{test}} \cdot l_{\text{span}}^3}{48 \cdot E_0 \cdot 1.15 \cdot I}$$

$$w = \begin{pmatrix} 9.394 \\ 18.788 \end{pmatrix} \cdot \text{mm}$$

Where I is increased with 15% because of deflection calculations

Appendix C1 – Convergence for number of elements

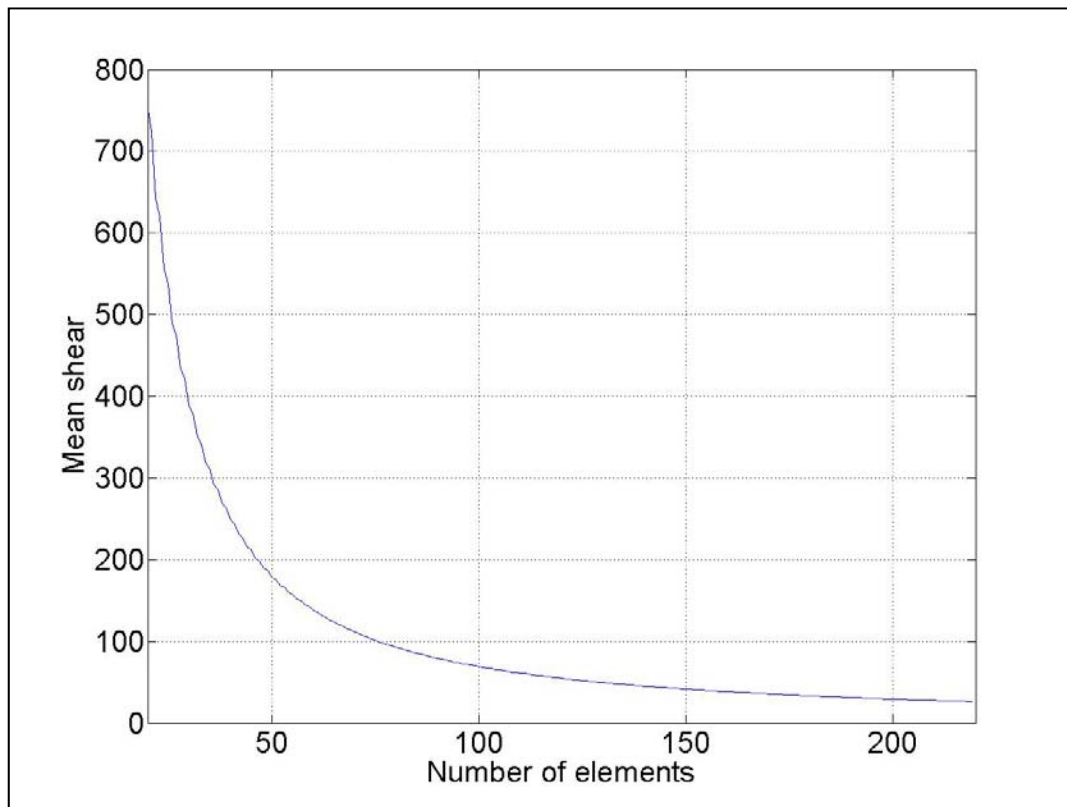


Figure C.1 Convergence, mean shear force versus number of elements.

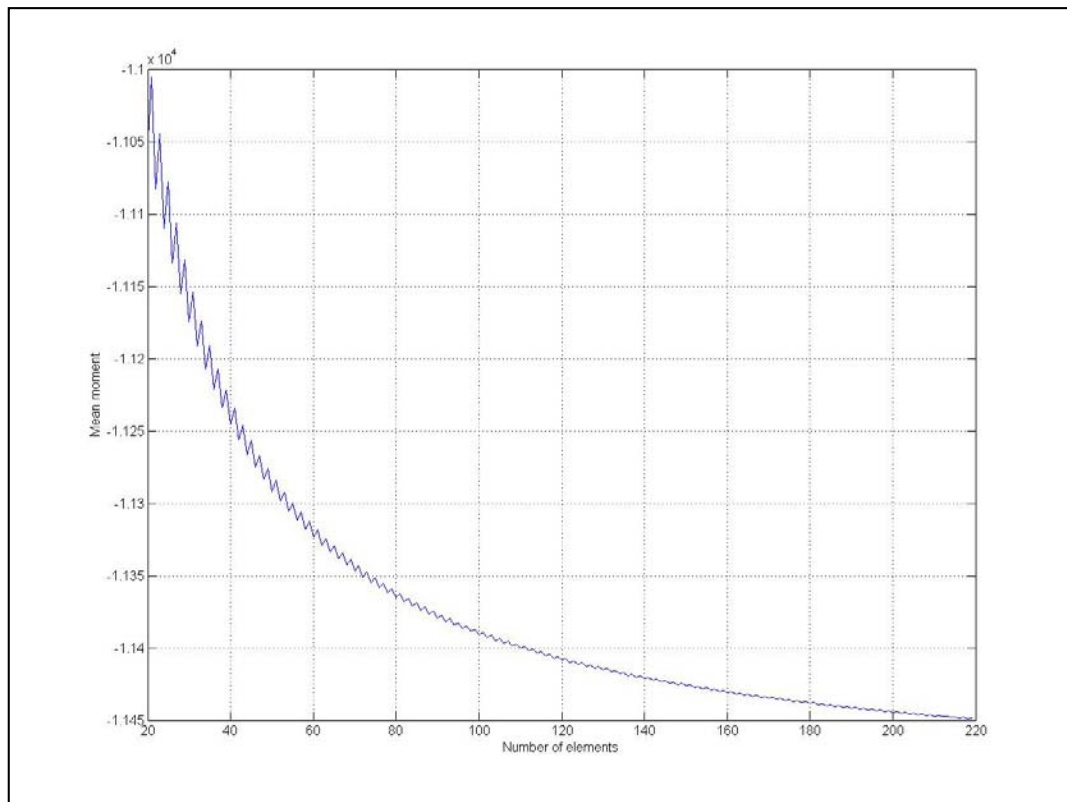


Figure C.2 Convergence, mean moment versus number of elements.

Appendix C2 – Behaviour of beam on elastic foundation

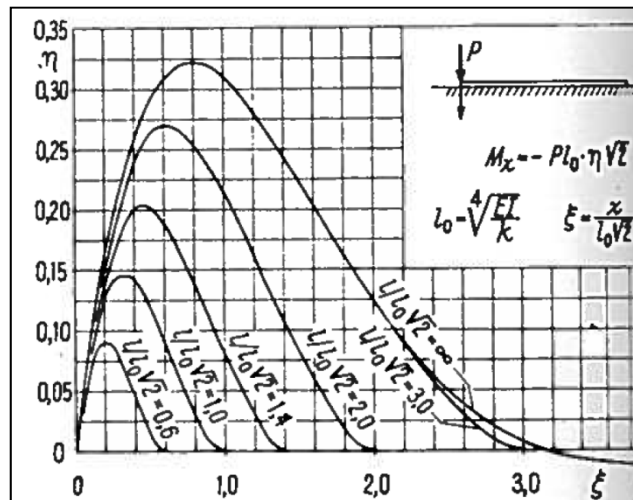


Figure C.3 Influence-lines for moment in beam on elastic foundation, Figure from BYGG1 p.648

$$k = \frac{48 \cdot E_X \cdot I_X}{l_{\text{deck}}^3}$$

$$l_0 = \sqrt[4]{\frac{E_y \cdot I_y}{k}} \quad \frac{l_{\text{span}}}{l_0 \sqrt{2}} \quad \xi = \frac{x}{l_0 \sqrt{2}}$$

$$M = -P \cdot l_0 \cdot \eta \cdot \sqrt{2}$$

CASE 1, 1000 N.

$$E_X := 12 \cdot 10^9 \quad P := 1000 \quad h := 0.495$$

$$I_y := \frac{w h^3}{12} \quad E_y := 0.02 E_X \quad l_{\text{span}} := 5 \quad w := 1 \quad l_{\text{deck}} := 10$$

$$I_X := \frac{h^3}{12} \quad k := \frac{48 \cdot E_X \cdot I_X}{l_{\text{deck}}^3}$$

$$l_0 := \sqrt[4]{\frac{E_y \cdot I_y}{k}} = 0.803$$

$$x := 0.5$$

$$\xi := \frac{x}{l_0 \sqrt{2}} = 0.44 \quad \frac{l_{\text{span}}}{l_0 \sqrt{2}} = 4.401$$

$$\eta := 0.275$$

$$M_x := -P \cdot l_0 \cdot \eta \cdot \sqrt{2} = -312.46$$

$$x_w := 1$$

$$\xi_w := \frac{x_w}{l_0 \sqrt{2}} = 0.88 \quad \frac{l_{\text{span}}}{l_0 \sqrt{2}} = 4.401$$

$$\eta_w := 0.32$$

$$M_{x_w} := -P \cdot l_0 \cdot \eta_w \cdot \sqrt{2} = -363.59$$

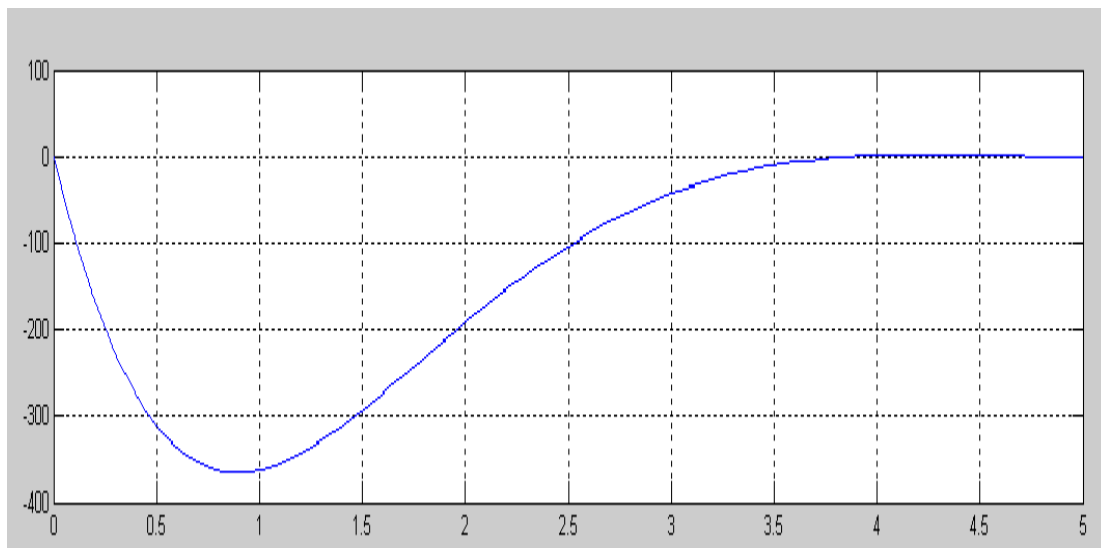
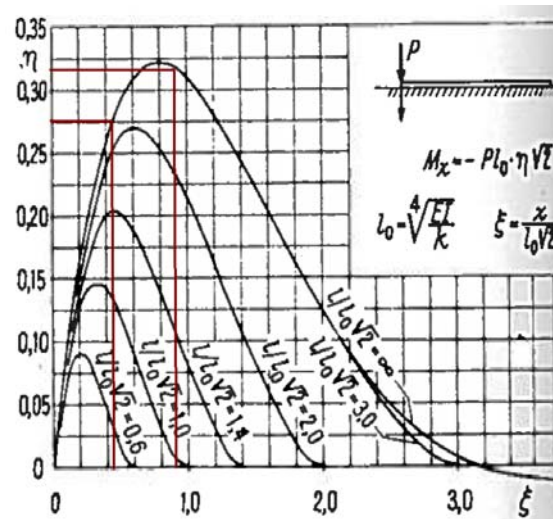


Figure C.4 Top right. Influence-lines for moment in beam on elastic foundation with values for the calculations to the left. Bottom. Y-axis: Moment distribution from CALFEM, X-axis: width of plate.

CASE 2, 1300 N.

$$E_x := 11.887 \cdot 10^9 \quad P := 1300 \quad h := 0.033$$

$$I_y := \frac{wh^3}{12} \quad E_y := 0.173 E_x \quad l_{\text{span}} := 1.8 \quad w := 1 \quad l_{\text{deck}} := 2$$

$$I_x := \frac{h^3}{12} \quad k := \frac{48 \cdot E_x \cdot I_x}{l_{\text{deck}}^3}$$

$$l_0 := \sqrt[4]{\frac{E_y \cdot I_y}{k}} = 0.412$$

$$x := 0.3$$

$$\xi := \frac{x}{l_0 \sqrt{2}} = 0.858 \quad \frac{l_{\text{span}}}{l_0 \sqrt{2}} = 3.089$$

$$\eta := 0.32$$

$$M_x := -P \cdot l_0 \cdot \eta \cdot \sqrt{2} = -242.428$$

$$x := 1$$

$$\xi := \frac{x}{l_0 \sqrt{2}} = 1.716 \quad \frac{l_{\text{span}}}{l_0 \sqrt{2}} = 3.089$$

$$\eta := 0.177$$

$$M_w := -P \cdot l_0 \cdot \eta \cdot \sqrt{2} = -134.093$$

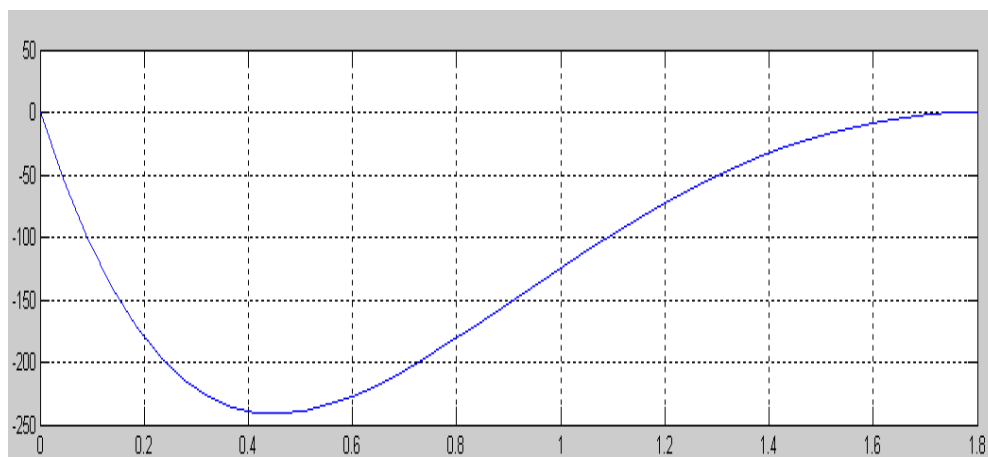
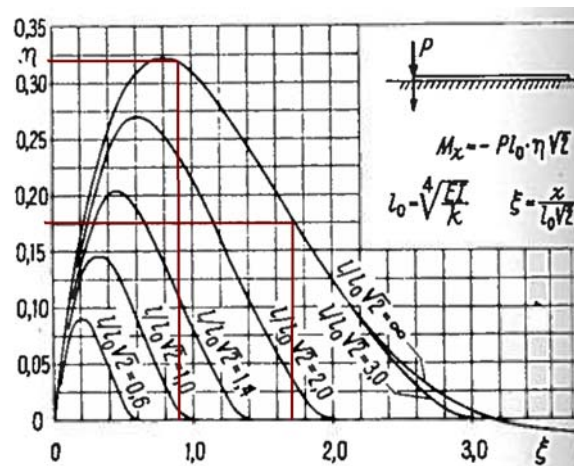


Figure C.5 Top right. Influence-lines for moment in beam on elastic foundation with values for the calculations to the left. Bottom. Y-axis: Moment distribution from CALFEM, X-axis: width of plate.

CASE 3, 480 N.

$$E_x := 11.887 \cdot 10^9 \quad P := 480 \quad h := 0.033$$

$$I_y := \frac{wh^3}{12} \quad E_y := 0.173 E_x \quad l_{\text{span}} := 0.3 \quad w := 1 \quad l_{\text{deck}} := 2$$

$$I_x := \frac{h^3}{12} \quad k := \frac{48 \cdot E_x \cdot I_x}{l_{\text{deck}}^3}$$

$$l_0 := \sqrt[4]{\frac{E_y \cdot I_y}{k}} = 0.412$$

$$x := 0.1$$

$$\xi := \frac{x}{l_0 \sqrt{2}} = 0.172 \quad \frac{l_{\text{span}}}{l_0 \sqrt{2}} = 0.515$$

$$\eta := 0.075$$

$$M_x := -P \cdot l_0 \cdot \eta \cdot \sqrt{2} = -20.979$$

$$x := 0.2$$

$$\xi := \frac{x}{l_0 \sqrt{2}} = 0.343 \quad \frac{l_{\text{span}}}{l_0 \sqrt{2}} = 0.515$$

$$\eta := 0.035$$

$$M_x := -P \cdot l_0 \cdot \eta \cdot \sqrt{2} = -9.79$$

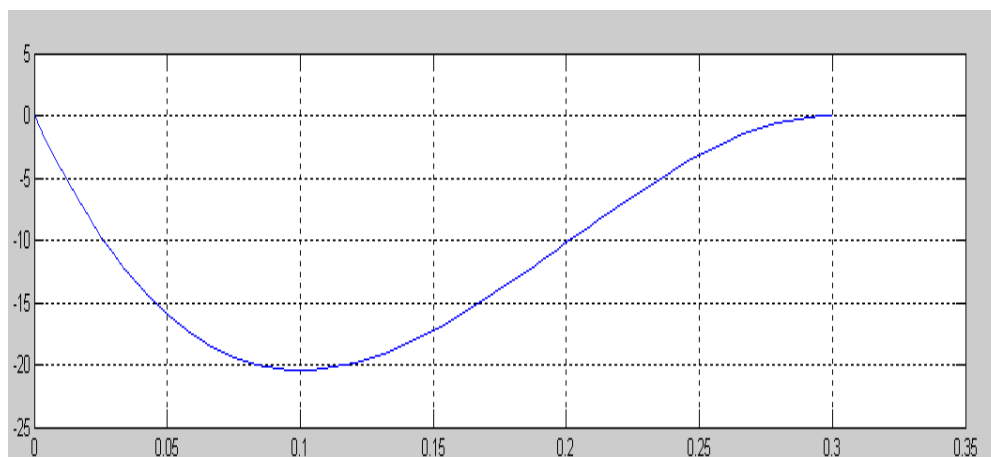
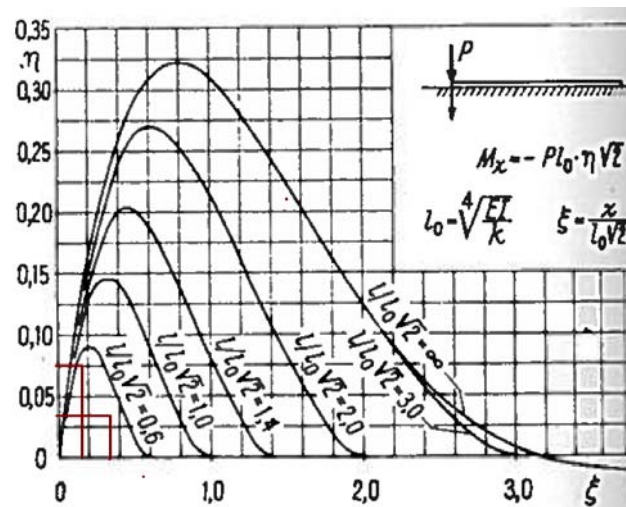


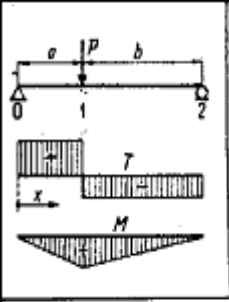
Figure C.6 Top right. Influence-lines for moment in beam on elastic foundation with values for the calculations to the left. Bottom. Y-axis: Moment distribution from CALFEM, X-axis: width of plate.

Appendix D1 – Convergence for creep

Table D.1 Convergence for creep with loading and unloading.

Loading			Unloading	
[min]	Time [sec]	def [mm]	Time [sec]	def [mm]
	10	14,486	1210	0,696
	20	14,546	1220	0,676
	30	14,59	1230	0,666
	40	14,621	1240	0,652
	50	14,647	1250	0,648
1	60	14,667	1260	0,642
	80	14,7	1280	0,632
	100	14,725	1300	0,623
2	120	14,747	1320	0,616
	150	14,775	1350	0,608
3	180	14,797	1380	0,601
4	240	14,834	1440	0,589
5	300	14,864	1500	0,58
6	360	14,888	1560	0,572
7	420	14,91	1620	0,567
8	480	14,928	1680	0,561
9	540	14,945	1740	0,557
10	600	14,961	1800	0,553
11	660	14,976	1860	0,55
12	720	14,989	1920	0,546
13	780	15	1980	0,544
14	840	15,012	2040	0,542
15	900	15,022	2100	0,539
16	960	15,032	2160	0,537
17	1020	15,042	2220	0,535
18	1080	15,051	2280	0,533
19	1140	15,061	2340	0,531
20	1200	15,068	2400	0,53

Appendix D2 – Computations for modulus of elasticity



$R_A = \frac{Pb}{l}$	$w_a = Pb \left(1 - \frac{b^2}{l^2}\right)$	$M_x^{0-1} = \frac{Pbx}{l}$
$R_B = \frac{Pa}{l}$	$w_b = Pa \left(1 - \frac{a^2}{l^2}\right)$	$M_x^{1-2} = \frac{Pa(l-x)}{l}$
$T_x^{0-1} = R_A$	$y_{\text{mitt}} = \frac{Pa(3l^2 - 4a^2)}{48EI}$	$M_{\text{max}} = M_1 = \frac{Pab}{l}$
$T_x^{1-2} = -R_B$	$(a < b)$	
$y^{0-1} = \frac{Plbx}{6EI} \left(1 - \frac{b^2}{l^2} - \frac{x^2}{l^2}\right)$		
$y^{1-2} = \frac{Pla(l-x)}{6EI} \left(\frac{2x}{l} - \frac{a^2}{l^2} - \frac{x^2}{l^2}\right)$		
$y_1 = \frac{Pa^2b^3}{3EI}$		
Beträffande R, T och M jfr : 415 A. Beträffande y jfr : 414 och : 909 A.		

Load

$$P := 19.9 \text{ kg} \cdot g = 196.035 \text{ N}$$

$$d := 200 \text{ mm}$$

For Ex

$$h := 0.033 \text{ m}$$

$$a_1 := \frac{1-d}{2} = 0.9 \text{ m}$$

$$a_2 := \frac{1+d}{2} = 1.1 \text{ m}$$

$$b_1 := 1 - a_1$$

$$b_2 := 1 - a_2$$

$$y_{1_midspan} = P \cdot \frac{l \cdot a_1 \left(1 - \frac{1}{2}\right)}{6 \cdot E \cdot I} \cdot \left[1 - \frac{a_1^2}{l^2} - \frac{\left(\frac{1}{2}\right)^2}{l^2}\right]$$

$$y_{1_midspan_E} := P \cdot \frac{l \cdot a_1 \left(1 - \frac{1}{2}\right)}{6 \cdot I} \cdot \left[1 - \frac{a_1^2}{l^2} - \frac{\left(\frac{1}{2}\right)^2}{l^2}\right] = 5.973 \times 10^6 \cdot \text{m} \cdot \text{Pa}$$

$$y_{2_midspan} = \frac{P \cdot l \cdot b_2 \cdot l}{2 \cdot 6 \cdot E \cdot I} \cdot \left[1 - \frac{b_2^2}{l^2} - \frac{\left(\frac{1}{2}\right)^2}{l^2}\right]$$

$$y_{2_midspan_E} := \frac{P \cdot l \cdot b_2 \cdot l}{2 \cdot 6 \cdot I} \cdot \left[1 - \frac{b_2^2}{l^2} - \frac{\left(\frac{1}{2}\right)^2}{l^2}\right] = 5.973 \times 10^6 \cdot \text{m} \cdot \text{Pa}$$

$$y_{\text{tot}} \cdot E = y_{1_midspan} \cdot E + y_{2_midspan} \cdot E \quad y_{\text{tot}1} := 1.005 \text{mm}$$

$$E_x := \frac{y_{1_midspan_E} + y_{2_midspan_E}}{y_{\text{tot}1}} = 11.887 \text{GPa}$$

For Ey

$$l := 1.8 \text{m} \quad h := 0.033 \text{m} \quad b := 2 \text{m}$$

$$a_1 := \frac{l-d}{2} = 0.8 \text{m} \quad a_2 := \frac{l+d}{2} = 1 \text{m}$$

$$b_1 := l - a_1 \quad b_2 := l - a_2$$

$$I := \frac{b \cdot h^3}{12}$$

$$y_{1_midspan} = P \cdot \frac{l \cdot a_1 \left(1 - \frac{1}{2}\right)}{6 \cdot E \cdot I} \cdot \left[1 - \frac{a_1^2}{l^2} - \frac{\left(\frac{1}{2}\right)^2}{l^2}\right]$$

$$y_{1_midspan_E} := P \cdot \frac{l \cdot a_1 \left(1 - \frac{1}{2}\right)}{6 \cdot I} \cdot \left[1 - \frac{a_1^2}{l^2} - \frac{\left(\frac{1}{2}\right)^2}{l^2}\right] = 3.906 \times 10^6 \cdot \text{m} \cdot \text{Pa}$$

$$y_{2_midspan} = \frac{P \cdot l \cdot b_2 \cdot l}{2 \cdot 6 \cdot E \cdot I} \cdot \left[1 - \frac{b_2^2}{l^2} - \frac{\left(\frac{1}{2}\right)^2}{l^2}\right]$$

$$y_{2_midspan_E} := \frac{P \cdot l \cdot b_2 \cdot l}{2 \cdot 6 \cdot I} \cdot \left[1 - \frac{b_2^2}{l^2} - \frac{\left(\frac{1}{2}\right)^2}{l^2}\right] = 3.906 \times 10^6 \cdot \text{m} \cdot \text{Pa}$$

$$y_{\text{tot}} \cdot E = y_{1_midspan} \cdot E + y_{2_midspan} \cdot E \quad y_{\text{tot}2} := 3.808666667 \text{mm}$$

$$E_y := \frac{y_{1_midspan_E} + y_{2_midspan_E}}{y_{\text{tot}2}} = 2.051 \cdot \text{GPa}$$

Caclulated E, according to STEP1

$$EI = \sum_i (E_i I_i)$$

$$E_0 := 13.8 \text{ GPa} \quad E_{90} := 0.43 \text{ GPa}$$

$$b := 1$$

$$d := \frac{0.033}{11}$$

$$E_{\text{paralell}} I = E_0 \left[\frac{9 \cdot d^3}{12} + 2 \cdot (2 \cdot d) \cdot [(1.5 \cdot d)^2 + (4.5 \cdot d)^2] \right] + E_{90} \left[\frac{2 \cdot d^3}{12} + 2 \cdot (1 \cdot d) \cdot (3 \cdot d)^2 \right]$$

$$E_{\text{paralell}} := \frac{E_0 \left[\frac{9 \cdot d^3}{12} + 2 \cdot (2 \cdot d) \cdot [(1.5 \cdot d)^2 + (4.5 \cdot d)^2] \right] + E_{90} \left[\frac{2 \cdot d^3}{12} + 2 \cdot (1 \cdot d) \cdot (3 \cdot d)^2 \right]}{\frac{(11 \cdot d)^3}{12}} = 11.36 \text{ GPa}$$

$$E_{\text{perpendicular}} I = E_0 \left[\frac{2 \cdot d^3}{12} + 2 \cdot (1 \cdot d) \cdot (3 \cdot d)^2 \right] + E_{90} \left[\frac{9 \cdot d^3}{12} + 2 \cdot (2 \cdot d) \cdot [(1.5 \cdot d)^2 + (4.5 \cdot d)^2] \right]$$

$$E_{\text{perpendicular}} := \frac{E_0 \left[\frac{2 \cdot d^3}{12} + 2 \cdot (1 \cdot d) \cdot (3 \cdot d)^2 \right] + E_{90} \left[\frac{9 \cdot d^3}{12} + 2 \cdot (2 \cdot d) \cdot [(1.5 \cdot d)^2 + (4.5 \cdot d)^2] \right]}{\frac{(11 \cdot d)^3}{12}} = 2.61 \text{ GPa}$$

Appendix D3 – Procedure for testing of LVL

Dimensions of tested plates $L \times B = 2 \times (0.3, 0.6, 0.9, 1.8)$ and $1.4 \times 1.8 \text{ m}^2$.

Applied load, $P = 0.46, 0.872, 1.302, 1.744$ and 1.310 kN .

Procedure:

1. Place first plate on supports
2. Load with P at $Lc1$ as can be seen in *Figure D1*
3. Deformations are measured after five minutes
4. Unload, remaining deformations are noted five minutes after unloading
5. Remove transducers at position 9, 10, 11 and change the boundary conditions so that the plate is no longer free for uplift, for boundary conditions see *Picture D1 and D2*
6. Change from $LC1$ to $LC2$ and redo the same procedure as for $LC1$
7. Redo step 1-7 for the next plate

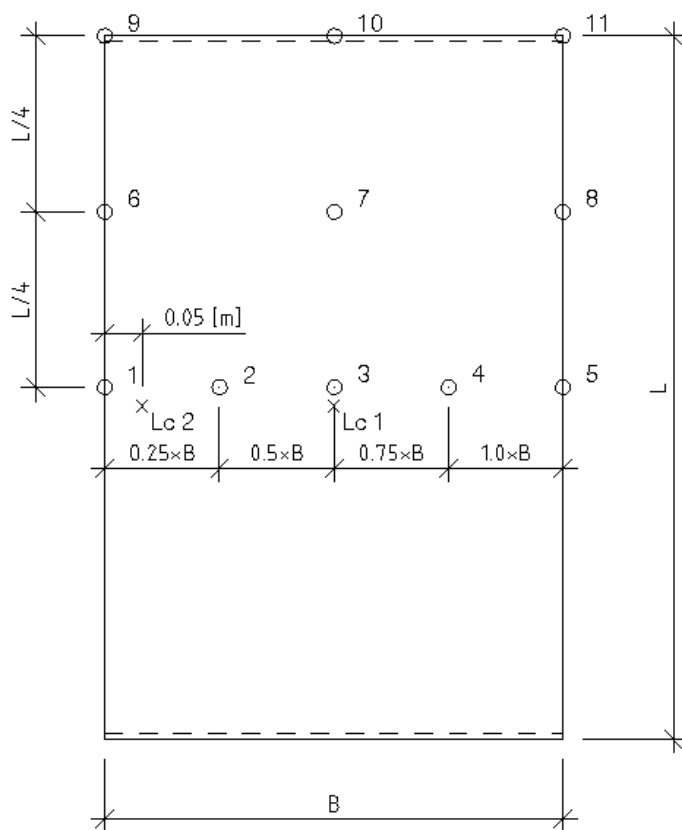


Figure D.1 Load placement and measure points for the simply supported plates.



Picture D.1 Support conditions when simply supported.



Picture D.2 Support conditions when fixed.

Appendix D4 – Expected plate deflections

Expected plate deflection according to different hand-calculation methods

Reference: Z:\Skolan\Exjobb\Till Storegate\MOE from experiment.xmcd

ORIGIN:= 1

Dimensions and indata for the test

$$E_x := E_x = 11.887 \text{ GPa}$$

From Appendix D2, according to our test

$$E_y := E_y = 2.051 \text{ GPa}$$

$$G_0 := 600 \frac{\text{N}}{\text{mm}^2}$$

From manufactures, Table 2.7 Kerto Teknisk handbok from Moelven

Dimensions of plates

$$l_{\text{span}} := 2 \text{ m}$$

Length of span

$$b_{\text{deck}} := \begin{pmatrix} 1800 \\ 900 \\ 600 \\ 300 \end{pmatrix} \text{ mm}$$

Width of plates

$$t := 33 \text{ mm}$$

Thickness of plates

Loads

$$P := \begin{bmatrix} (2.5 + 45 + 44.4 + 43.9 + 42) \text{ kg} \\ (2.5 + 44.4 + 43.9 + 42) \text{ kg} \\ (2.5 + 42 + 44.4) \text{ kg} \\ (2.5 + 44.4) \text{ kg} \end{bmatrix} \cdot g = \begin{pmatrix} 1.744 \\ 1.302 \\ 0.872 \\ 0.46 \end{pmatrix} \cdot \text{kN}$$

Parameters that will be used in calculations

$$C_B := 1.0$$

No effects from butt joints

$$l_{\text{bridge}} := 15 \text{ m}$$

Length of bridge that our scale tests are based on.

$$\eta := \frac{l_{\text{bridge}}}{l_{\text{span}}} = 7.5$$

Factor that the calculated effective width should be scaled with

Expected deflections according to the different hand calculation methods

Ritter

$$b_{\text{ritter}} := \eta \cdot b_{\text{deck}} = \begin{pmatrix} 13.5 \\ 6.75 \\ 4.5 \\ 2.25 \end{pmatrix} \text{ m} \quad \text{Width of scaled bridge}$$

Effective width

$$\alpha := \frac{2 \cdot G_0}{\sqrt{E_0 \cdot C_B \cdot E_{90}}} = 0.243$$

$$\theta := \frac{b_{\text{ritter}}}{2 \cdot l_{\text{bridge}}} \cdot \left(\frac{E_0 \cdot C_B}{E_{90}} \right)^{0.25} = \begin{pmatrix} 0.698 \\ 0.349 \\ 0.233 \\ 0.116 \end{pmatrix}$$

a - Parameter for the Decks torsional stiffness

? - Relation between the deck stiffness in longitudinal and transversal direction

$$D_{w_ritter} := 1800 \text{ mm}$$

From diagram according to Ritter (1990), and modified by Dahl (2002).

$$D_w := \frac{D_{w_ritter}}{\eta} = 0.24 \text{ m}$$

Scaled width with respect to scale factor

Second moment of inertia, I, and deflection, w.

$$I_w := \frac{D_w \cdot t^3}{12} = 7.187 \times 10^{-7} \text{ m}^4$$

$$w_{\text{Ritter}} := \frac{P_4 \cdot l_{\text{span}}^3}{48 \cdot E_0 \cdot 1.33 I_w} = 6.746 \text{ mm}$$

For the load P=0.46 kN

Where I is increased due to deflection calculations.

Eurocode 5

Effective width

$$b_w := 0.6 \text{ m}$$

Width of wheel

$$\beta := 45 \text{ deg}$$

Dispersion angle according to EN 1995-2:2004 (E), Table 5.2

$$a := 0.5\text{m}$$

For cross laminated timber according to EN 1995-2:2004 (E), Table 5.3

$$b_{w_middle} := b_w + \eta \cdot t \cdot \sin(\beta) = 0.775\text{m}$$

$$D_{w_EC5} := b_{w_middle} + a$$

$$D_{w_EC5} = 1.275\text{m}$$

$$D_{w_scaled} := \frac{D_{w_EC5}}{\eta} = 0.17\text{m}$$

Scaled width with respect to scale factor

Second moment of inertia, I , and deflection, w .

$$I_w := \frac{D_w \cdot t^3}{12} = 5.091 \times 10^{-7} \text{ m}^4$$

$$w_{EC5} := \frac{P_4 \cdot l_{span}^3}{48 \cdot E_0 \cdot I} = 12.667\text{mm}$$

For the load $P=0.46 \text{ kN}$

Crews

Distribution width

$$D_w = \left[\left(\frac{E_0}{10000} \right)^{0.50} + \frac{L}{25} + 0.45 \right] \cdot C_B \quad \text{for a single lane bridge}$$

$$D_{w_crews} := \left[\left(\frac{E_0}{10000 \text{ MPa}} \right)^{0.50} + \frac{l_{bridge}}{25 \cdot \text{m}} + 0.45 \right] \cdot C_B \cdot 1\text{m}$$

$$D_{w_crews} = 2.14\text{m}$$

$$D_{w_scaled} := \frac{D_{w_crews}}{\eta} = 0.285\text{m}$$

Scaled width with respect to scale factor

Second moment of inertia, I , and deflection, w .

$$I_w := \frac{C_B \cdot D_w \cdot t^3}{12} = 8.546 \times 10^{-7} \cdot \text{m}^4$$

$$w_{\text{Crews}} := \frac{P_4 \cdot l_{\text{span}}^3}{48 \cdot E_0 \cdot I} = 7.546 \text{ mm}$$

For the load $P=0.46 \text{ kN}$

West Virginia University

Distribution width

$$D_w = (b_f + 2 \cdot t) \cdot C_B$$

$$b_f := \frac{b_w}{\eta} = 0.08 \text{ m}$$

Scaled wheel width with respect to scale factor

$$D_{w_W.V.U} := (b_f + 2 \cdot t) \cdot C_B$$

$$D_{w_W.V.U} = 0.146 \text{ m}$$

calculated distribution width according to W.V.U metl

$$D_{w_W.V.U} := D_{w_W.V.U} = 0.146 \text{ m}$$

Second moment of inertia, I, and deflection, w.

$$I_w := \frac{D_w \cdot t^3}{12} = 4.372 \times 10^{-7} \text{ m}^4$$

$$w_{W.V.U} := \frac{P_4 \cdot l_{\text{span}}^3}{48 \cdot E_0 \cdot 1.15 \cdot I} = 12.825 \text{ mm}$$

For the load $P=0.46 \text{ kN}$

Appendix D5 – Results from plate behaviour test

This section gives results from our tests performed on LVL plates with different dimensions and applied loads. All plates have the same thickness, 33mm.

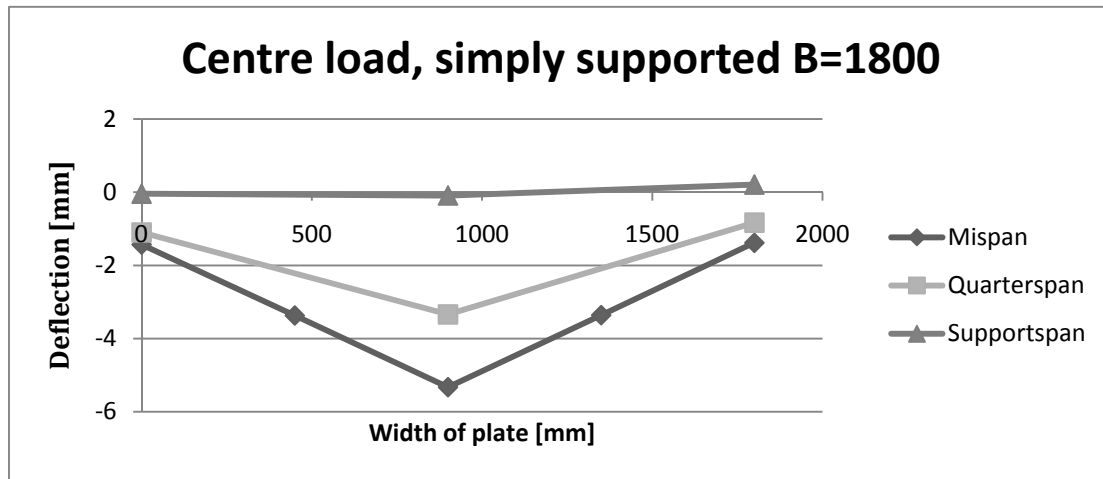


Figure D.2 Deflections for simply supported plate with dimensions $L \times B = 2 \times 1.8 \text{ m}^2$. Applied load $P=1.303 \text{ kN}$ in the middle of the plate.

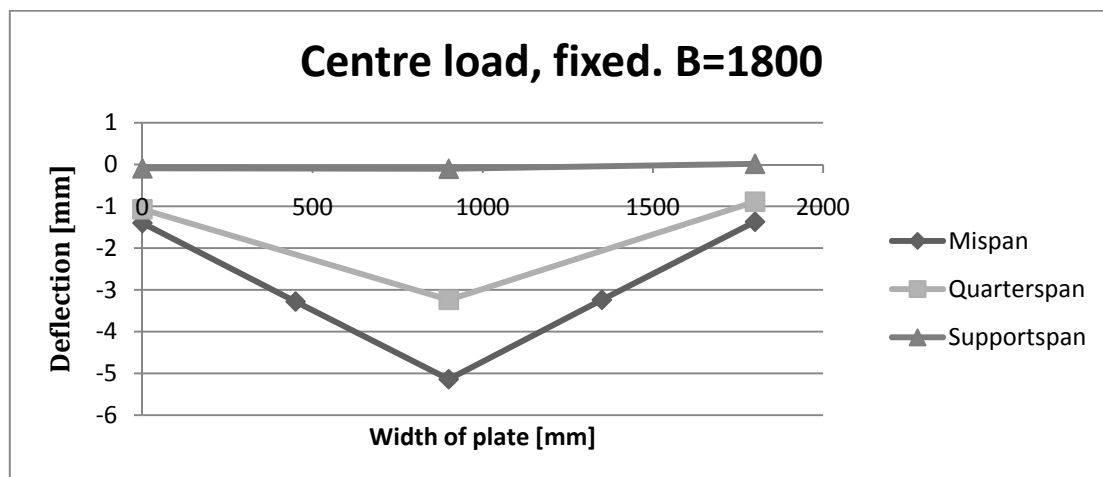


Figure D.3 Deflections for fixed plate with dimensions $L \times B = 2 \times 1.8 \text{ m}^2$. Applied load $P=1.303 \text{ kN}$ in the middle of the plate.

Table D.2 Measured deflections for the plate with dimensions $L \times B = 2 \times 1.8$ m^2 . Applied load $P=1.303$ kN in the centre of the plate (measure point 3). Simply supported and fixed respectively.

LC1, simply	mm	Measure point	Deflection
Midspan	0	1	-1,43
	450	2	-3,37
	900	3	-5,33
	1350	4	-3,36
	1800	5	-1,38
Quarter span	0	6	-1,1
	900	7	-3,34
	1800	8	-0,83
Support span	0	9	-0,04
	900	10	-0,09
	1800	11	0,21

LC1, fixed	mm	Measure point	Deflection
Midspan	0	1	-1,4
	450	2	-3,28
	900	3	-5,14
	1350	4	-3,24
	1800	5	-1,37
Quarter span	0	6	-1,07
	900	7	-3,24
	1800	8	-0,89
Support span	0	9	-0,09
	900	10	-0,1
	1800	11	0,02

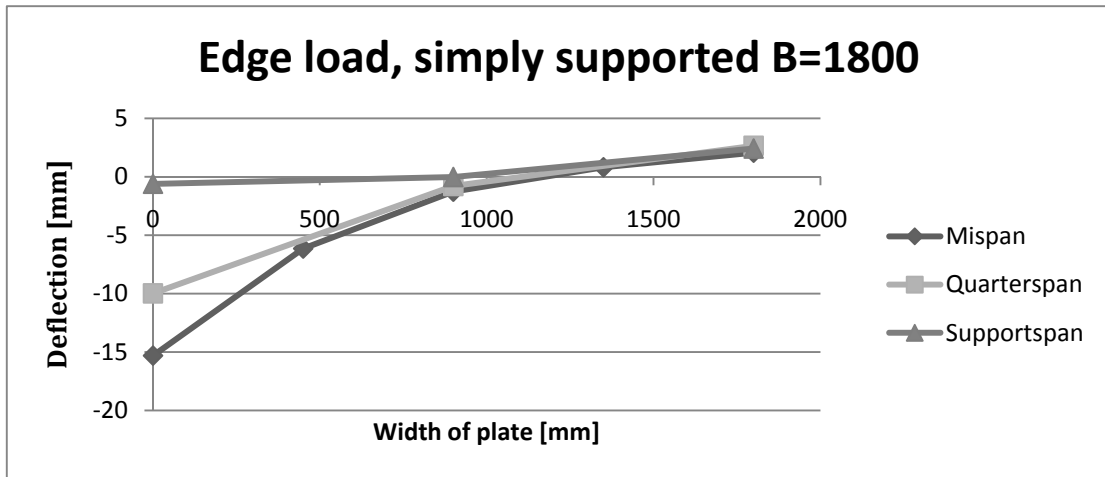


Figure D.5 Deflections for simply supported plate with dimensions $L \times B = 2 \times 1.8 \text{ m}^2$. Applied load $P=1.303 \text{ kN}$ at the edge of the plate.

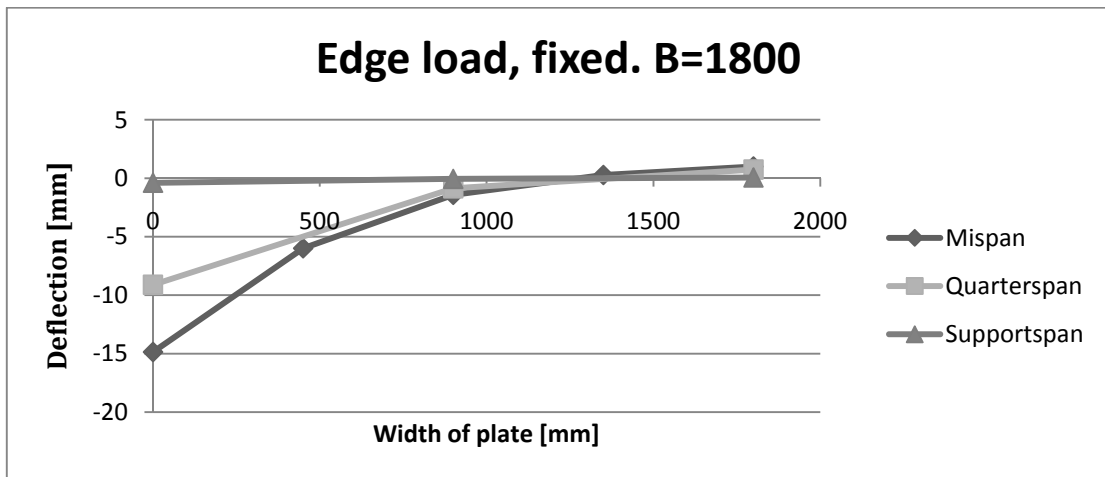


Figure D.6 Deflections for fixed plate with dimensions $L \times B = 2 \times 1.8 \text{ m}^2$. Applied load $P=1.303 \text{ kN}$ at the edge of the plate.

Table D.3 Measured deflections for the plate with dimensions $L \times B = 2 \times 1.8 \text{ m}^2$. Applied load $P=1.303 \text{ kN}$ at the edge of the plate (measure point 1). Simply supported and fixed respectively.

LC2, simply	mm	Measure point	Deflection
Midspan	0	1	-15,31
	450	2	-6,14
	900	3	-1,27
	1350	4	0,82
	1800	5	2,07
Quarter span	0	6	-9,98
	900	7	-0,78
	1800	8	2,66
Support span	0	9	-0,6
	900	10	-0,02
	1800	11	2,42

LC2, fixed	mm	Measure point	Deflection
Midspan	0	1	-14,864
	450	2	-5,99
	900	3	-1,424
	1350	4	0,28
	1800	5	1,006
Quarter span	0	6	-9,11
	900	7	-0,86
	1800	8	0,74
Support span	0	9	-0,39
	900	10	-0,06
	1800	11	0,06

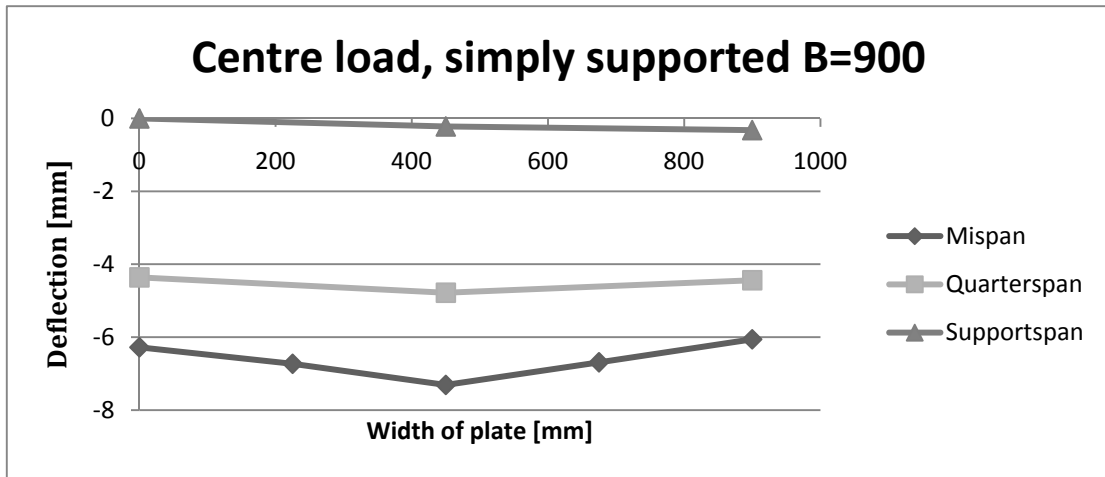


Figure D.8 Deflections for simply supported plate with dimensions $L \times B = 2 \times 0.9 \text{ m}^2$. Applied load $P=1.303 \text{ kN}$ in the middle of the plate.

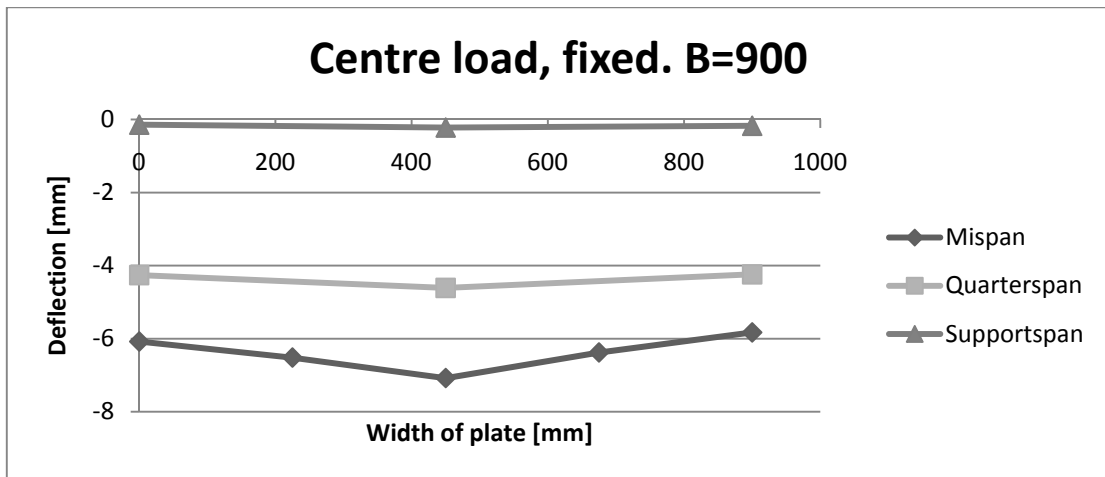


Figure D.9 Deflections for fixed plate with dimensions $L \times B = 2 \times 0.9 \text{ m}^2$. Applied load $P=1.303 \text{ kN}$ in the middle of the plate.

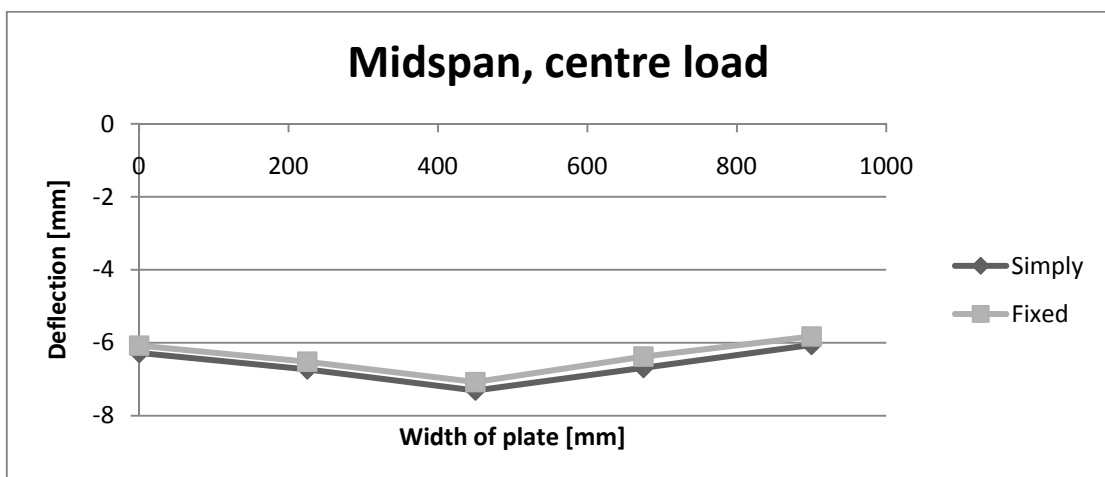


Figure D.10 Deflections in the mid span for simply supported and fixed plate, with dimensions $L \times B = 2 \times 0.9 \text{ m}^2$. Applied load $P=1.303 \text{ kN}$ in the middle of the plate.

Table D.4 Measured deflections for the plate with dimensions $L \times B = 2 \times 0.9$ m^2 . Applied load $P=1.303$ kN in the centre of the plate (measure point 3). Simply supported and fixed respectively.

LC1, simply	mm	Measure point	Deflection
Midspan	0	1	-6,28
	225	2	-6,73
	450	3	-7,31
	675	4	-6,69
	900	5	-6,06
Quarter span	0	6	-4,36
	450	7	-4,78
	900	8	-4,44
Support span	0	9	0
	450	10	-0,22
	900	11	-0,32

LC1, fixed	mm	Measure point	Deflection
Midspan	0	1	-6,08
	225	2	-6,52
	450	3	-7,08
	675	4	-6,38
	900	5	-5,83
Quarter span	0	6	-4,26
	450	7	-4,61
	900	8	-4,24
Support span	0	9	-0,14
	450	10	-0,22
	900	11	-0,17

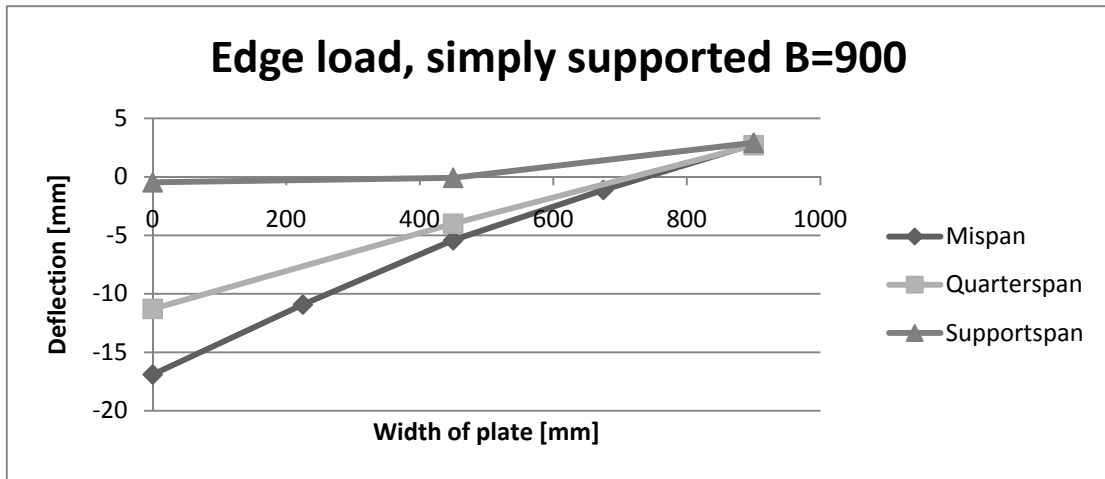


Figure D.11 Deflections for simply supported plate with dimensions $L \times B = 2 \times 0.9 \text{ m}^2$. Applied load $P=1.303 \text{ kN}$ at the edge of the plate.

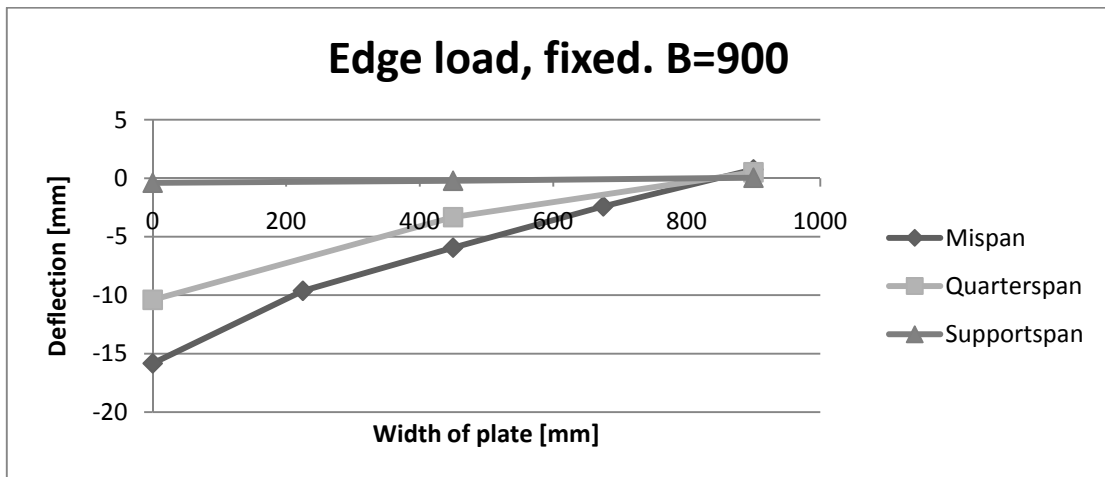


Figure D.12 Deflections for fixed plate with dimensions $L \times B = 2 \times 0.9 \text{ m}^2$. Applied load $P=1.303 \text{ kN}$ at the edge of the plate.

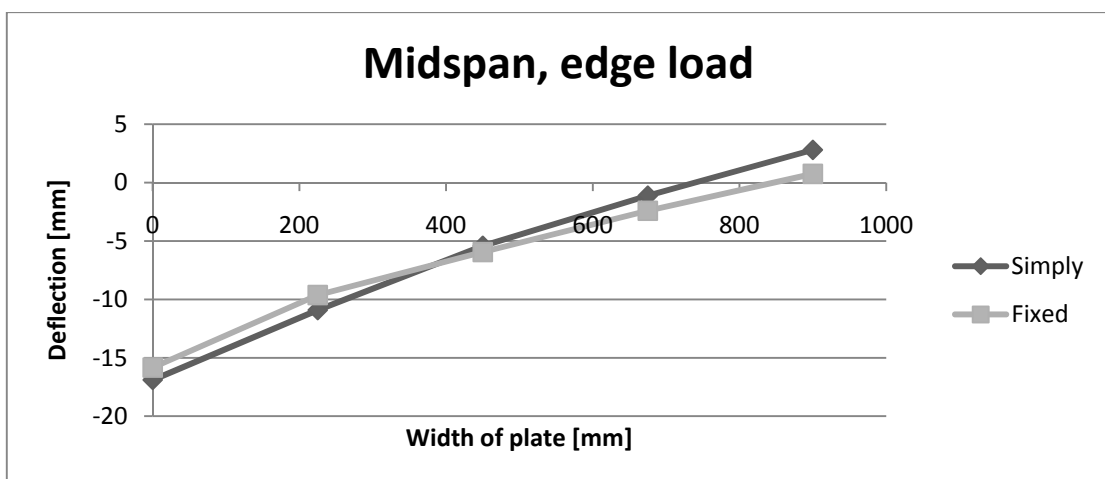


Figure D.13 Deflections in mid span for simply supported and fixed plate, with dimensions $L \times B = 2 \times 0.9 \text{ m}^2$. Applied load $P=1.303 \text{ kN}$ at the edge of the plate.

Table D.5 Measured deflections for the plate with dimensions $L \times B = 2 \times 0.9 \text{ m}^2$. Applied load $P=1.303 \text{ kN}$ at the edge of the plate (measure point 1). Simply supported and fixed respectively.

LC2, simply	mm	Measure point	Deflection
Midspan	0	1	-16,9
	225	2	-10,92
	450	3	-5,42
	675	4	-1,12
	900	5	2,8
Quarter span	0	6	-11,29
	450	7	-4
	900	8	2,71
Support span	0	9	-0,47
	450	10	-0,08
	900	11	2,92

LC2, fixed	mm	Measure point	Deflection
Midspan	0	1	-15,837
	225	2	-9,63
	450	3	-5,945
	675	4	-2,41
	900	5	0,752
Quarter span	0	6	-10,4
	450	7	-3,33
	900	8	0,51
Support span	0	9	-0,39
	450	10	-0,22
	900	11	0,04

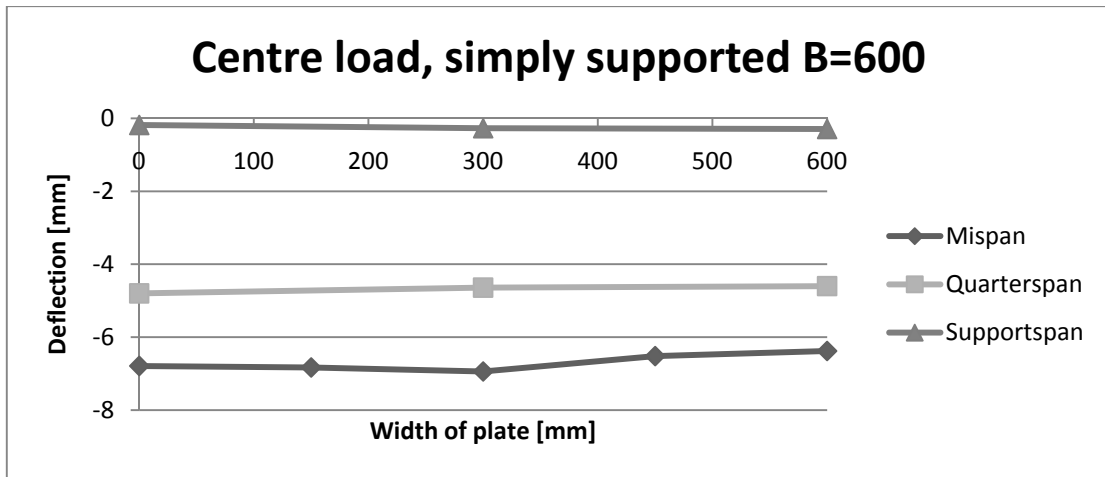


Figure D.14 Deflections for simply supported plate with dimensions $L \times B = 2 \times 0.6 \text{ m}^2$. Applied load $P=0.872 \text{ kN}$ in the middle of the plate.

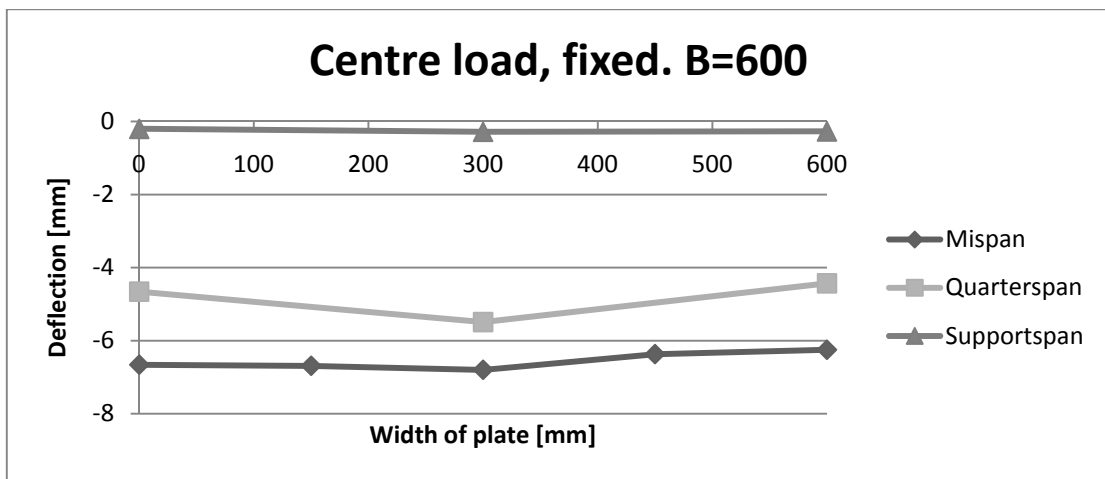


Figure D.15 Deflections for fixed plate with dimensions $L \times B = 2 \times 0.6 \text{ m}^2$. Applied load $P=0.872 \text{ kN}$ in the middle of the plate.

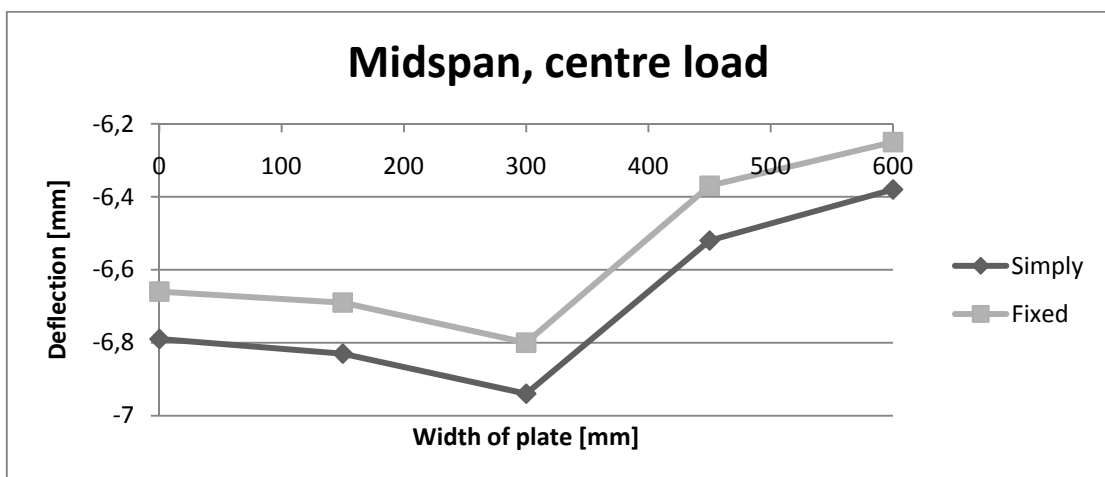


Figure D.16 Deflections in the mid span for simply supported and fixed plate, with dimensions $L \times B = 2 \times 0.6 \text{ m}^2$. Applied load $P=0.872 \text{ kN}$ in the middle of the plate.

Table D.6 Measured deflections for the plate with dimensions $L \times B = 2 \times 0.6 \text{ m}^2$. Applied load $P=0.872 \text{ kN}$ in the centre of the plate (measure point 3). Simply supported and fixed respectively.

LC1, simply	mm	Measure point	Deflection
Midspan	0	1	-6,79
	150	2	-6,83
	300	3	-6,94
	450	4	-6,52
	600	5	-6,38
Quarter span	0	6	-4,8
	300	7	-4,64
	600	8	-4,6
Support span	0	9	-0,18
	300	10	-0,27
	600	11	-0,29

LC1, fixed	mm	Measure point	Deflection
Midspan	0	1	-6,66
	150	2	-6,69
	300	3	-6,8
	450	4	-6,37
	600	5	-6,25
Quarter span	0	6	-4,66
	300	7	-5,49
	600	8	-4,43
Support span	0	9	-0,2
	300	10	-0,28
	600	11	-0,27

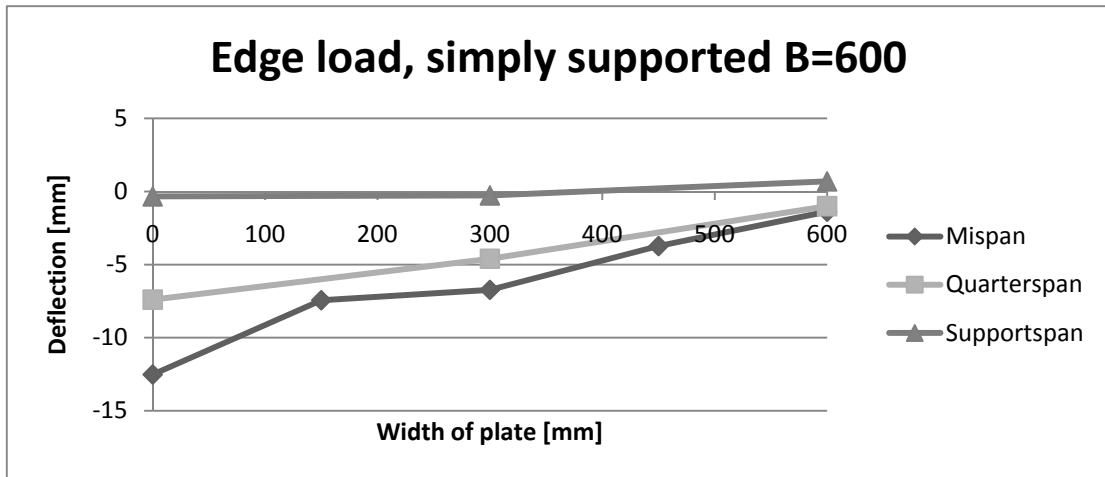


Figure D.17 Deflections for simply supported plate with dimensions $L \times B = 2 \times 0.6 \text{ m}^2$. Applied load $P=0.872 \text{ kN}$ at the edge of the plate.

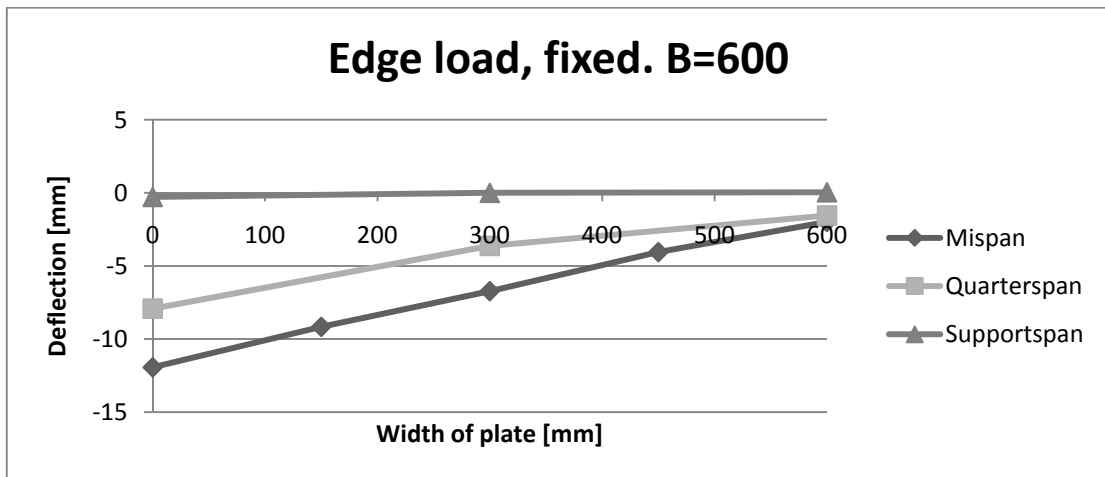


Figure D.18 Deflections for fixed plate with dimensions $L \times B = 2 \times 0.6 \text{ m}^2$. Applied load $P=0.872 \text{ kN}$ at the edge of the plate.

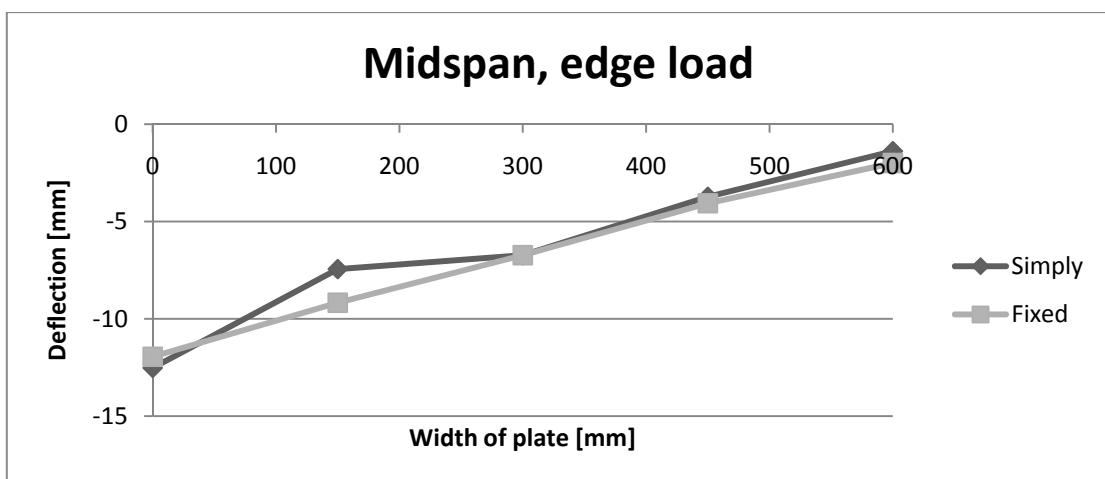


Figure D.19 Deflections in mid span for simply supported and fixed plate, with dimensions $L \times B = 2 \times 0.6 \text{ m}^2$. Applied load $P=0.872 \text{ kN}$ at the edge of the plate.

Table D.7 Measured deflections for the plate with dimensions $L \times B = 2 \times 0.6 \text{ m}^2$. Applied load $P=0.872 \text{ kN}$ at the edge of the plate (measure point 1). Simply supported and fixed respectively.

LC2, simply	mm	Measure point	Deflection
Midspan	0	1	-12,52
	150	2	-7,44
	300	3	-6,73
	450	4	-3,73
	600	5	-1,38
Quarter span	0	6	-7,4
	300	7	-4,6
	600	8	-1
Support span	0	9	-0,34
	300	10	-0,27
	600	11	0,69

LC2, fixed	mm	Measure point	Deflection
Midspan	0	1	-11,945
	150	2	-9,17
	300	3	-6,728
	450	4	-4,06
	600	5	-1,99
Quarter span	0	6	-7,92
	300	7	-3,63
	600	8	-1,55
Support span	0	9	-0,28
	300	10	0
	600	11	0,04

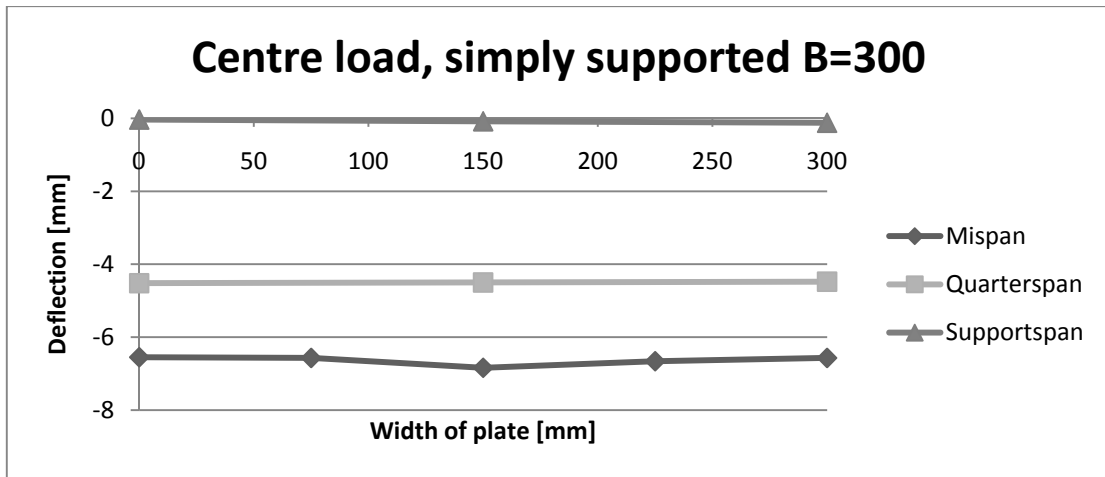


Figure D.20 Deflections for simply supported plate with dimensions $L \times B = 2 \times 0.3 \text{ m}^2$. Applied load $P=0.460 \text{ kN}$ in the middle of the plate.

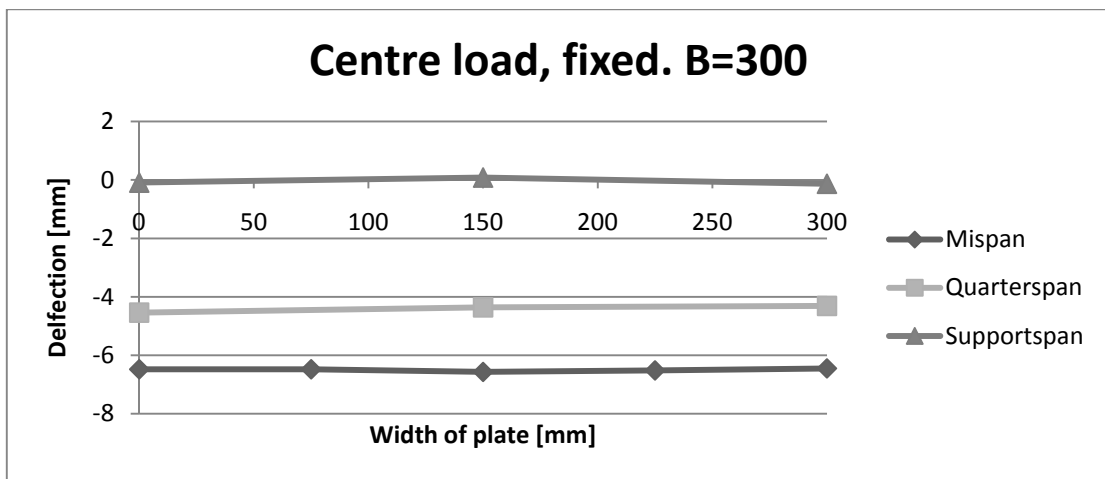


Figure D.21 Deflections for fixed plate with dimensions $L \times B = 2 \times 0.3 \text{ m}^2$. Applied load $P=0.460 \text{ kN}$ in the middle of the plate.

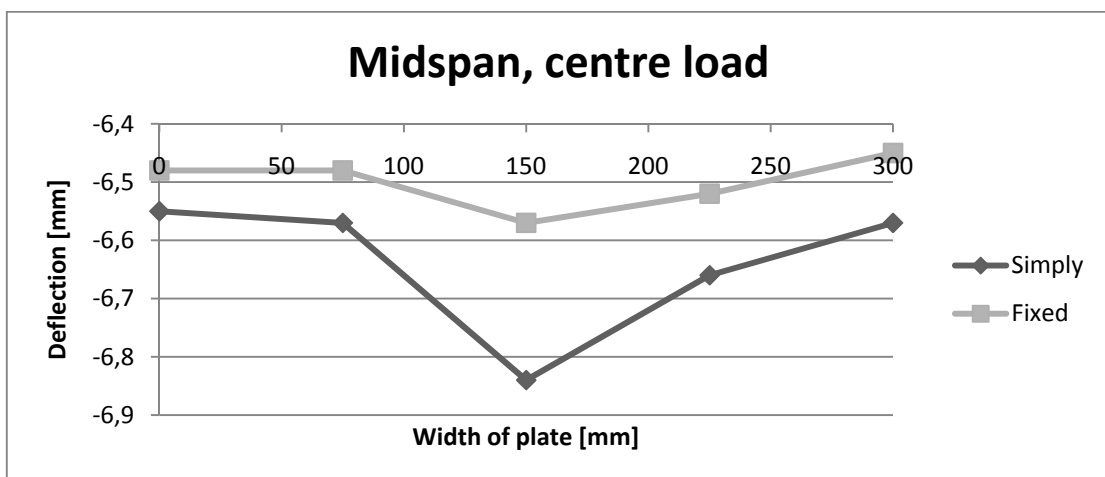


Figure D.22 Deflections in the mid span for simply supported and fixed plate, with dimensions $L \times B = 2 \times 0.3 \text{ m}^2$. Applied load $P=0.460 \text{ kN}$ in the middle of the plate.

Table D.8 Measured deflections for the plate with dimensions $L \times B = 2 \times 0.3 \text{ m}^2$. Applied load $P=0.460 \text{ kN}$ in the centre of the plate (measure point 3). Simply supported and fixed respectively.

LC1, simply	mm	Measure point	Deflection
Midspan	0	1	-6,55
	75	2	-6,57
	150	3	-6,84
	225	4	-6,66
	300	5	-6,57
Quarter span	0	6	-4,52
	150	7	-4,5
	300	8	-4,48
Support span	0	9	-0,03
	150	10	-0,08
	300	11	-0,12

LC1, fixed	mm	Measure point	Deflection
Midspan	0	1	-6,48
	75	2	-6,48
	150	3	-6,57
	225	4	-6,52
	300	5	-6,45
Quarter span	0	6	-4,54
	150	7	-4,36
	300	8	-4,31
Support span	0	9	-0,09
	150	10	0,08
	300	11	-0,13

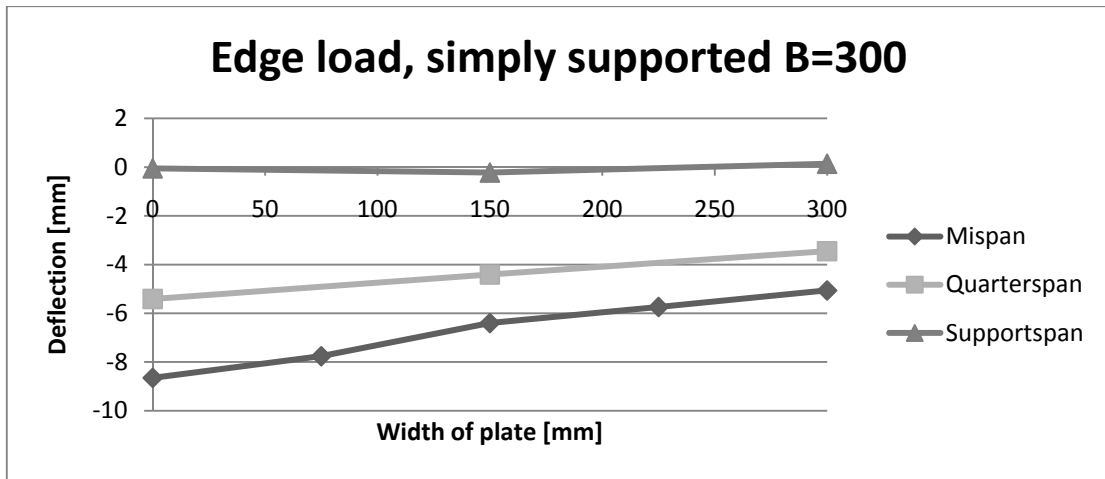


Figure D.23 Deflections for simply supported plate with dimensions $L \times B = 2 \times 0.3 \text{ m}^2$. Applied load $P=0.460 \text{ kN}$ at the edge of the plate.

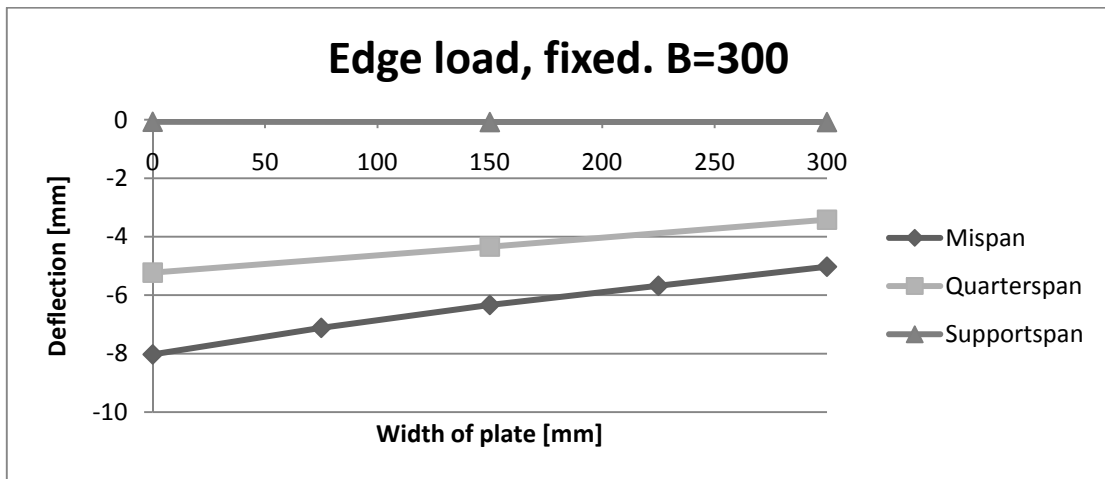


Figure D.24 Deflections for fixed plate with dimensions $L \times B = 2 \times 0.3 \text{ m}^2$. Applied load $P=0.460 \text{ kN}$ at the edge of the plate.

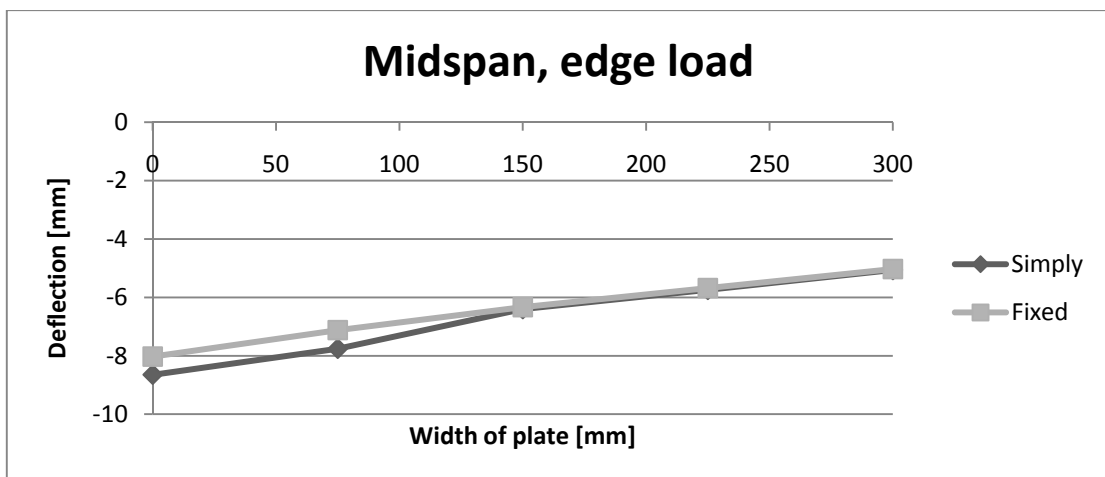


Figure D.25 Deflections in mid span for simply supported and fixed plate, with dimensions $L \times B = 2 \times 0.3 \text{ m}^2$. Applied load $P=0.460 \text{ kN}$ at the edge of the plate.

Table D.9 Measured deflections for the plate with dimensions $L \times B = 2 \times 0.3 \text{ m}^2$. Applied load $P=0.460 \text{ kN}$ at the edge of the plate (measure point 1). Simply supported and fixed respectively.

LC2, simply	mm	Measure point	Deflection
Midspan	0	1	-8,65
	75	2	-7,76
	150	3	-6,4
	225	4	-5,74
	300	5	-5,06
Quarter span	0	6	-5,41
	150	7	-4,41
	300	8	-3,45
Support span	0	9	-0,05
	150	10	-0,22
	300	11	0,14

LC2, fixed	mm	Measure point	Deflection
Midspan	0	1	-8,028
	75	2	-7,12
	150	3	-6,335
	225	4	-5,68
	300	5	-5,027
Quarter span	0	6	-5,23
	150	7	-4,34
	300	8	-3,42
Support span	0	9	-0,07
	150	10	-0,08
	300	11	-0,08

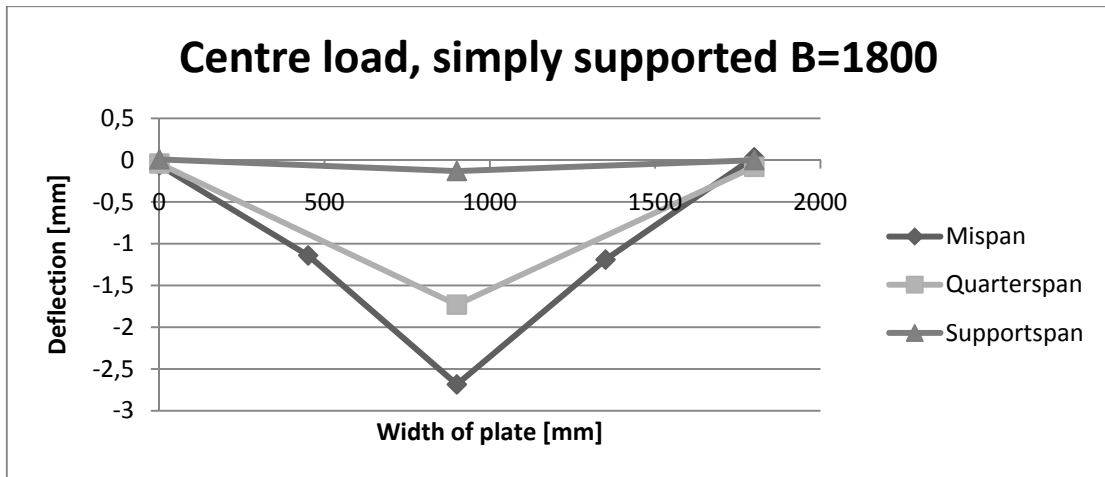


Figure D.26 Deflections for simply supported plate with dimensions $L \times B = 1.4 \times 1.8 \text{ m}^2$. Applied load $P=1.310 \text{ kN}$ in the middle of the plate.

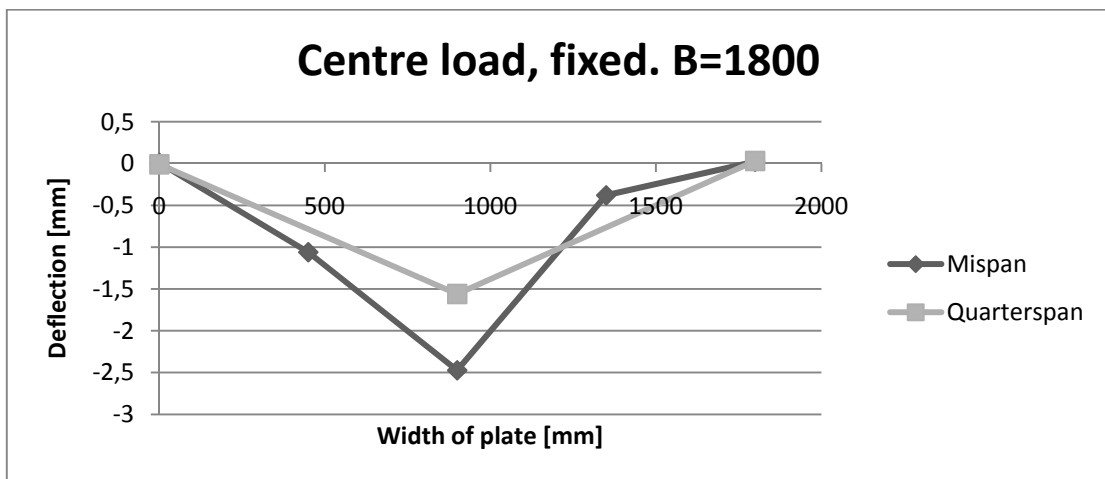


Figure D.27 Deflections for fixed plate with dimensions $L \times B = 1.4 \times 1.8 \text{ m}^2$. Applied load $P=1.310 \text{ kN}$ in the middle of the plate.

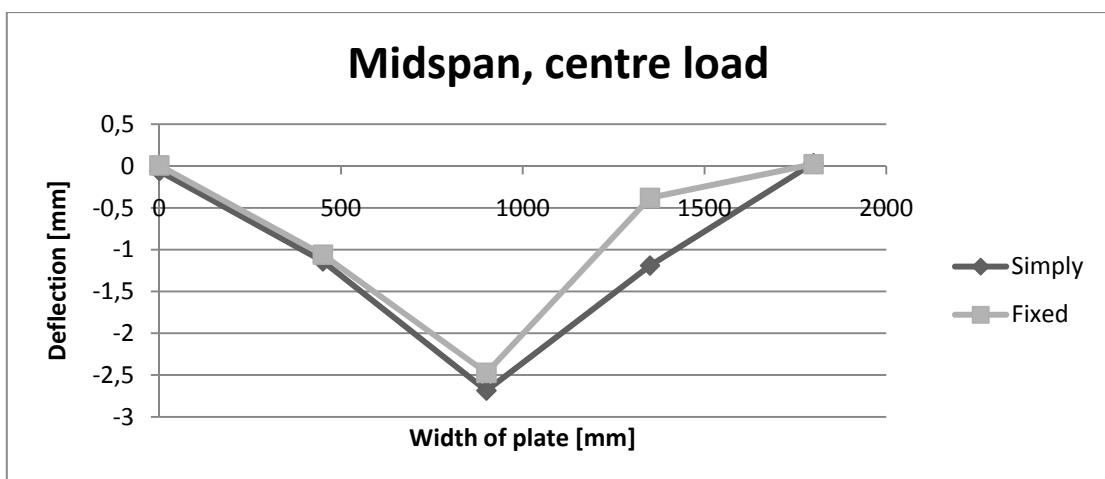


Figure D.28 Deflections in the mid span for simply supported and fixed plate, with dimensions $L \times B = 1.4 \times 1.8 \text{ m}^2$. Applied load $P=1.310 \text{ kN}$ in the middle of the plate.

Table D.10 Measured deflections for the plate with dimensions $L \times B = 1.4 \times 1.8$ m^2 . Applied load $P=1.310$ kN in the centre of the plate (measure point 3). Simply supported and fixed respectively.

LC1, simply	mm	Measure point	Deflection
Midspan	0	1	-0,059
	450	2	-1,14
	900	3	-2,686
	1350	4	-1,19
	1800	5	0,035
Quarter span	0	6	-0,04
	900	7	-1,73
	1800	8	-0,08
Support span	0	9	0,01
	900	10	-0,13
	1800	11	0

LC1, fixed	mm	Measure point	Deflection
Midspan	0	1	0,008
	450	2	-1,06
	900	3	-2,474
	1350	4	-0,38
	1800	5	0,022
Quarter span	0	6	-0,01
	900	7	-1,56
	1800	8	0,03

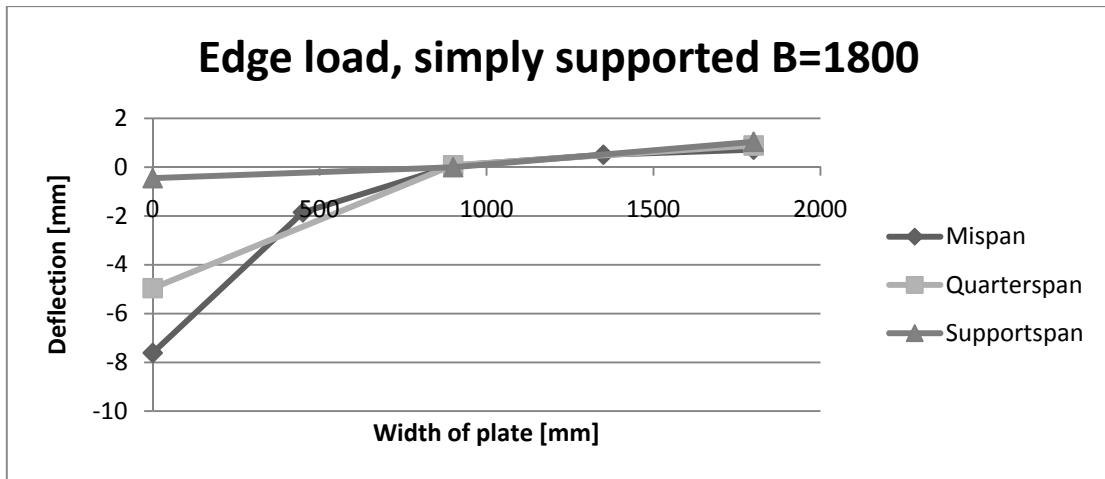


Figure D.29 Deflections for simply supported plate with dimensions $L \times B = 1.4 \times 1.8 \text{ m}^2$. Applied load $P=1.310 \text{ kN}$ at the edge of the plate.

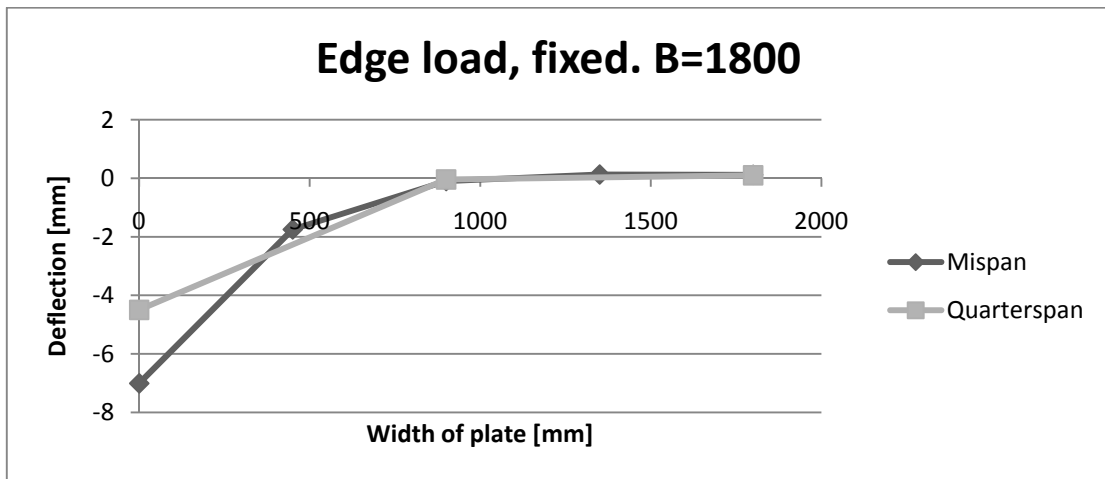


Figure D.30 Deflections for fixed plate with dimensions $L \times B = 1.4 \times 1.8 \text{ m}^2$. Applied load $P=1.310 \text{ kN}$ at the edge of the plate.

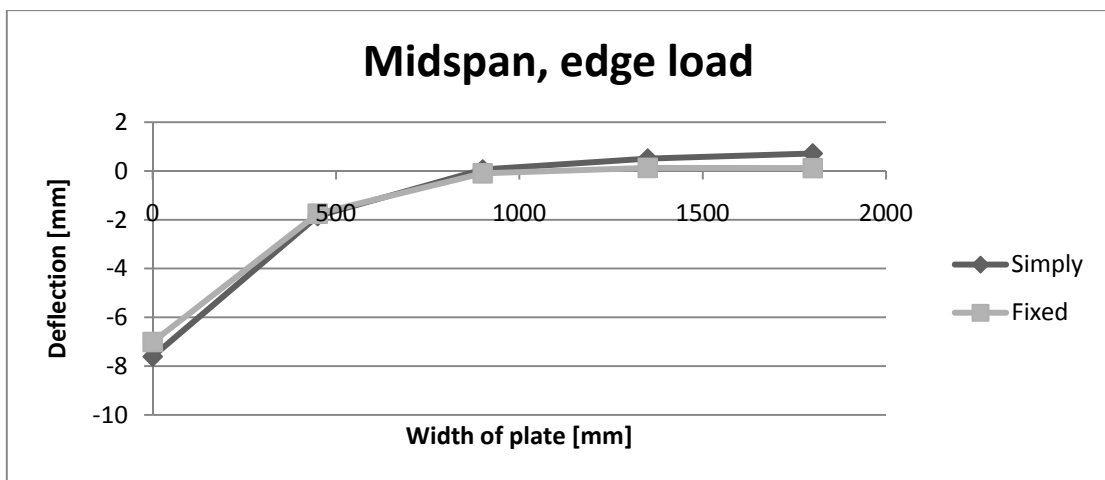


Figure D.31 Deflections in mid span for simply supported and fixed plate, with dimensions $L \times B = 1.4 \times 1.8 \text{ m}^2$. Applied load $P=1.310 \text{ kN}$ at the edge of the plate.

Table D.11 Measured deflections for the plate with dimensions $L \times B = 1.4 \times 1.8 \text{ m}^2$. Applied load $P=1.310 \text{ kN}$ at the edge of the plate (measure point 1). Simply supported and fixed respectively.

LC2, simply	mm	Measure point	Deflection
Midspan	0	1	-7,611
	450	2	-1,85
	900	3	0,064
	1350	4	0,51
	1800	5	0,719
Quarter span	0	6	-4,96
	900	7	0,08
	1800	8	0,89
Support span	0	9	-0,45
	900	10	0
	1800	11	1,04

LC2, fixed	mm	Measure point	Deflection
Midspan	0	1	-7,012
	450	2	-1,75
	900	3	-0,096
	1350	4	0,13
	1800	5	0,119
Quarter span	0	6	-4,5
	900	7	-0,04
	1800	8	0,1

Appendix E1 – Results from parameter study

In Table E.1-E.3 results from the parameter are presented where the relations between x and y varies for the different tables.

Table E.1 *Values from parameter study*

l_{dist} [m]	x [-]	y [-]	X_{je} (500 kN)	X_{je} (600 kN)
10	1.99	0.1	0.96	1.02
9	2.24	0.112	0.94	1.02
8	2.56	0.128	0.93	1.02
7	2.94	0.147	0.93	1.03
6	3.74	0.187	0.91	1.05
5	5.8	0.29	0.84	1.06

Table E.2 *Values from parameter study*

l_{dist} [m]	x [-]	y [-]	X_{je} (500 kN)	X_{je} (600 kN)
10	1.2	0.24	0.93	1.03
9	1.33	0.26	0.92	1.03
8	1.52	0.30	0.9	1.03
7	1.75	0.35	0.9	1.04
6	2.20	0.44	0.87	1.05
5	3.20	0.64	0.8	1.08

Table E.3 *Values from parameter study*

l_{dist} [m]	x [-]	y [-]	X_{je} (500 kN)	X_{je} (600 kN)
10	0.7	0.35	0.92	1.02
9	0.89	0.445	0.91	1.02
8	1.00	0.5	0.9	1.03
7	1.16	0.58	0.89	1.04
6	1.43	0.715	0.86	1.05
5	2.05	1.025	0.79	1.06